"INTENSITY MEASUREMENTS WITH A CURVED CRYSTAL GAMMA RAY SPECTROMETER"

by

A. J. COCHRAN, B.Sc.

Thesis submitted to the University of Edinburgh for the Degree of Doctor of Philosophy, October 1955.

ACKNOWLEDGEMENTS

I should like to thank Dr M. A. S. Ross and Professor N. Feather for their continued interest in the work described here, and for much helpful advice. Thanks are also due to many other members of the staff of the Edinburgh University Natural Philosophy Department, particularly Dr J. Hughes, with whom I had many helpful discussions. I am also indebted to the Department of Scientific and Industrial Research for providing a maintenance allowance during the first year of research.

A.J.C.

C O N T E N T S

Chapter		Page
1.	THE INSTRUMENT	1
	Introduction - The Need for Focussing Spectrometers	1
	Basic Theory and Description	2
	Alternative Source Positions	3
	Object of Present Research	5
2.	INTERPRETATION OF MICROPHOTOMETER READINGS	7
	Procedure for Microphotometering	7
	Averaging Over a Number of Traverses	12
3.	SENSITIVITY-ENERGY CALIBRATION OF THE INSTRUMENT	16
	Introduction	16
	Theoretical Calibration	17
	Experimental Calibration	25
	Comparison of Calculated and Experimental Curves	35
	Selection of Best Curve	37
	Effect of Different Curvature of the Crystal	39
	Reflecting Power of Mica	39
4.	POSITION OF THE SOURCE FOR INTENSITY MEASUREMENTS	41

Chapter		Page
5.	THE FLUORESCENCE YIELDS OF THE L LEVELS OF BISMUTH BY INTENSITY MEASUREMENTS ON THE RaD SPECTRUM	44
	Introduction	44
	Previous Work on L Fluorescence Yields	45
	Equations Governing the Fluorescence Yields	46
	Experimental Values for Bismuth	52
	Calculation of the Yields	64
	Mode of Disintegration of RaD	70
6.	THE FLUORESCENCE YIELDS OF THE L LEVELS OF URANIUM AND BISMUTH	72
	Introduction	72
	Experimental Values for 92 U	73
	Calculation of Yields	76
	Experimental Values for Am^{241} Disintegration	78
	Fitting Uranium Yields to Am^{241}	90
7.	ENERGY MEASUREMENTS	92
	Introduction	92
	Method of Measuring Energy I	92
	II	93
	Americium 241	95
	Xenon 133	96
8.	CONCLUSION	99
	REFERENCES	103

CHAPTER 1

THE INSTRUMENT

INTRODUCTION - THE NEED FOR FOCUSSING SPECTROMETERS

Since the early years of this centure X-ray spectra have been studied by crystalline diffraction methods using plane crystals. To get good resolution with these the beam incident on the crystal must be narrowly defined by a system of fine slits (or possibly by using another crystal - which is effectively the same thing). This means that only a very small fraction of the total radiation impinges on the crystal and though this is not a prohibitive objection when dealing with the radiation from an X-ray tube it becomes a great disadvantage if the method is to be adapted to measurements on weak spectra. If this is desired very long exposures are required. Intensity can, of course, be increased at the expense of resolution by widening the slits but it is not desirable to carry this too far and any spectrometer has to compromise between the two, with a bias towards one or the other depending on the information required from it.

The two pioneers of curved crystal spectrometers, Dumond and Cauchois, were, about 1930, faced with this problem in different ways. Dumond wanted to measure the change in wavelength of X-rays after Compton scattering, and Cauchois was interested in the X-ray spectra of gases. In both cases the intensity available, coupled with the resolution required, made conventional spectrometers impracticable and they both concluded

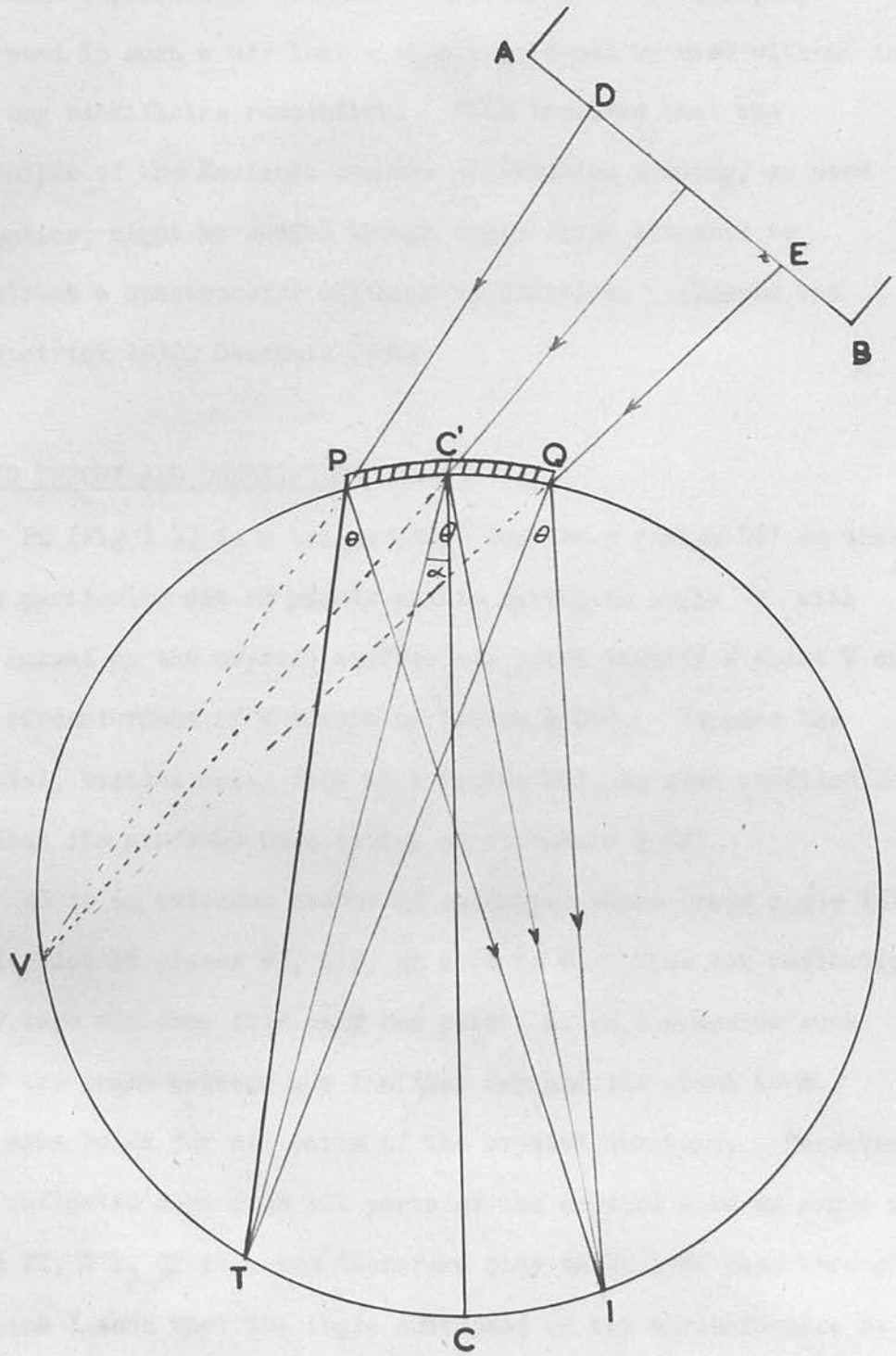

Fig 1.1 : Exact focussing spectrometer

that the experimental technique would have to be radically improved in such a way that a wide beam could be used without in any way sacrificing resolution. Both realised that the principle of the Rowlands concave diffraction grating, as used in optics, might be useful though their first attempts to construct a spectrometer differed in practice. (Dumond and Kirkpatrick 1930, Cauchois 1934)

BASIC THEORY AND DESCRIPTION

PQ (Fig 1.1) is a thin crystal bent to a radius CC' so that some particular set of atomic planes making an angle α with the normal to the crystal surface all point towards a point T on the circumferance of a circle of radius $\frac{1}{2}$ CC'. Suppose the crystal, besides being bent to a radius CC', is also profiled so that its surfaces have radius of curvature $\frac{1}{2}$ CC'.

AB is an extended source of radiation whose Bragg angle for reflection at planes PT, C'T, QT etc. is θ. Then for reflection at P rays can come from only one point, D, on the source such that the angle between the incident ray and the plane is θ. The same holds for all parts of the crystal aperture. Moreover, the reflected rays from all parts of the crystal make an angle θ with PT, C'T, QT etc. and therefore they themselves pass through a point I such that the angle subtended on the circumference by arc TI is θ.

At first Dumond (1930) considered that crystals could not be ground and bent with the necessary precision so his first attempt

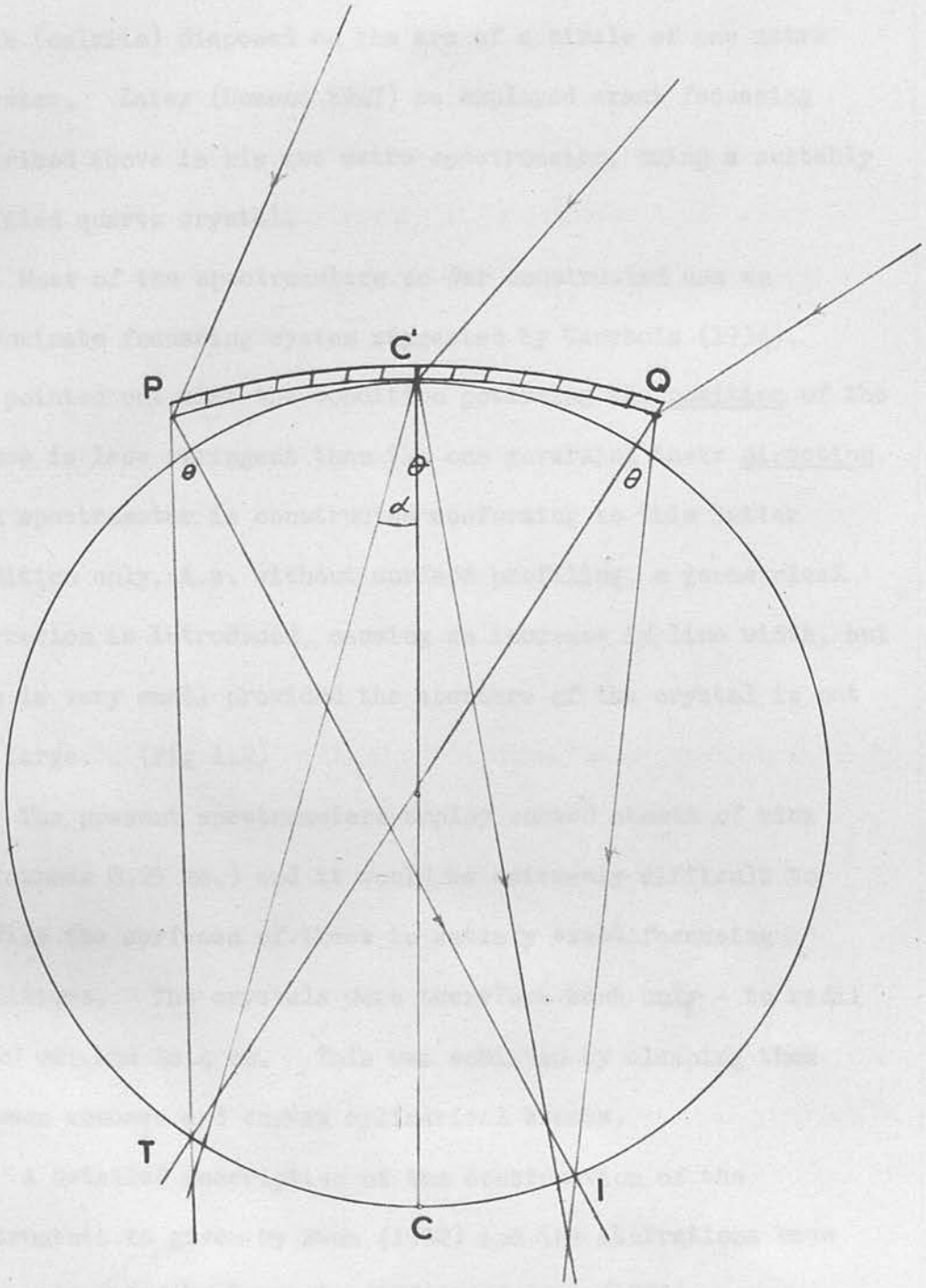

Fig 1.2 : Approximate focussing spectrometer

at building such an instrument consisted of 50 small crystal units (calcite) disposed on the arc of a circle of one metre diameter. Later (Dumond 1947) he employed exact focussing described above in his two metre spectrometer, using a suitably profiled quartz crystal.

Most of the spectrometers so far constructed use an approximate focussing system suggested by Cauchois (1934). She pointed out that the condition governing the position of the planes is less stringent than the one governing their direction. If a spectrometer is constructed conforming to this latter condition only, i.e. without surface profiling, a geometrical aberration is introduced, causing an increase in line width, but this is very small provided the aperture of the crystal is not too large. (Fig 1.2)

The present spectrometers employ curved sheets of mica (thickness 0.25 mm.) and it would be extremely difficult to profile the surfaces of these to satisfy exact focussing conditions. The crystals were therefore bent only - to radii of 20 cm. and 46.4 cm. This was achieved by clamping them between concave and convex cylindrical blocks.

A detailed description of the construction of the instruments is given by Ewan (1952) and the aberrations have been calculated by Cauchois (1934) and Ewan (1952).

ALTERNATIVE SOURCE POSITIONS

The instrument can be used in two ways

(a) with a line source at I, which can move round the circle, and a counter at AB with suitable collimation,

or (b) with an extended source at AB and a detector on the circumference of the circle. This may be either photographic film or a moving counter and fine slit.

If a counter is used, then with method (a) each atom of the source will have the solid angle subtended by the whole crystal aperture to radiate into, whereas with method (b) the solid angle for each atom is the one subtended by a very narrow zone of the crystal. Thus if a counter is to be used (a) is better than (b).

However to record a spectrum consisting of several lines by method (a) involves taking a large number of readings, shifting the position of source and counter each time. If method (b) is used with film round the circumference of the circle then a large part of the spectrum will be recorded at once. Also, if a strong source is used (and sources of several millicuries are necessary) it can be spread out and this reduces self-absorption. This is of particular importance if low energy radiation is being studied. For higher energies (above 150 Kev say) the photographic method loses its advantage because self-absorption is not important and the film is not very sensitive to radiation of high energy.

The method employed therefore depends on what we want to

measure with the instrument. When the spectrometers were constructed by Ewan the first object was to measure γ-ray energies and scan γ-ray spectra to search for lines whose existence was doubtful. This was to be done in the energy range below 100 Kev - the region where β-ray spectrometers are least suited. Hence for reasons stated above the spectrometers were adapted to the photographic method of recording and this is also the best method for the present research.

The original intention was to use X-ray film as the detector but all the intensity measurements have been made using Ilford G 5 β-sensitive nuclear emulsion plates, 200μ thick, as they are more than ten times as sensitive as X-ray film over most of the energy range. The use of a flat plate instead of film curved on an arc of the focussing circle introduces a further aberration but, if the plate is placed tangential to the circle at a point near the lines under investigation, the aberration is small. In any case the instrument is designed primarily to measure intensity rather than energy.

OBJECT OF PRESENT RESEARCH

The object of the present research was to attempt to make intensity measurements of lines in the γ-ray and X-ray spectra from various radioactive sources and to make deductions from these measurements where possible. From the experience gained in doing this we can assess in what circumstances these spectrometers, in their present form, are good instruments for

measuring relative intensities, we can estimate upper and lower energy limits of usefulness, and we can suggest modifications which might improve their performance.

CHAPTER 2

INTERPRETATION OF MICROPHOTOMETER READINGS

The γ- and X-ray spectra recorded on the Ilford G 5 plates have been scanned by a Hilger and Watts microphotometer. If relative intensities of lines are to be measured it is necessary to know exactly what the microphotometer readings mean in terms of relative intensity on the plates.

Suppose the intensities of two lines of energies E_1 and E_2 are as $n_1 : n_2$ and suppose the sensitivity of the apparatus to E_1 and E_2 is S_1 and S_2 respectively. (The sensitivity varies with energy in a way which will be discussed in the next chapter.) Then the ratio of the intensities on the plate is $n_1 S_1 : n_2 S_2$.

Expressed differently, this is the ratio of the number of developed grains produced on the plate by line E_1 to that produced by E_2

or, $$\frac{\text{"blackening" due to } E_1}{\text{"blackening" due to } E_2}$$

We must ensure that the microphotometer observations do, in fact, give the ratio as $n_1 s_1 : n_2 s_2$

PROCEDURE FOR MICROPHOTOMETERING

Very briefly the microphotometer operates as follows:

A diminished image of a line filament is formed by a lens system and focussed on the plate. The light transmitted through

the plate is collected by another lens system and brought to a focus, greatly magnified, on the slit of a photo-cell. The photo-cell is connected to a sensitive galvanometer whose deflection is proportional to the amount of light received through the slit. The final image is so much magnified that only a small fraction of the light from the first image enters the slit. In this particular instrument the slit width and height were adjustable but were normally used with values which corresponded to a height of 1 mm. and a width of 0.025 mm. on the plate. Henceforth "slit width" will be taken as meaning effective width on the plate.

The plate can be moved in a direction perpendicular to the length of the slit by means of a fine screw and the method used to record spectra is to set the plate up so that the lines on it are accurately parallel to the slit and note the galvanometer deflection at points roughly one slit width apart as the slit passes along the plate (strictly as the plate moves past the light).

The lines on a plate are usually at least a centimetre long so that several traverses of a plate can be made at different "heights" on the plate. This is desirable because with G 5 emulsion there are considerable background fluctuations which can be reduced by averaging the results of, say, 10 traverses. This might introduce complications in the interpretation of the results so for the moment let us consider only the readings from one traverse across a spectrum. In what way are these readings

connected with the quantity called "blackening" which we have defined above?

Two assumptions are made:

(1) That the number of grains developed in an exposure of time t to radiation of a given energy is porportional to t.

$$n = c_1 t \qquad (c_1 = \text{constant})$$

(2) That the light transmitted through the plate (i.e. the galvanometer deflection) is given by

$$I = I_o e^{-c_2 n} \qquad (c_2 = \text{constant})$$

where I_o is the transmitted intensity at a clear part of the plate.

Combining (1) and (2):

$$I = I_o e^{-kt} \qquad (k = \text{constant})$$

or $\log I_o - \log I = kt. \propto n$ ("blackening") ...(2.1)

Since all lines are not the same breadth or shape the blackening is obtained not simply by subtraction but by finding the area enclosed between log I and log I_o over the whole breadth of the line.

The two original assumptions might be invalid for a very black line.

(1) Some of the incident photons might be absorbed in grains already rendered developable, i.e. $n < c_1 t$.

(2) Some of the developed grains might be "in the shadow" of others, i.e. $I > I_o e^{-c_2 n}$

To test whether relation (2.1) held for dark lines, different

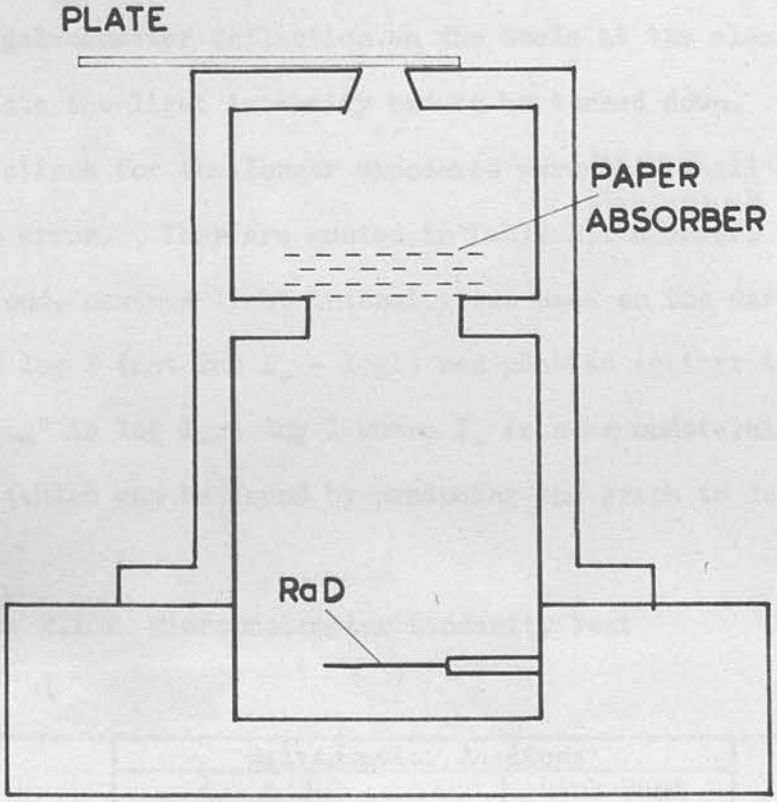

Fig 2.1 : Linearity test - the apparatus

parts of a G 5 200μ plate were exposed for 50, 40, 30, 20 and 10 minutes to the electromagnetic radiation from RaD (46.5 Kev γ-rays and RaE L X-rays, 10-16 Kev, the β-rays from RaD and RaE being absorbed in filter paper) as in fig 2.1.

Each exposure gave a broad band with a sharp edge. At first the value of log I_o in each case was taken as the deflection just to the clear side of the edge and I as that on the dark side. This was not found to be satisfactory since to keep the galvanometer deflection on the scale at the clear part of the plate the light intensity had to be turned down. Then the deflections for the longer exposures were very small and so liable to error. They are quoted in Table 2.1 however.

Instead, maximum light intensity was used on the dark band only, and log I (not log I_o - logI) was plotted against time. "Blackening" is log I_o - log I where I_o is some undetermined constant (which can be found by producing the graph to cut t = o).

Table 2.1 : Microphotometer Linearity Test

Exposure (mins)	Galvanometer Readings			Log_{10} I
	Clear Part	Dark Band	Dark Band with full Intensity (I)	
50	42	0.6	1.15	0.061
40	45	1.2	2.45	0.389
30	46	2.7	6.1	0.785
20	45	6.4	14.0	1.146
10	47	13.8	31.5	1.498

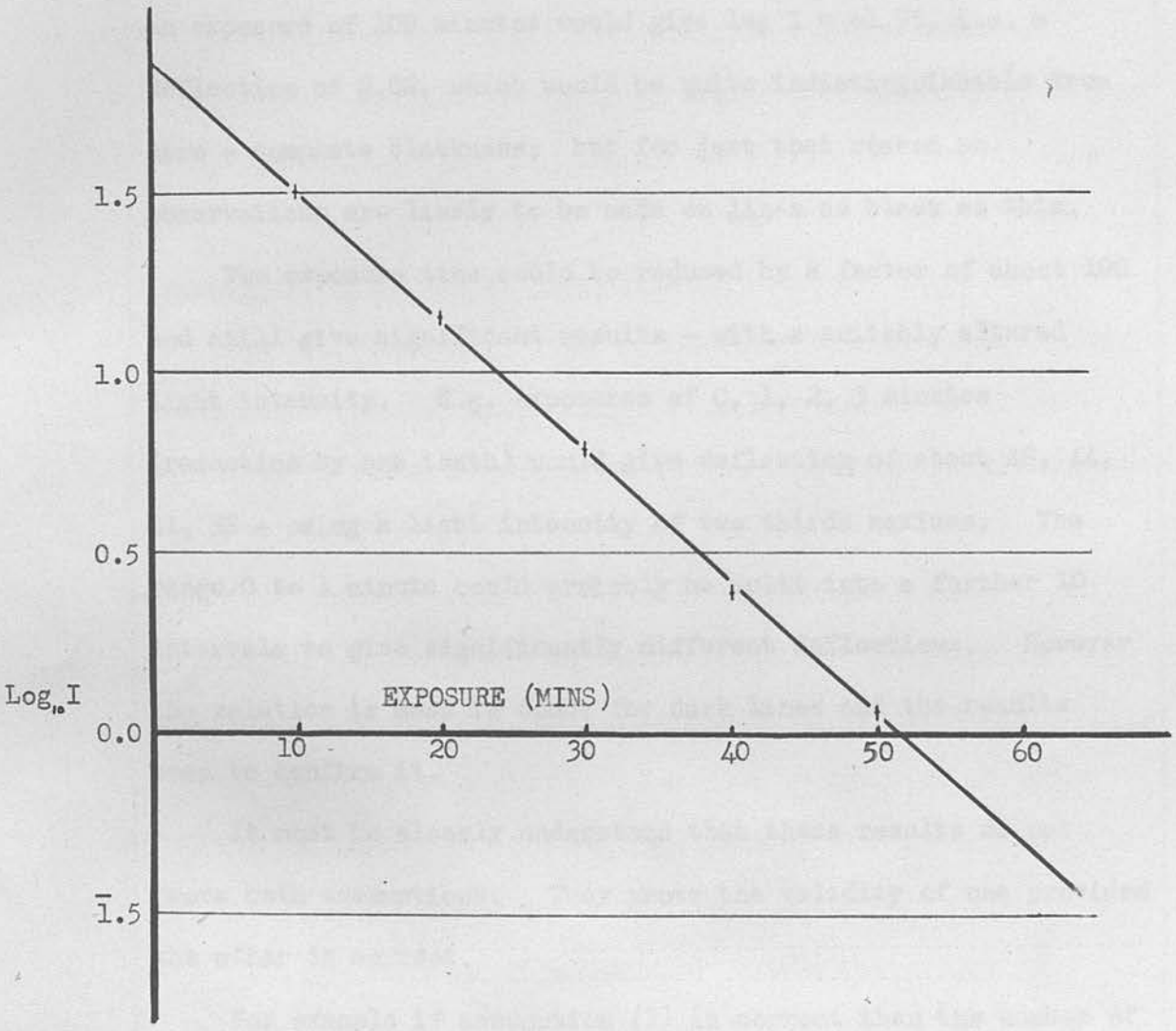

Fig 2.2 : Linearity test - relation between transmitted intensity and exposure time

The graph of $\log_{10} I$ against time (Fig 2.2) is a straight line over the above range.

It is almost impossible to extend the range upwards. For example, assuming approximate linearity beyond t = 50 minutes an exposure of 100 minutes would give log I = -1.75, i.e. a deflection of 0.02, which would be quite indistinguishable from zero - complete blackness; but for just that reason no observations are likely to be made on lines as black as this.

The exposure time could be reduced by a factor of about 100 and still give significant results - with a suitably altered light intensity. E.g. exposures of 0, 1, 2, 3 minutes (reduction by one tenth) would give deflection of about 48, 44, 41, 38 - using a light intensity of two thirds maximum. The range 0 to 1 minute could probably be split into a further 10 intervals to give significantly different deflections. However the relation is most in doubt for dark lines and the results seem to confirm it.

It must be clearly understood that these results do not prove both assumptions. They prove the validity of one provided the other is correct.

For example if assumption (1) is correct then the number of grains i.e. "blackening" in each of the dark bands is truly in the ratio 1 : 2 : 3 : 4 : 5 and hence the straight line graph proves that assumption (2) is valid. Conversely if assumption (2) is correct the straight line graph proves that the number of grains developed are in the ratios 1 : 2 : 3 : 4 : 5 for exposures

of 10, 20, 30, 40 and 50 minutes and so proves assumption (1).

An examination of the plate by means of a high power microscope shows that even for the darkest lines the grains occupy only a small fraction of the total area in any field so that assumption (1) is a reasonable one. Hence relative intensities of lines are given to a good approximation by taking the area between log I and log I_o on microphotometer traces.

AVERAGING OVER A NUMBER OF TRAVERSES

We have seen earlier in this chapter that it is desirable to average (or sum) the results of as many traverses of the plate as possible to reduce the effect of background fluctuations to a minimum.

The correct procedure is to obtain the galvanometer readings for each of the traverses, find the logarithm for each point and sum them for corresponding points on different traverses. This is a long and tedious process and it would reduce the labour if it were legitimate to sum the galvanometer readings and use the logarithm of these sums.

It is therefore of interest to find out when this is allowed.

Suppose we have a plate which has two lines A and B on it and which has a uniform background - i.e. I_o is constant over the whole plate except for the lines. (This is of course an erroneous assumption for we should require only one traverse if it were so. However it does not affect the conditions which

determine whether the above approximation is allowed and it simplifies the argument.)

Suppose we make n traverses across the plate and suppose that to span line A, p readings are required, and to span line B, q are required. These readings are all the same distance apart - equal to the width of slit, let us suppose, though this is not necessary.

At the j^{th} point (j = 1 to p) on line A on traverse r (r = 1 to n) let the transmitted intensity (i.e. galvanometer deflection) $= I_{Ar}^{j}$

Then blackening in the area round j on the r^{th} traverse

$$= \log I_o - \log I_{Ar}^{j}$$

Blackening at j over n traverses

$$= \sum_{r=1}^{n} \left\{ \log I_o - \log I_{Ar}^{j} \right\}$$

$$= n \log I_o - \sum_{r=1}^{n} \log I_{Ar}^{j}$$

$\therefore$ Total blackening on whole line A

$$= \sum_{j=1}^{p} \left\{ n \log I_o - \sum_{r=1}^{n} \log I_{Ar}^{j} \right\}$$

A similar expression gives the blackening on B so that the ratio A : B

$$= \frac{\sum_{j=1}^{p} \left\{ n \log I_o - \sum_{r=1}^{n} \log I_{Ar}^{j} \right\}}{\sum_{i=1}^{q} \left\{ n \log I_o - \sum_{r=1}^{n} \log I_{Br}^{i} \right\}} \qquad (2.2)$$

where I_{Br}^{i} is the intensity at the i^{th} point on line B on the r^{th} traverse.

This expression (2.2) is the ratio of true blackening.

If we add galvanometer readings and then take logarithms we get a quantity which we shall call "pseudo-blackening".

Then the pseudo-blackening round j on A over n traverses

$$= \log n I_{o} - \log \sum_{r=1}^{n} I_{Ar}^{j}$$

$\therefore$ Total pseudo-blackening on whole line

$$= \sum_{j=1}^{p} \left\{ \log n I_{o} - \log \sum_{r=1}^{n} I_{Ar}^{j} \right\}$$

$$\therefore \text{Ratio A : B} = \frac{\sum_{j=1}^{p} \left\{ \log n I_{o} - \log \sum_{r=1}^{n} I_{Ar}^{j} \right\}}{\sum_{i=1}^{q} \left\{ \log n I_{o} - \log \sum_{r=1}^{n} I_{Br}^{i} \right\}} \qquad (2.3)$$

Expression (2.2) = (2.3) only when

$$I_{A1}^{j} = I_{A2}^{j} = \ldots = I_{Ar}^{j} = \ldots I_{An}^{j} = I_{A}^{j}$$

$$I_{B1}^{i} = I_{B2}^{i} = \ldots = I_{Br}^{i} = \ldots I_{Bn}^{i} = I_{B}^{i}$$

Then (2.2) becomes

$$\frac{\sum_{j=1}^{p} \left\{ n \log I_{o} - n \log I_{A}^{j} \right\}}{\sum_{i=1}^{q} \left\{ n \log I_{o} - n \log I_{B}^{i} \right\}} = \frac{\sum_{j=1}^{p} \log \frac{I_{o}}{I_{A}^{j}}}{\sum_{i=1}^{q} \log \frac{I_{o}}{I_{B}^{j}}}$$

and (2.3) becomes

$$\frac{\sum_{j=1}^{p} (\log n I_o - \log n I_A^j)}{\sum_{i=1}^{q} (\log n I_o - \log n I_B^i)} = \frac{\sum_{j=1}^{p} \log \frac{I_o}{I_A^j}}{\sum_{i=1}^{q} \log \frac{I_o}{I_B^i}}$$

The labour saving procedure therefore gives the same result as the exact method only if galvanometer readings at the same points on each traverse are equal. However the method is accurate enough if the galvanometer readings are approximately equal and this should nearly always be the case if the plate is properly set up in the microphotometer.

If this method is to be used we must, in addition to setting the plate up very carefully guard against two possible sources of error.

(i) The lines on the plate must not be bent. This can happen if the emulsion is distorted while processing the plates.

(ii) Traverses must not be made near the ends of lines on a plate because intensity falls off there compared with the middle of the lines. This is because only part of the source is being used to form the ends of the lines.

Bearing these two points in mind it is usually sufficiently accurate to use this shorter method and unless otherwise stated this is the procedure which has been adopted.

CHAPTER 3

SENSITIVITY-ENERGY CALIBRATION OF THE INSTRUMENT

INTRODUCTION

The instrument is to be used primarily to measure intensities rather than energies - i.e. to compare intensities of the components of a γ-ray spectrum, or to compare the intensities of γ-rays with fluorescent X-rays caused by internal conversion. It is therefore essential to know how the sensitivity of the apparatus varies for different radiation energies. It is evident that it must vary for, besides the variation due to different absorptions in the path from source to plate (in air and crystal), there will be less easily calculable, and probably more rapid variations in the sensitivity of the plate and reflecting power of the crystal for different energies.

A sensitivity calibration of the apparatus has been done theoretically and experimentally. For reasons discussed later the experimental method is not easy to carry out and it involves the assumption of some not very well established data. On the other hand it does use the instrument in exactly the way it is used for measurements on γ-ray sources, and so any unknown effects are automatically included in the calibration. The calculated curve involves the use of fairly well established data - absorption coefficients and K fluorescence yields - but it takes account only of the absorption of the radiation by the photographic emulsion and absorption in the path from source to

emulsion. There may be other effects for which no allowance has been made. In addition a simplifying assumption has to be made about the amount of fluorescent X-rays absorbed in the emulsion.

THEORETICAL CALIBRATION

The variation in plate sensitivity can be calculated if we assume that all the developed grains are caused by electrons ejected from atoms of the emulsion - either directly by the incident radiation or after some secondary process such as Auger electron emission.

Primary Photo-electrons

Let there be N_o photons of energy E incident normally on the plate. Then the number incident on a layer of thickness dx at depth x $= N = N_o e^{-\mu x}$

where μ = total linear absorption coefficient of the emulsion for radiation of energy E.

$\therefore$ The number of photons absorbed by photo-ionization in the K level of a particular element in the layer dx

$$= N \tau_K \rho \, dx = N_o \tau_K \rho e^{-\mu x} dx$$

where τ_K is the mass absorption coefficient for radiation of energy E in the K shell of the element, and ρ is the density of the element in the emulsion.

$\therefore$ Total number of photons absorbed in the K shell of the element in the whole emulsion (depth X) $= N_o \tau_K \rho \, \frac{1 - e^{-\mu X}}{\mu}$ (3.1)

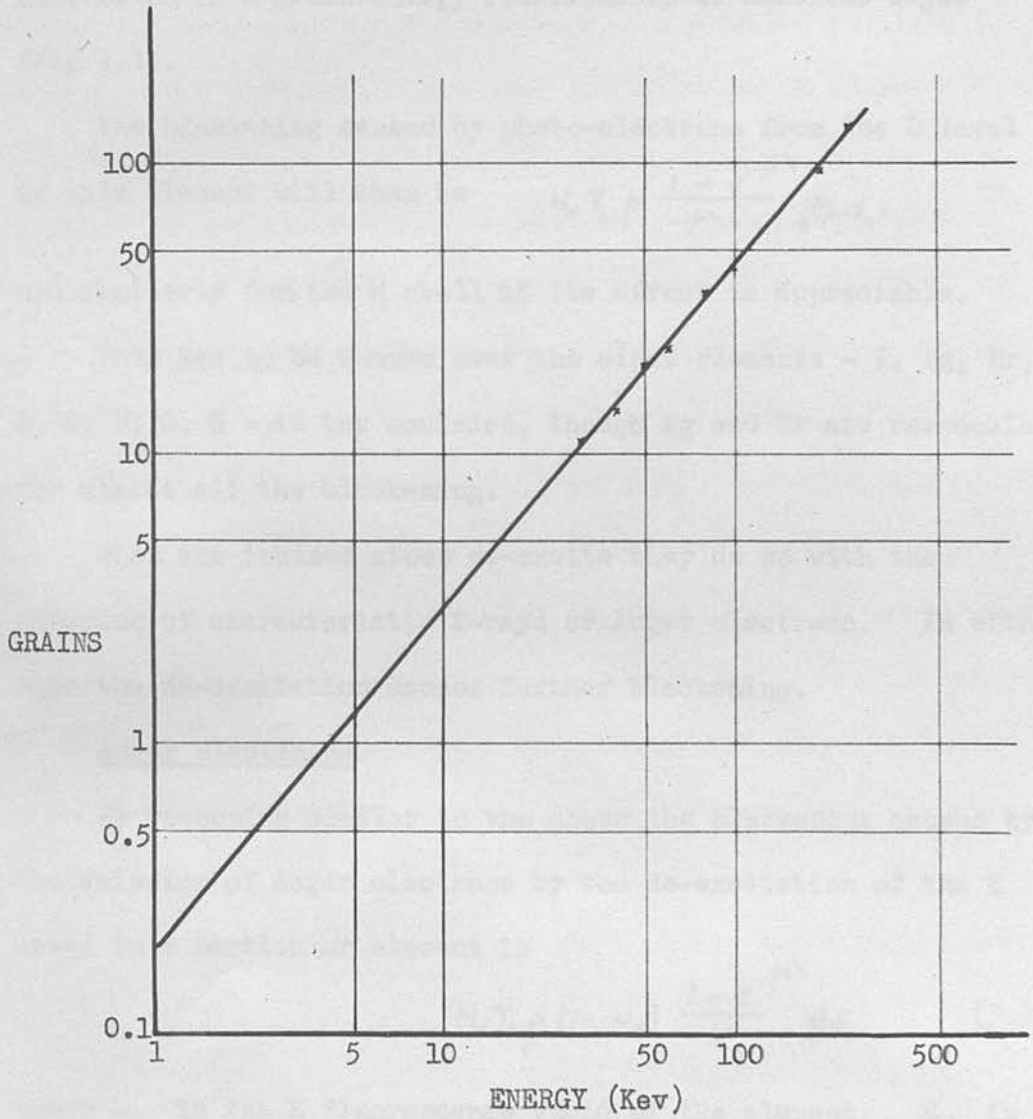

Fig 3.1 : Grain-energy relationship for G5 emulsion

∴ Blackening caused by ejection of photo-electrons from K shell of the element $= N_0 \tau_K \rho \frac{1 - e^{-\mu x}}{\mu} g_{(E-E_K)}$ (3.2)

where E_K is the ionization energy of the K level of the element and $g_{(E-E_K)}$ is the average number of grains produced by an electron of energy $E - E_K$. The values used were those determined in a grain-energy relationship of Ross and Zajac (Fig 3.1).

The blackening caused by photo-electrons from the L level of this element will then be $N_0 \tau_L \rho \frac{1 - e^{-\mu x}}{\mu} g_{(E-E_L)}$

and similarly for the M shell if its effect is appreciable.

This has to be summed over the eight elements - I, Ag, Br, S, O, N, C, H - in the emulsion, though Ag and Br are responsible for almost all the blackening.

When the ionized atoms de-excite they do so with the emission of characteristic X-rays or Auger electrons. In either case the de-excitation causes further blackening.

Auger Blackening.

By reasoning similar to the above the blackening caused by the emission of Auger electrons by the de-excitation of the K level in a particular element is

$$N_0 \tau_K \rho (1 - \omega_K) \frac{1 - e^{-\mu x}}{\mu} g_{E_A} \qquad (3.3)$$

where ω_K is the K fluorescence yield of the element. E_A is the average energy of the Auger electrons which is accurately enough E_K. The reason for this is that after emission of an Auger electron the atom can de-excite in several ways. All of

these involve low energy X-rays or electrons so that the entire energy is likely to be absorbed in the emulsion. The total number of grains produced in the process will, therefore, not differ much from the number produced by an electron of energy E_K.

Fluorescent X-rays

To find the blackening by fluorescent X-rays is more difficult since they are emitted in all directions and at all depths in the emulsion. A method for calculation of the effect will be outlined.

Let us for simplicity consider that the emulsion consists only of silver and bromine. Then a typical fluorescent X-ray process would be for a silver atom to be ionized in the K shell by incident radiation and to emit a K X-ray photon. This travels some distance in the emulsion before being absorbed in the K shell of bromine, so knocking out a photo-electron which will cause blackening. This atom will de-excite either by Auger emission or by emission of bromine K X-rays which can in turn be absorbed. But for the moment let us consider only the first process - the blackening by the "primary" fluorescent X-rays.

The following symbols will be used.

N_o : the number of photons incident on the emulsion per unit area.

ρ, ρ' : densities of silver and bromine respectively in the emulsion.

μ : total linear absorption coefficient of the emulsion for incident radiation.

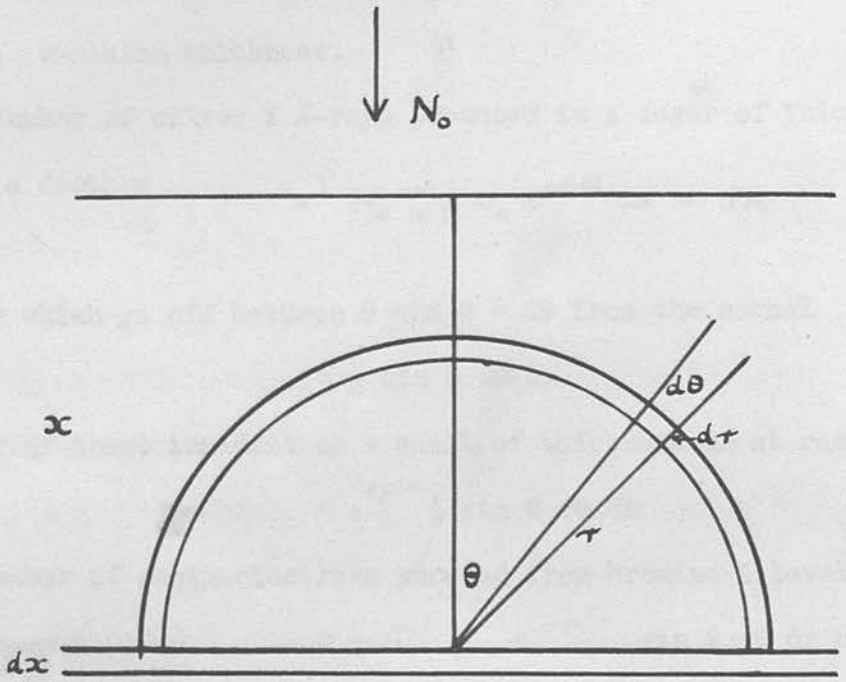

Fig 3.2 : Absorption of fluorescent X-rays

μ' : total linear absorption coefficient of the emulsion for silver K radiation.

τ_K : mass absorption coefficient of incident radiation in K shell of silver.

τ_K' : mass absorption coefficient of silver K radiation in K shell of bromine.

ω_K : K fluorescence yield of silver.

X : emulsion thickness.

Number of silver K X-rays produced in a layer of thickness dx at a depth x

$$= N_0 \tau_K \rho \omega_K e^{-\mu x} dx = dn$$

Number which go off between θ and $\theta + d\theta$ from the normal

$$= \tfrac{1}{2} \sin\theta \, d\theta \, dn$$

Number of these incident on a shell of thickness dr at radius r

$$= e^{-\mu' r} \tfrac{1}{2} \sin\theta \, d\theta \, dn$$

$\therefore$ Number of photo-electrons knocked from bromine K level in dr

$$= \tfrac{1}{2} \tau_K' \rho' e^{-\mu' r} \sin\theta \, d\theta \, dr \, dn$$

$\therefore$ Total number of bromine K photo-electrons ejected by Ag X-rays going off in $d\theta$ from layer dx

$$= \tfrac{1}{2} \tau_K' \rho' \sin\theta \, d\theta \, dn \int_0^{x \sec\theta} e^{-\mu' r} dr.$$

provided $\theta < \pi/2$

(If $\theta > \pi/2$ limits are 0 to $(X - x) \sec\theta$)

This expression is

$$\frac{\tau_K \tau_K' \rho \rho' N_0 \omega_K}{2\mu'} \left\{1 - e^{-\mu' x \sec\theta}\right\} e^{-\mu x} \sin\theta \, dx \, d\theta \quad (3.4)$$

for $\theta < \pi/2$ with a similar expression for $\theta > \pi/2$

Extending this to cover all layers (x = o to X) the number of bromine K photo-electrons ejected becomes

$$A \sin\theta \int_0^X (1 - e^{-\mu' x \sec\theta}) e^{-\mu x} \, dx \, d\theta$$

where A is a constant equal to the expression before the bracket in expression (3.4).

On integration this is

$$A \sin\theta \left\{ \frac{1 - e^{-\mu X}}{\mu} - \frac{1 - e^{-(\mu' \sec\theta + \mu)X}}{\mu' \sec\theta + \mu} \right\} d\theta \qquad (3.5)$$

To find the total number of bromine K electrons emitted by silver K X-rays at all angles $(< \pi/2)$ this expression (3.5) must be integrated between O and $\pi/2$. The second term is not integrable however.

We can get a good approximation by doing a summation.

The probability of a photon being emitted between θ and $\theta + d\theta$ of the normal is $P(\theta) = \frac{1}{2} \sin\theta \, d\theta$ so that expression (3.5) can be written

$$2A \left\{ \frac{1 - e^{-\mu X}}{\mu} - \frac{1 - e^{-(\mu' \sec\theta + \mu)X}}{\mu' \sec\theta + \mu} \right\} P(\theta) \qquad (3.6)$$

Now $P(\theta)$ can be evaluated for small angular zones (of say 5°).

i.e. $P(2\frac{1}{2})$ = probability of emission into a zone within 5° of the normal $= \frac{1}{2}(1 - \cos 5^\circ)$

$P(7\frac{1}{2})$ = probability of emission into a zone between 5° and 10° of the normal $= \frac{1}{2}(\cos 5^\circ - \cos 10^\circ)$

$P(a) = \frac{1}{2}\left[\cos (a - 2\frac{1}{2})^\circ - \cos (a + 2\frac{1}{2})^\circ\right]$

$P(87\frac{1}{2}) = \frac{1}{2}(\cos 85^\circ - 0)$

Hence the number of bromine K X-rays emitted by absorption of fluorescent K radiation from silver will be given by

$$\sum_{\theta=2\frac{1}{2}^\circ}^{87\frac{1}{2}^\circ} 2A\left\{\frac{1-e^{-\mu x}}{\mu} - \frac{1-e^{-(\mu'\sec\theta+\mu)x}}{\mu'\sec\theta+\mu}\right\} P(\theta)$$

$$+ \sum_{\theta=92\frac{1}{2}^\circ}^{177\frac{1}{2}^\circ} 2A\left\{\text{a similar expression}\right\} P(\theta) \qquad (3.7)$$

and the blackening will be found by multiplying this by the number of grains appropriate to the process (i.e. ejection from the K shell of bromine by 22 Kev photon).

To calculate blackening in this way for sufficient energies to draw a curve is long and laborious. Double and triple processes must be included in the calculation - for example fluorescent silver K X-rays can excite bromine K X-rays which in turn can excite silver L X-rays.

This summation was therefore done only for two values of incident energy and used as a check for the following very simple approximation.

Approximate Fluorescent X-ray Blackening

Again we consider only bromine and silver. The blackening by "primary" photo-electrons and Auger electrons was calculated for a number of energies and a graph drawn (fig 3.3, lower curve). The units of "sensitivity" are the average number of grains developed per incident photon, though this is of little importance since we require only ratios. The two discontinuities are at energies corresponding to the K absorption edges of bromine and silver.

For incident energies less than 13.5 Kev neither bromine nor silver K will be excited. Hence the fluorescent X-ray effect adds nothing to the first curve for these energies (except the small amount caused by silver and bromine L - we neglect this).

Bromine K radiation is excited by all incident photons with energy greater than 13.5 Kev. By equation (3.1) the number of bromine atoms ionized in the K shell per incident quantum is $\tau_K \rho \frac{1 - e^{-\mu x}}{\mu}$ where μ is again the total absorption coefficient of the emulsion for the given energy, τ_K applies to photo-absorption in the K level of bromine and ρ is the density of bromine in the emulsion.

I.e. the number of bromine K X-rays produced per incident quantum

$$= n_K(Br) = \tau_K \omega_K \rho \frac{1 - e^{-\mu x}}{\mu}$$

where ω_K = K fluorescence yield.

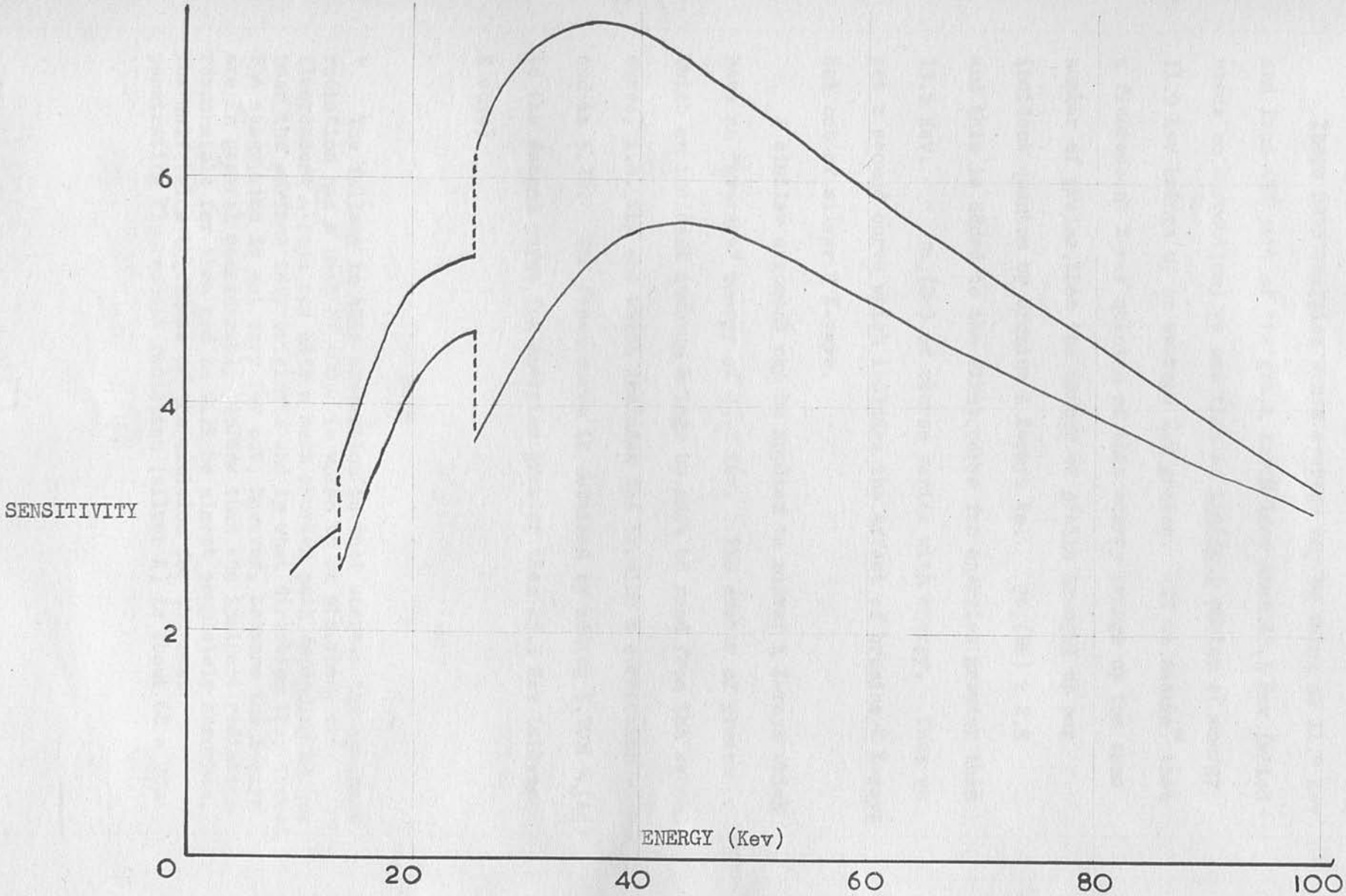

Fig 3.3 : Calculated sensitivity-energy relation for G5 emulsion - lower curve excludes fluorescent X-rays

These have energies whose average may be taken as 11.9 Kev and from the part of the graph for E less than 13.5 Kev (which needs no correction) we see that an incident photon of energy 11.9 Kev brings up on average 2.8 grains. If we assume* that a fluorescent X-ray quantum of this energy brings up the same number of grains, then the number of grains brought up per incident quantum by bromine K X-rays is $n_K(Br) \times 2.8$ and this is added to the first curve for energies greater than 13.5 Kev. $n_K(Br)$ of course varies with energy. Thus we get a second curve which includes the effect of bromine K X-rays but not of silver K X-rays.

A similar argument can be applied to silver K X-rays which have an "average" energy of 22.2 Kev. The number of grains which an incident quantum brings up must be read from the second curve, i.e. the one which includes the bromine K correction - and is 5.20. The final curve is obtained by adding $5.20 \times n_K(Ag)$ to the second curve for energies greater than 25.5 Kev (silver K edge).

* The fallacy in this assumption is that whereas the incident radiation has a path of 200μ in which to be absorbed, the fluorescent X-rays may have a much shorter path depending on how near the surface they originate and in what direction they travel. The assumption is not very far out, however, because the X-rays are in general considerably softer than the incident radiation responsible for them and so will be almost completely absorbed. The half value thickness of the emulsion for the most penetrating fluorescent radiation (silver K) is about 60 - 70μ

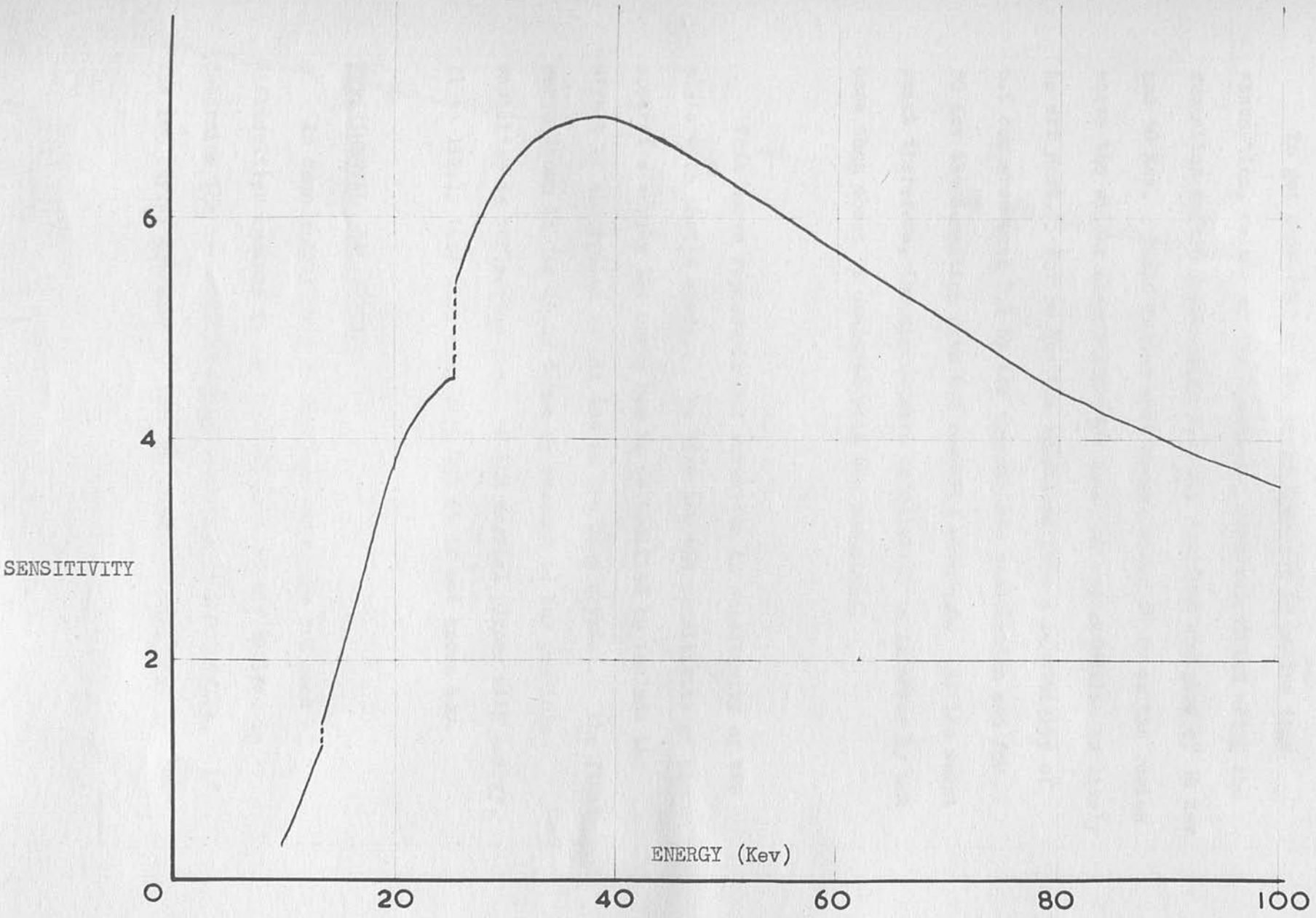

Fig 3.4 : Calculated sensitivity-energy relation for whole apparatus

The final curve obtained is the upper one in fig 3.3.

To get some idea of the error involved in making this assumption, values of the blackening were calculated using the summation method (expression 3.7) for incident energies of 30 Kev and 50 Kev. These values were chosen since it is in the region above the silver absorption edge that the approximation is likely to err most. For 30 Kev the summation gave a sensitivity of 6.8 compared with 7.1 by the approximate calculation and for 50 Kev the summation gave 6.5 compared with 6.6. At its worst point therefore, the approximate calculation is in error by not more than about 5% compared with the summation.

This curve represents the variation in sensitivity of the plate with photon energy. To find how the sensitivity of the apparatus varies the curve has to be modified to include the effect of absorption in air and in the mica crystal. The final curve shown in fig (3.4) takes no account of any possible variation in reflecting power of the crystal planes with energy. It is likely that this does vary but it is not known how.

EXPERIMENTAL CALIBRATION

As some simplifying assumptions were made and some difficulties ignored in the calculation, it was decided to determine the sensitivity-energy relation experimentally. If the two curves are more or less in agreement then this is

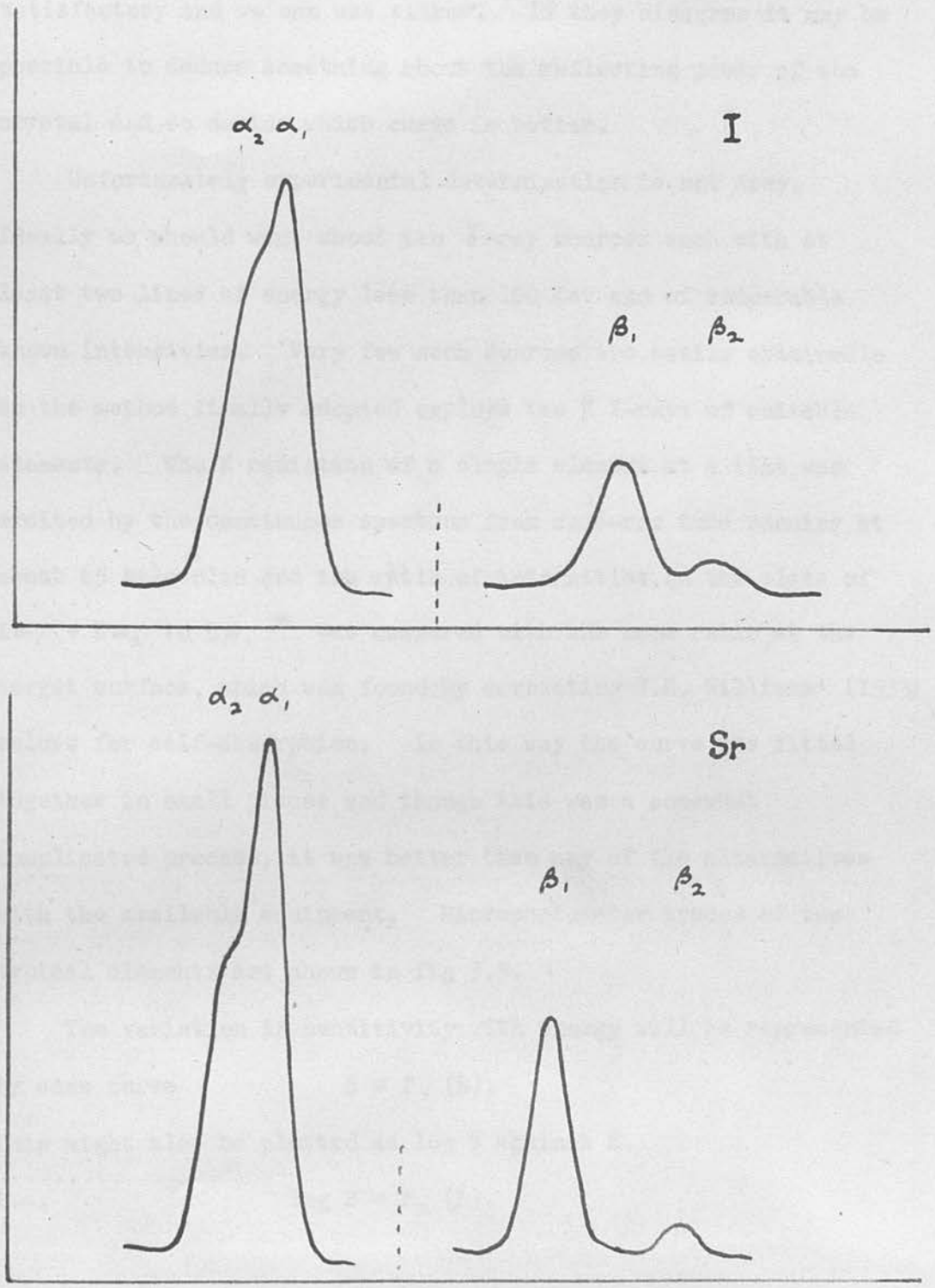

Fig 3.5 : Microphotometer traces of two elements used in the sensitivity-energy calibration

satisfactory and we can use either. If they disagree it may be possible to deduce something about the reflecting power of the crystal and so decide which curve is better.

Unfortunately experimental determination is not easy. Ideally we should want about ten γ-ray sources each with at least two lines of energy less than 100 Kev and of comparable known intensities. Very few such sources are easily obtainable so the method finally adopted employs the K X-rays of suitable elements. The K radiation of a single element at a time was excited by the continuous spectrum from an X-ray tube running at about 65 kilovolts and the ratio of intensities on the plate of $K\alpha_1 + K\alpha_2$ to $K\beta_1$ * was compared with the same ratio at the target surface, which was found by correcting J.H. Williams' (1933) values for self-absorption. In this way the curve was fitted together in small pieces and though this was a somewhat complicated process, it was better than any of the alternatives with the available equipment. Microphotometer traces of two typical elements are shown in fig 3.5.

The variation in sensitivity with energy will be represented by some curve $S = f_1(E)$.

This might also be plotted as log S against E.

i.e. $\log S = f_2(E)$.

* This ratio was taken in preference to α_1/β_1 because α_1 and α_2 were at best only partially resolved.

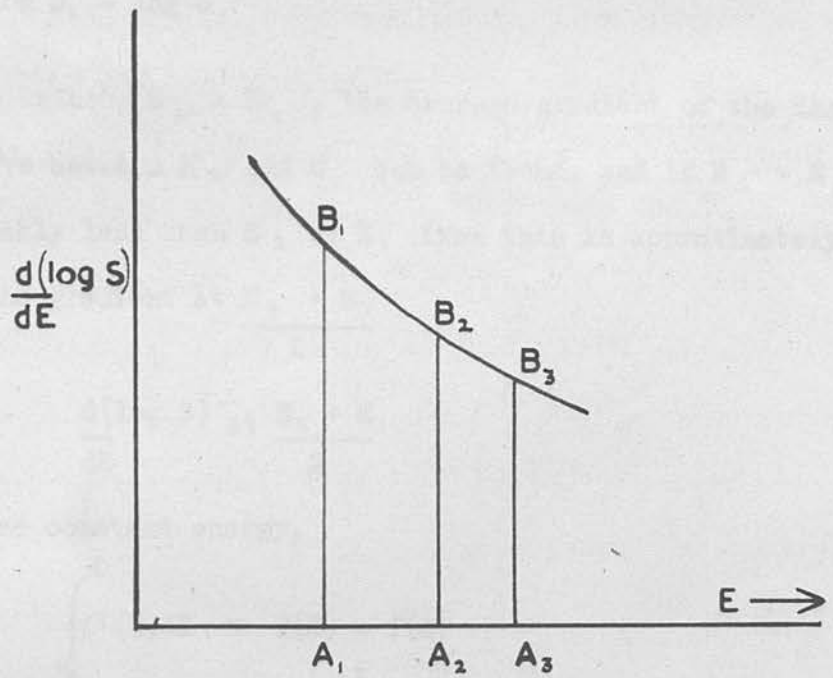

Fig 3.6

The experimental observations consist of a number of ratios of $S_2 : S_1$ for two energies E_2, E_1 not differing by much. i.e. They give ratios of pairs of ordinates in curve (1) or they give differences of pairs of ordinates in curve (2) since

$$\log \frac{S_2}{S_1} = \log S_2 - \log S_1$$

Since we know $E_2 - E_1$, the average gradient of the log S-energy curve between E_2 and E_1 can be found, and if $E_2 - E_1$ is appreciably less than E_2 or E_1 then this is approximately equal to the gradient at $\frac{E_2 + E_1}{2}$

i.e. $$\frac{d(\log S)}{dE} \text{ at } \frac{E_2 + E_1}{2}$$

If A is some constant energy,

$$\int_A^E f'(E)dE = f(E) - f(A)$$

$$\therefore \quad f(E) = \int_A^E \frac{d(\log S)}{dE} dE + \log S_A$$

$$\therefore \quad S_E = S\, e^{\int_A^E \frac{d(\log S)}{dE} dE}$$

Now if $\frac{d(\log S)}{dE}$ is plotted against E, and if the area under the curve to the left of A_1B_1 (Fig 3.6) is assumed to be some constant K then area $A_1B_1B_2A_2$ + K represents $\log S_{A_2}$ + constant and area $A_1B_1B_3A_3$ represents $\log S_{A_3}$ + constant.
i.e. the difference in the two areas represents $\log S_{A_3} - \log S_{A_2}$

A curve can then be plotted, log S against energy in which

there is an arbitrary constant of addition. If we wish a sensitivity-energy curve this constant becomes a constant multiplying factor.

Correction to Williams' Relative Intensities

The ratios of Williams (quoted in Compton & Allison, 1935) are the relative intensities at the target surface when the X-rays are excited by electron bombardment. In our case the X-rays are excited by the white radiation from an X-ray tube falling on a thick target (except in two cases). The ratio will not necessarily be the same.

The fundamental quantity is, of course, the relative transition probability and Williams carried out a calculation to find whether these probabilities for $K\alpha_1$ and $K\beta_1$ differed significantly from ratios at the target surface. He found that the correction factor to be applied to β_1'/α_1 varied from 0.97 in 24 Cr to 1.00 in 52 Te - i.e. it was within the experimental error. His ratios of $K\beta_1$ to $K\alpha_1$ are therefore the relative probability of these transitions. However since the exciting radiation from the tube in our case penetrates deeper into the target than the electrons in Williams' experiment there is likely to be some correction needed to fix the relative intensities at the surface of our target.

Suppose the exciting radiation is monochromatic of energy E; that the total linear absorption coefficient of the target for E is μ; and that the linear absorption coefficient for E in the K shell of the target element is τ_K.

The targets were placed so that both the exciting incident radiation and the part of the emerging fluorescent radiation which passes through the crystal made an angle of about 45° with the target surface.

Let N_o photons be incident at 45° on the target

$\therefore$ Number of photons reaching a depth $x = N_o e^{-\mu\sqrt{2}x}$

$\therefore$ Number of K ionizations in a layer of thickness dx at depth $x = N_o e^{-\mu\sqrt{2}x} \tau_K dx$

$\therefore$ Number of Kα X-rays produced $= N_o e^{-\mu\sqrt{2}x} \tau_K dx \, p_\alpha$

where p_α is the probability of a Kα transition.

The number going off in a direction suitable for collection by the crystal ($\sim 45^\circ$) will be a constant fraction of this

$$= A N_o p_\alpha \tau_K e^{-\mu x} dx \qquad (A = \text{constant})$$

Let μ_α = total linear absorption coefficient of Kα X-rays in the target.

$\therefore$ Number of suitable Kα X-rays reaching the target surface from layer dx

$$= A p_\alpha N_o \tau_K e^{-(\mu+\mu_\alpha)\sqrt{2}x} dx$$

and the total number from all depths will be found by integrating from 0 to ∞ with the result

$$\frac{A p_\alpha N_o \tau_K}{(\mu+\mu_\alpha)\sqrt{2}}$$

A similar expression can be derived for Kβ_1, with p_β and μ_β replacing p_α and μ_α respectively and so the ratio of

$$K\alpha/K\beta_1 = \frac{p_\alpha(\mu+\mu_\beta)}{p_\beta(\mu+\mu_\alpha)}$$

Now p_α / p_β is the ratio given by Williams so we have to multiply this by a factor $\frac{\mu+\mu_\beta}{\mu+\mu_\alpha}$ which will be appreciably different from unity.

The value of μ will be an average value over the energy region from the K edge of the target element to the maximum exciting voltage of the tube and weighted according to the spectrum of the tube. This is not accurately known and hence to find accurate values for μ it is necessary to do absorption experiments with foils of each of the target elements.

However it is not necessary to know μ accurately. Since μ varies, very roughly, from 2 to 4 times μ_α or μ_β, $\frac{\mu+\mu_\beta}{\mu+\mu_\alpha}$ does not depend critically on μ. For example, unless the spectrum shape of the tube is quite abnormal we can say that the average μ for tin will <u>certainly</u> lie between 15 and 25 (the probable range is smaller).

Now for tin $\mu_\alpha = 11.6$

$\mu_\beta = 8.4$

i.e. $\frac{\mu+\mu_\beta}{\mu+\mu_\alpha}$ lies between 0.88 and 0.91 - a variation which is within the limits of experimental error.

Hence to find the correction factors $\frac{\mu+\mu_\beta}{\mu+\mu_\alpha}$ the spectrum of the tube running at 65 kilovolts was assumed to be similar to those found by Ulrey (1918) and the weighted mean of μ found for the various target elements. In certain cases the target material was a compound but the additional elements involved were always so light as to be ignored (oxygen usually). In two cases (tin and silver) the targets were thin foils and no correction

Table 3.1

A Element	B $K\alpha$	C $K\beta_1$	D Relative intensity on plate of α/β_1	E Actual Relative Intensity (Williams)	F Absorption correction	G $\frac{S(\beta_1)}{S(\alpha)}$	H $\log_{10}\frac{S(\beta_1)}{S(\alpha)} = R$	I Gradient of log curve $= \frac{R}{\beta_1 - \alpha}$
58Ce	34.58	39.25	4.98	4.67	1.11	0.85 ± 0.04	-0.071	-0.0152
56Ba	32.04	36.34	4.87	4.78	1.11	0.88 ± 0.04	-0.056	-0.0130
53I	28.50	32.29	4.90	4.90	1.12	0.89 ± 0.04	-0.051	-0.0134
50Sn	25.18	28.48	4.46	5.00	1.00	1.12 ± 0.04	0.049	-
49In	24.13	27.27	4.26	5.03	1.13	1.04 ± 0.04	0.017	-
48Cd	23.12	26.09	3.84	5.07	1.13	1.17 ± 0.04	0.068	-
47Ag	22.10	24.97	5.12	5.12	1.00	1.00 ± 0.04	0.000	0.0000
45Rh	20.17	22.75	4.07	5.21	1.15	1.11 ± 0.04	0.045	0.0176
42Mo	17.45	19.59	3.81	5.30	1.16	1.20 ± 0.05	0.079	0.0370
38Sr	14.15	15.84	3.22	5.54	1.16	1.48 ± 0.05	0.170	0.1008
35Br	11.91	13.3	2.86	5.86	1.18	1.74 ± 0.07	0.241	0.173
33As	10.53	11.7	2.56	6.14	1.20	2.00 ± 0.08	0.301	0.257
30Zr	8.63	9.55	1.66	6.92	1.22	3.42 ± 0.14	0.534	0.580

Notes on table 3.1

Columns B and C: Energies in Kev Column B: Weighted mean of α_1 and α_2. Column F: This is the factor $\frac{\mu + \mu_\alpha}{\mu + \mu_\beta}$

Column G: Sensitivity ratio obtained thus: $\frac{E}{D.F}$ The errors arise chiefly from errors in column D (estimated at 3 - 4% in most cases) and column F (2 - 3% in most cases).

was applied.

The relevant data are shown in table 3.1 and from this a curve was plotted from 0 to 40 Kev. As observed before there were two discontinuities - at 13.5 Kev and at 25.5 Kev.

It would be incorrect to say that the gradient of the log curve at the mean of two points which bridge a jump (e.g. indium $K\alpha$ = 24.1 Kev, $K\beta_1$ = 27.3 Kev) is equal to the average gradient between these points, for the term "average gradient" has no physical meaning in such a case. The log S-energy curve was therefore plotted in three sections ($E < 13.5$, $13.5 < E < 25.5$, $25.5 < E$) by the method indicated earlier. These three sections had to be fitted together. This can be done either by using elements whose α and β lines lie on either side of the edge or by direct measurement of the jump ratio. For the silver K edge there were three elements, 48 Cd, 49 In and 50 Sn, which were suitable, and a direct measurement was also made on a plate exposed to the continuous spectrum. This latter measurement gave a ratio of 1.27:1 which was consistent with the ratio deduced from the three $\alpha:\beta$ ratios.

For the bromine edge only a direct measurement was made - 1.105:1.

Curve Beyond 40 Kev.

Using the above results a curve can be plotted from about 8 - 40 Kev but to use this method beyond 40 Kev involves the use of rare earth elements which are difficult to obtain. However since the calculated curve suggests that the sensitivity falls

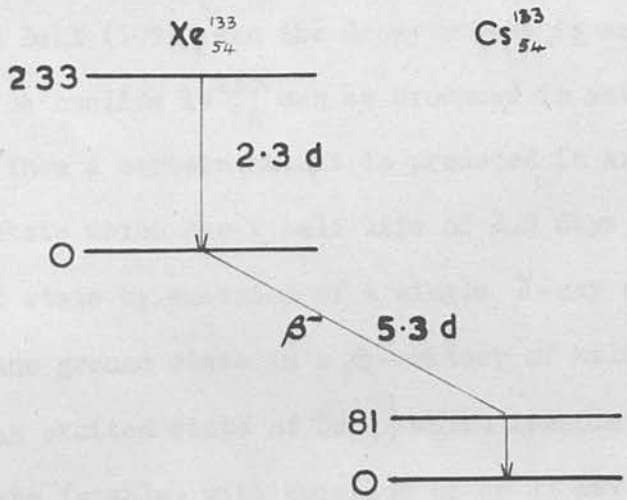

Fig 3.7 : Decay scheme of Xe^{133}. (energies in Kev)

off fairly smoothly above 40 Kev, it would be helpful if a measurement could be made on even one γ-ray source which has a line in the 40-100 Kev range and another in the 8-40 Kev range. The relative intensities of the two lines would have to be known, or measured in a different way.

Xenon 133 is suitable and a source of about one curie strength was obtained from A.E.R.E., Harwell.

Xe^{133} has been investigated by several authors, among them Bergström and Thulin (1950, 1951), Goldhaber and Hill (1952), Graham and Bell (1953), and the decay scheme is as shown in fig (3.7). The nuclide Xe^{133}_{54} can be produced in several ways but in all of them a certain amount is produced in an excited isomeric state which has a half life of 2.3 days and goes to the ground state by emission of a single γ-ray of energy 233 Kev. Xe^{133}_{54} in the ground state is a β-emitter of half life 5.3 days going to an excited state of Cs^{133}_{55} which immediately goes to the ground state (stable) with emission of an 81 Kev γ-ray.* By internal conversion of the 81 Kev γ-ray in the K shell the K fluorescent X-rays of Cs are emitted and since they have energy of about 31 Kev the ratio of K to γ would be a useful one for extending the calibration curve.

From the results of Graham and Bell (1953) who give the K internal conversion coefficient as 1.77 ± 0.15 the relative intensities of K X-rays and γ-ray can be calculated as 1.5 : 1

* The energy of the γ-ray was measured. See Chapter 7

with an error of about 10% due in part to uncertainty in the K fluorescence yield of Cs. This has been estimated as 0.85 ± 0.05, a value based on the results for 54 Xe of Auger (1925), Martin et al. (1937), West and Rothwell (1950), Bergström and Thulin (1950) and for 56 Ba of Backhurst (1936), and on the theoretical (non-relativistic) value of 0.88 for Cs.

The Xenon source used in this particular experiment was adsorbed on a piece of charcoal which was situated in a bulb blown at the end of a piece of glass capillary tube. The radiation was therefore absorbed by an unknown thickness of glass before reaching the spectrometer. This is unsatisfactory as the 1.5 : 1 ratio is for absolute intensities. Rather than estimate the thickness of glass it was decided to measure the relative intensities coming through the glass by another method.

This was done by Hughes (private communication) using a proportional counter (Argon filled) with pulse analyser. The ratio of K X-rays to δ-ray for this particular source unit was found to be 1.4 : 1 with an error of about 10% which is not inconsistent with the 1.5 : 1 ratio since the X-rays will be absorbed to a greater extent than the δ-ray. Hughes could not resolve the Cs K X-rays from any possible Xe K X-rays which could occur by internal conversion of the 233 Kev γ-ray. However the first plate obtained from the source using the crystal spectrometer showed that the Xe X-rays were certainly less than $\frac{1}{10}$ as intense as Cs X-rays. Since the intensity of Xe X-rays is halved in 2.2 days and that of Cs in 5.3 days the ratio obtained by Hughes,

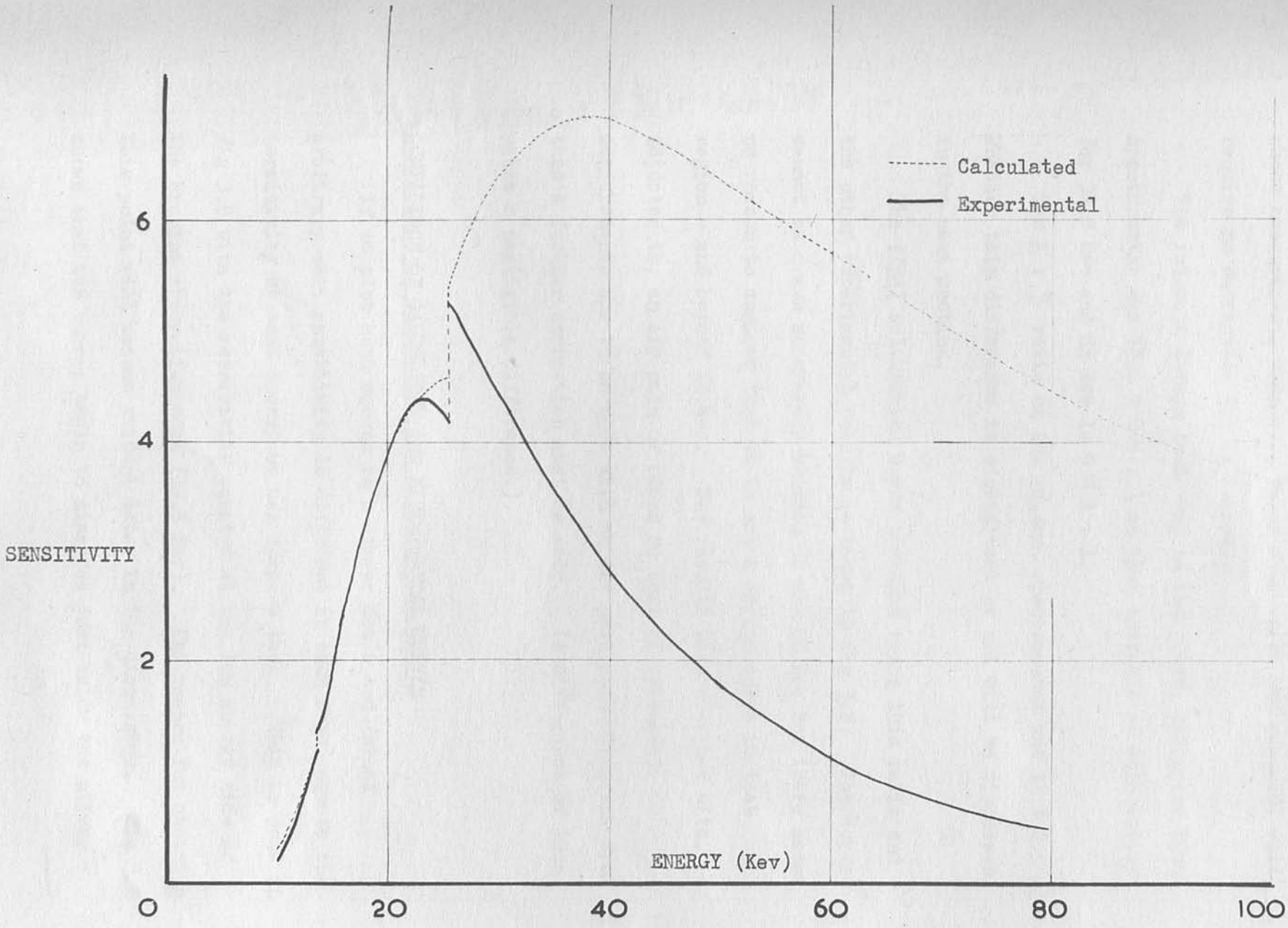

Fig 3.8 : Comparison of experimental and calculated calibration curves

whose measurements were made after four weeks had elapsed, will require no correction for Xe X-rays.

The ratio, K X-rays to γ -ray on the plate, using the 20cm. spectrometer was 12.6 ± 0.5 : 1 so that theratio of sensitivity for 31.5 Kev and 81 Kev is 9 ± 1 : 1.

The K : γ ratio on the 46.4cm. spectrometer was 11 ± 0.5 : 1. Whether this difference is significant or not will be discussed in the next section.

The final calibration curve obtained using this ratio and the other experimental results is shown in fig 3.8. The curve cannot be drawn accurately between 35 and 80 Kev but there seems no reason to suppose that it is not a smooth curve in that region - and beyond 80 Kev. The results were obtained with, or adjusted to, an air path of 60cms so that if intensity measurements are to be made with an air path much different from this a further correction must be made. (A difference of 10cm makes a negligible difference.)

COMPARISON OF CALCULATED AND EXPERIMENTAL CURVES

If we plot both curves on a linear scale and (since arbitrary unit sensitivity is different in each case) equate the sensitivity at some energy we can compare them. This is done in fig 3.8 with the sensitivity equated at the low energy side of the bromine absorption edge (13.5 Kev). The reason for choosing this point will become evident later in the discussion. Fig 3.8 shows that the curves begin to disagree just below the silver

edge and for energies above that are in violent disagreement. The reason for this is almost certainly that the reflecting power of the mica crystal decreases as the energy increases. No allowance was made in the calculation for such an effect.

The reflection coefficient for unbent crystals has been investigated both theoretically and experimentally by a number of authors - Darwin (1914), Allison (1927), Compton (1917), Bragg, James and Bosanquet (1921, 1922), Davis and Stempel (1921), Wagner and Kulenkampff (1922). Quantitative agreement between theory and experiment - and indeed between different experiments - is not good, but qualitatively it can be said that the reflection coefficient of the crystals investigated tends to increase with wave-length (i.e. as energy decreases). Very roughly most of the results suggest that the variation is with wave-length to a power near to, but not greater than unity. Particularly interesting in view of the shape of the curves in fig 3.8 are Wagner and Kulenkampff's results which show no significant variation with wave-length at wave-lengths greater than 1 A^{o} or so (energies less than 12.4 Kev).

Inspection of the two curves shows that they do agree quite well in the low energy region but at high energy, if the disagreement is caused purely by varying reflecting power, then this variation is more rapid than wave-length (1/E) to the first power. For example while the wave-length is multiplied by 2 (80 Kev - 40 Kev) the reflecting power increases by a factor 3.6.

This is not inconsistent with the previous results since in

this case we are dealing with reflections from a bent crystal. It is well known that the intensity of reflection of crystal planes depends to some extent on the mosaic structure (i.e. on the "degree of imperfection") of the crystal. It seems reasonable to suppose therefore that there are imperfections introduced when a crystal is bent and these alter not only the reflecting power but the way in which the reflecting power varies with wave-length. Lind, West and Dumond (1950) have investigated the reflection properties of the 310 planes of the bent quartz crystal used in their curved crystal spectrometer and find that for wave-lengths shorter than 0.5A^{o} (energy greater than 24.8Kev) the reflection coefficient varies approximately as λ^{2} $(1/E^{2})$, whereas for an unstressed crystal the variation is approximately as λ. They have not made any observations at wave-lengths greater than 0.5A^{o}. It appears that the reflecting power of the bent mica crystal does not vary with wave-length at energies below 20 Kev. Wagner and Kulenkampff's results give some support to this and while no theoretical investigation has been attempted it is conceivable that the power law variation could break down when the wave-length becomes comparable with the spacing between reflecting planes.

SELECTION OF BEST CURVE

Although the calculated curve makes no allowance for change in reflecting power it should not be immediately discarded. As we have seen from fig 3.8 the curves agree from about 12 - 22 Kev

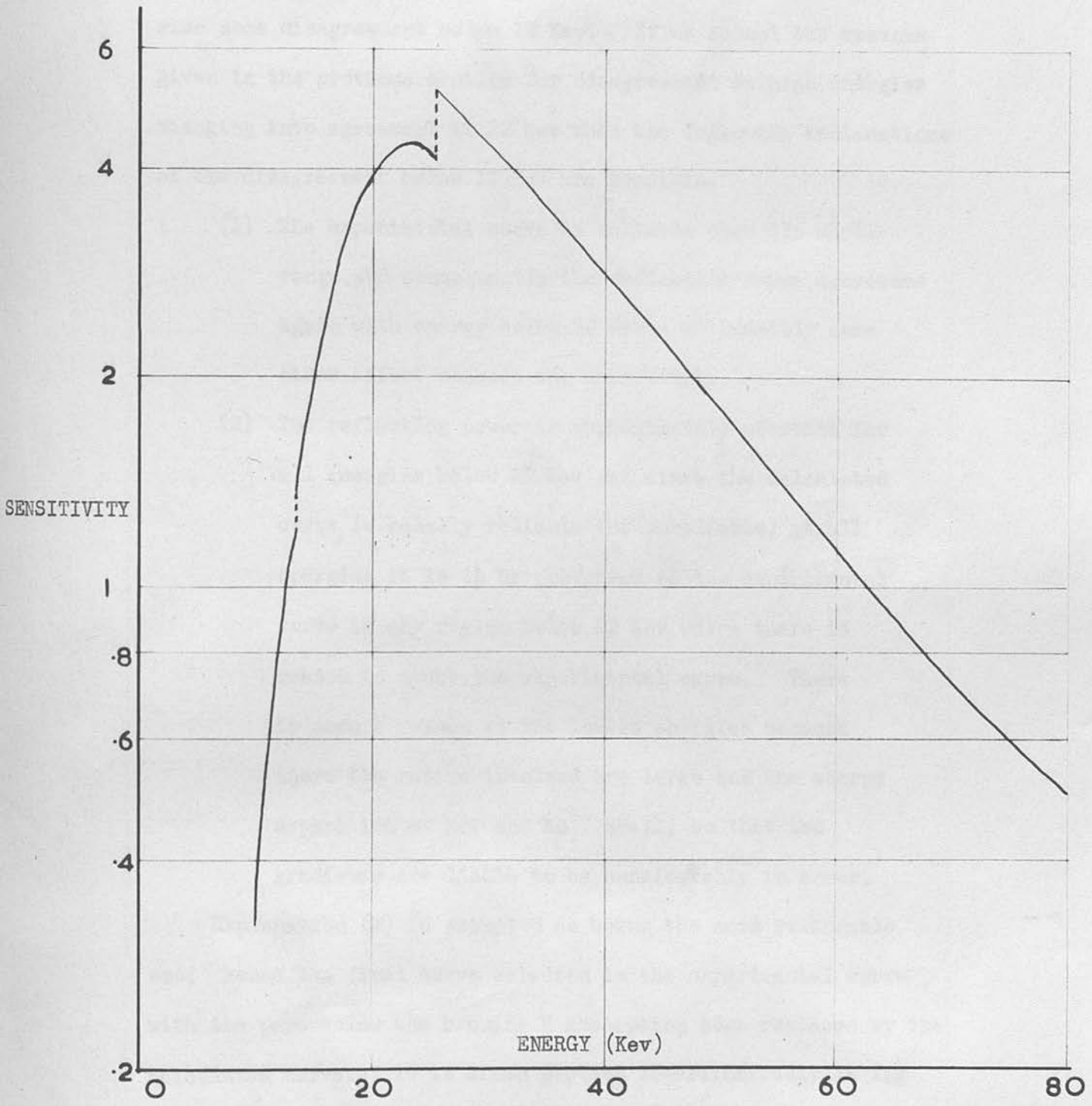

Fig 3.9 : "Best" curve representing sensitivity-energy relation for whole apparatus including an air path of 60 cm.

but in addition to the large disagreement above 22 Kev there is also some disagreement below 12 Kev. If we accept the reasons given in the previous section for disagreement at high energies changing into agreement at 22 Kev then the following explanations of the disagreement below 12 Kev are possible:

(1) The experimental curve is reliable over its whole range and consequently the reflecting power decreases again with energy below 12 Kev - or possibly some other effect reduces the sensitivity.

(2) The reflecting power is approximately constant for all energies below 22 Kev and since the calculated curve is equally reliable (or unreliable) at all energies it is to be preferred to the experimental curve in any region below 22 Kev where there is reason to doubt the experimental curve. There is such a reason at the lowest energies because there the ratios involved are large and the energy separation of $K\alpha$ and $K\beta$, small, so that the gradients are liable to be considerably in error.

Explanation (2) is accepted as being the more reasonable one; hence the final curve selected is the experimental curve with the part below the bromine K absorption edge replaced by the calculated curve. It is shown plotted logarithmically in fig 3.9.

EFFECT OF DIFFERENT CURVATURE OF THE CRYSTAL

If as Lind, West and Dumond suggest, a λ^2 law is obeyed for their quartz crystal (bent to 2 metres radius) and a λ law for an unstressed crystal, then there will be a range of curvature over which the variation will be as λ to powers between 1 and 2. It is therefore possible that with the mica crystal the reflecting power will fall off more rapidly with wave-length in the case of the 20 cm. radius crystal than in the case of the 46.4 cm. radius crystal. The Xe K X-ray to γ-ray ratio might then be smaller on plates exposed on the 46.4 cm. spectrometer than on the 20 cm. spectrometer. This is apparently confirmed by the results obtained - viz. 11 ± 0.5 and 12.6 ± 0.5 for large and small spectrometers respectively - but it is possible that the difference is not significant.

Hence the final curve shown in fig 3.9 applies to the 20 cm. spectrometer for all energies. It applies to the 46.4 cm. spectrometer for energies below about 25 Kev but for energies greater than that it might have to be slightly modified.

REFLECTING POWER OF MICA

The calibration curve which has finally evolved is believed to be the best obtainable from the available data. If we assume that the only large error in the first calculated curve is that caused by neglecting variation in reflecting power, then by comparing these two curves we can get some idea of how the reflecting power of mica bent to a radius of 20 cm. varies with

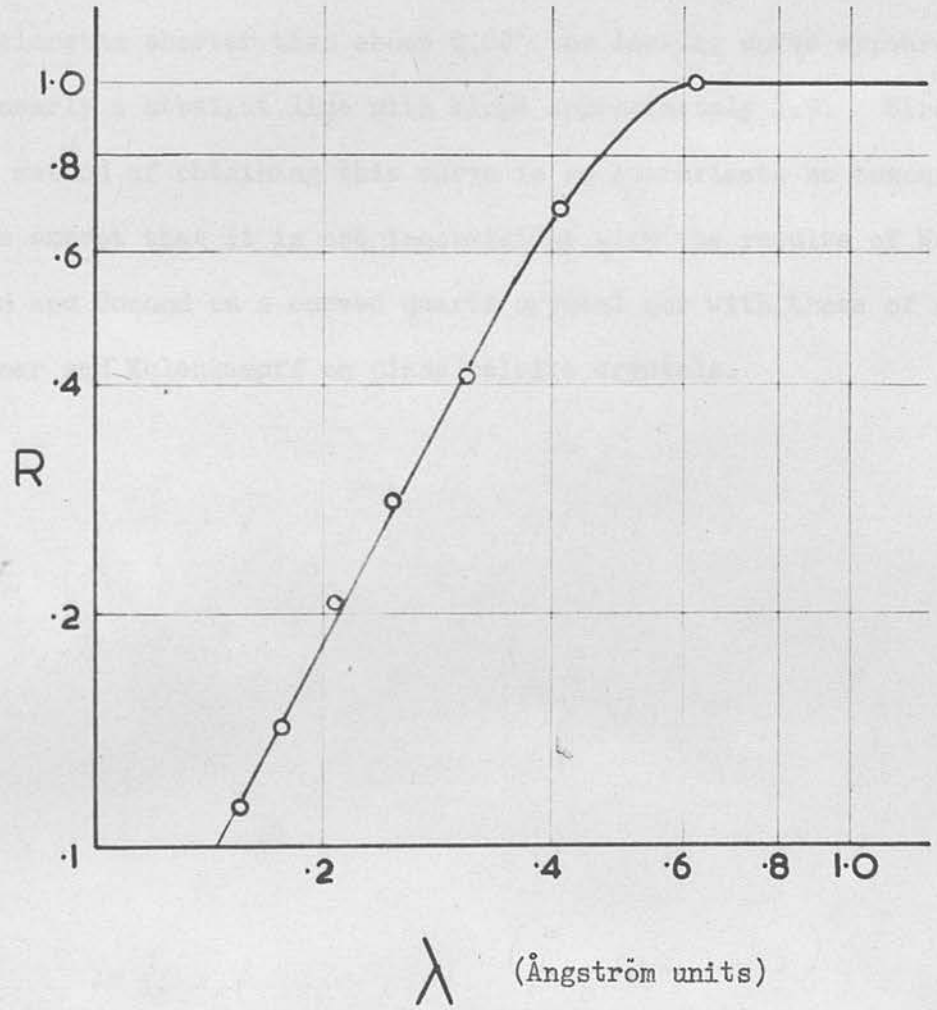

Fig 3.10 : Relation between reflecting power of the 100 planes of mica and wave-length

energy. This will be of no immediate practical importance as far as the present work is concerned but it may be of general interest in a field where many of the experimental results are not in good quantitative agreement. Fig 3.10 shows this variation plotted as log λ against log (reflecting power). At wavelengths shorter than about 0.6Å$^{\circ}$ the log-log curve appears to be nearly a straight line with slope approximately 1.9. Since the method of obtaining this curve is so approximate no comment is made except that it is not inconsistent with the results of West, Lind and Dumond on a curved quartz crystal nor with those of Wagner and Kulenkampff on plane calcite crystals.

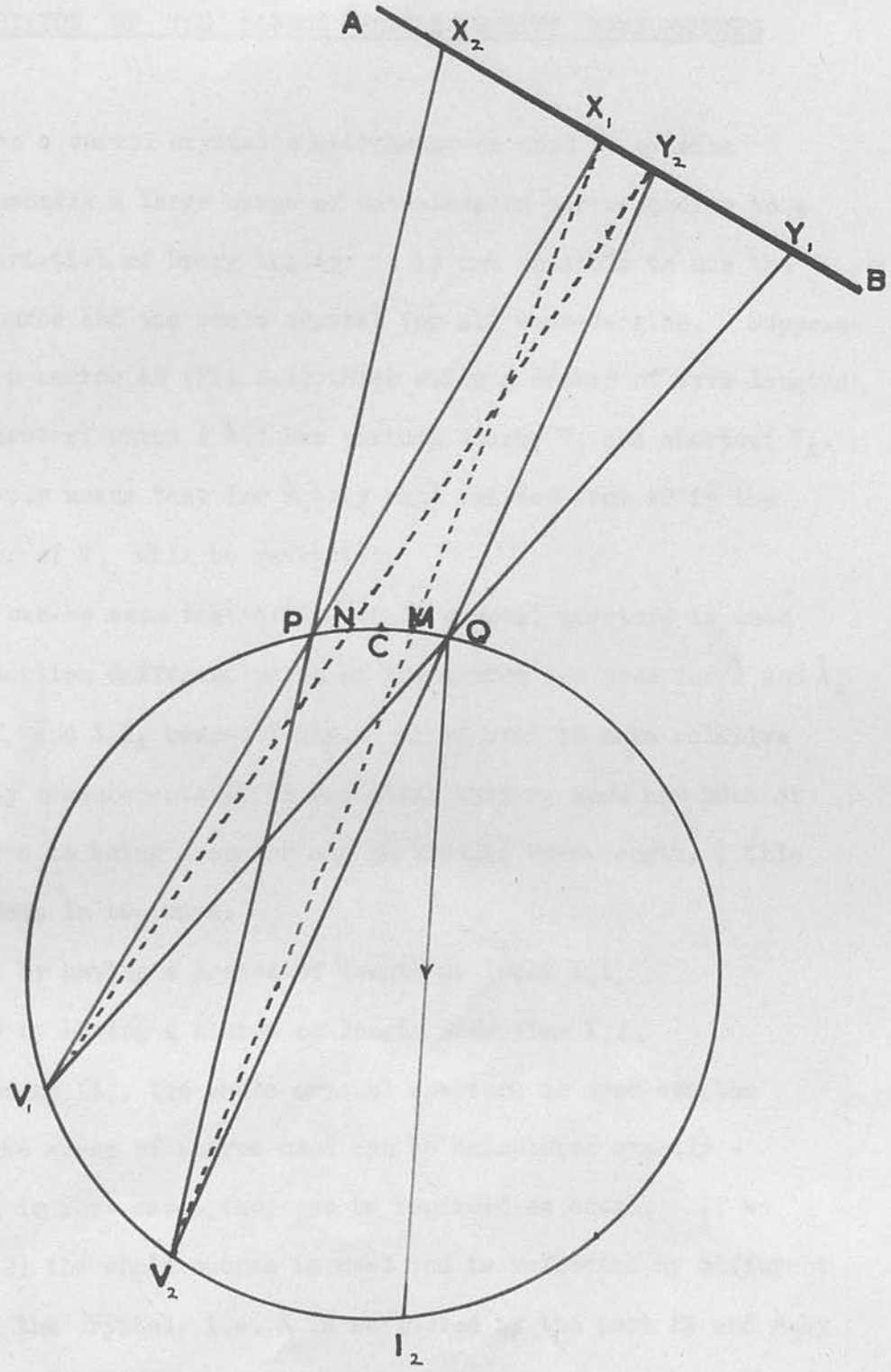

Fig 4.1 : Alternative source sizes for intensity measurements

CHAPTER 4

POSITION OF THE SOURCE FOR INTENSITY MEASUREMENTS

When a curved crystal spectrometer is used to examine simultaneously a large range of wave-lengths corresponding to a large variation of Bragg angles, it is not possible to use the whole source and the whole crystal for all wave-lengths. Suppose we have a source AB (Fig 4.1) which emits a number of wave-lengths the longest of which (λ_1) has virtual source V_1 and shortest V_2. This simply means that for λ_1 only rays emitted from AB in the direction of V_1 will be reflected.

It can be seen that if the whole crystal aperture is used for reflection different parts of the source are used for λ_1 and λ_2 viz. X_1Y_1 and X_2Y_2 respectively. If we want to make relative intensity measurements it is essential that we know how much of the source is being used for any particular wave-length. This can be done in two ways:

(1) by having a source of length at least X_2Y_1

(2) by having a source of length less than X_1Y_2

If we choose (1), the whole crystal aperture is used and the respective areas of source used can be calculated exactly - although in most cases they can be regarded as equal. If we choose (2) the whole source is used and is reflected by different parts of the crystal, i.e. λ_1 is reflected by the part PN and λ_2 by MQ.

There are two serious objections to (1):

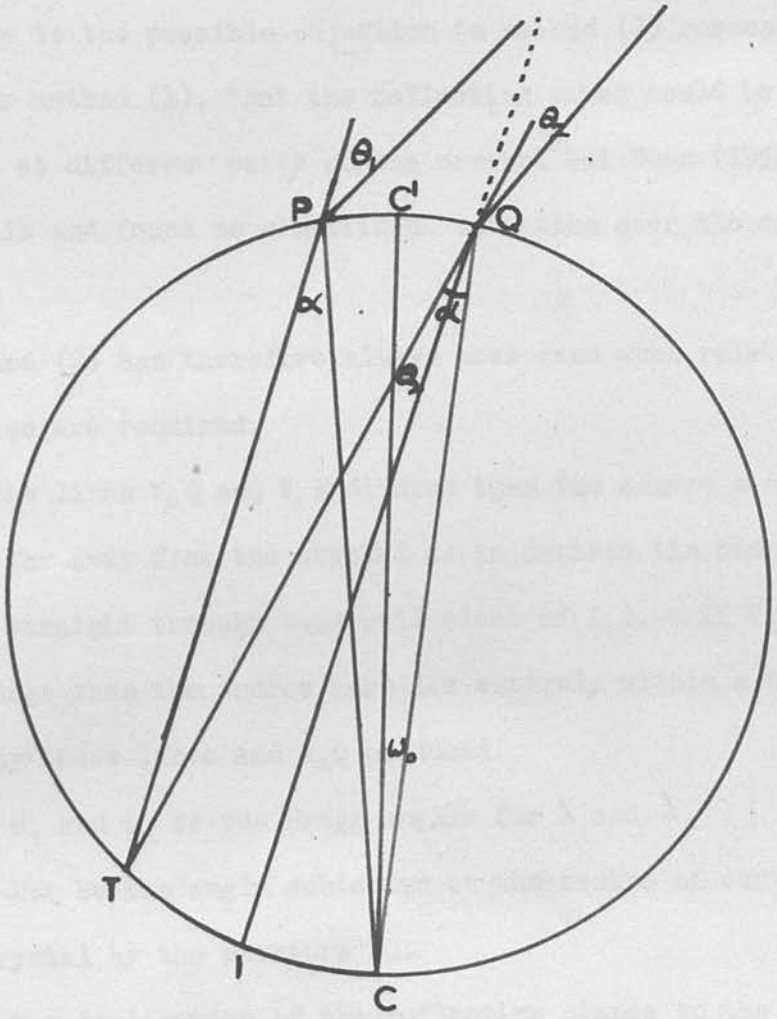

Fig 4.2 : Determination of source position

(a) No part of the source must be visible from I_2 and hence long sources are undesirable.

(b) The specific activity of the source would have to be the same over the whole source. A pin-hole photograph of the RaD source showed that this was not the case.

There is the possible objection to method (2) corresponding to (b) for method (1), that the reflecting power could be different at different parts of the crystal but Ewan (1952) has tested this and found no significant variation over the crystal aperture.

Method (2) has therefore always been used when relative intensities are required.

If the lines V_2Q and V_1P diverge then the source can be taken as far away from the crystal as is desired (in order to keep the straight through beam well clear of I_2). If V_2Q and V_1P converge then the source must lie entirely within a triangle bounded by these lines and I_2Q produced.

Let θ_1 and θ_2 be the Bragg angles for λ_1 and λ_2

Let $2\omega_o$ be the angle subtended at the centre of curvature, C, of the crystal by the aperture PQ.

Let α = inclination of the reflecting planes to the normal

C' = centre point of aperture.

From fig 4.2 it is seen that the angles that the three lines limiting the source position make with CC' are

Incident ray at P : $-\omega_o + \alpha + \theta_1$

Incident ray at Q : $\omega_o + \alpha + \theta_2$

Diffracted ray at Q : $\omega_o + \alpha - \theta_2$

ω_o and α are properties of the spectrometer and θ_1 and θ_2 depend on the wave-length range to be covered so by taking CC' and the tangent to the crystal surface at C' as axes these three lines can be drawn on squared paper and a suitable position for the source centre selected as a pair of co-ordinates.

The axis CC' is achieved in practice by a long brass tube which slides through a hole in a brass block and can be firmly clamped. The block is attached to the hard steel crystal clamping blocks by means of screws, which can be adjusted to make the tube accurately at right angles to the face of the steel block. A shorter brass tube is attached at right angles to the first and can also slide, thus supplying the other co-ordinate.

An error estimated at not more than 2 - 3 mm. in 100 cm. ($\sim \frac{1}{4}\%$) is possible in setting the co-ordinate system so whenever the wave-length range allowed it, the source was always placed so that its extremities were about one cm. clear of the two limiting lines. This was possible on every occasion except when measuring the relative intensity of the RaD 46.5 Kev γ-ray and RaE L γ X-rays.

CHAPTER 5

THE FLUORESCENCE YIELDS OF THE L LEVELS OF BISMUTH BY INTENSITY MEASUREMENTS ON THE RaD SPECTRUM

INTRODUCTION

The decay of RaD⟶RaE is very largely and possibly entirely by a single mode of β-disintegration with an end-point energy of 16 Kev leading to an excited state of the RaE nucleus. The de-excitation of this state takes place in a single stage by the emission of a γ-ray of energy 46.5 Kev. Other γ-rays have been reported by Tsien et al. (1946), Amaldi and Rassetti (1939), Salgueiro (1944), Frilley et al. (1951), Curran et al. (1949) and Cranberg (1950), but the results of these authors are somewhat conflicting and there are a like number who report no other transitions, Cork et al. (1951), Pringle (1951), Ross and Ewan (1953) and Kobayashi (1953) . None of these doubtful lines is of intensity comparable to the 46.5 Kev γ-ray except for one of about 7.3 Kev reported by Tsien et al., and Curran et al., but this has been accounted for by Wu et al. (1953) as copper K X-rays excited either in the counter or the source mounting. Hence for the purpose of this chapter it will be assumed that all other transitions except the 46.5 Kev one are negligible.

The γ-ray of this energy is highly converted in the L levels of RaE (Bi) and since the internal conversion coefficients for these levels can be estimated, a study of the relative intensities of the L X-ray spectrum will give some information about the

fluorescence yields. If sufficient additional data are available it will be possible to calculate completely the fluorescence, Auger and Coster-Kronig yields of the three L levels.

PREVIOUS WORK ON L FLUORESCENCE YIELDS

Direct measurements of the total fluorescence yield of the L shell were made for 21 elements in the range of Z from 40 to 92 by Lay (1934) using X-rays to excite the fluorescence and photographic film to record the intensities. Measurements of the fluorescence yields ω_1, ω_2 and ω_3, for the L_I, L_{II} and L_{III} levels, respectively, were made with ionization chambers by Küstner and Arends (1935) for seven elements between Z = 73 and Z = 83, but they took no account of the Coster-Kronig effect - namely the possibility of ionization being transferred from one L level to a higher L level (Coster and Kronig, 1935). Values of ω_3 are unaffected by this omission and if ionization transfers of the type $L_{II} \rightarrow L_{III}$ (N, O etc.) are of negligible intensity, values of ω_2 should also be unaffected. Measurements of ω_3 were also made by Stephenson (1937) for Pb, Th and U. His results are consistent with the corresponding ones of Küstner and Arends and this suggests that both sets of measurements for ω_3 are reliable.

Kinsey (1948a) calculated the values of ω_1, ω_2 and ω_3 for eight elements between Z = 73 and Z = 92 by estimating the radiation width of each sub-shell and dividing this by the total

width. His estimates were based on both theory and experiment and some simplifying assumptions were made. In a subsequent paper (Kinsey, 1948b) he published measurements of the absolute intensities of L X-rays excited by internal conversion of γ-radiation following the β-disintegration of the ThB, the α-disintegration of ThC and the β-disintegration of RaD. His results did not agree well with his calculations and he concluded that certain of his initial data were in error. A slight improvement was effected by modifying these data but agreement was still not good. Further experimental evidence would clearly be of value.

EQUATIONS GOVERNING THE FLUORESCENCE YIELDS

The equations formulated below are developments of those in Kinsey's first paper (1948a). They apply to the case where the primary ionization is produced by internal conversion of a single γ-ray but are easily adaptable to other methods of ionization by a suitable substitution for the phrase "per disintegration".

The following symbols are used:

n_1, n_2, n_3 : the numbers of primary ionizing events per disintegration in the $L_{\underline{I}}$, $L_{\underline{II}}$ and $L_{\underline{III}}$ levels respectively.

ω_1, ω_2, ω_3 : the fluorescence yields of the three L levels

a_1, a_2, a_3 : the Auger yields of the three L levels

f_{12}, f_{13}, f_{23} : the Coster-Kronig transition yields for transfer of ionization from the level represented by the first suffix to the level represented by the second suffix.

I, F, A : the total number per disintegration of L ionizations, L fluorescent quanta and L Auger electrons, respectively.

R : the total number of γ-ray quanta radiated per disintegration.

$1 : C_2 : C_3$: the relative numbers of primary ionizations in the three levels.

$1 : F_2 : F_3$: the relative numbers of L X-ray quanta from the three levels.

$1 : A_2 : A_3$: the relative numbers of Auger electrons from the three levels.

As in Kinsey's paper it is assumed here that the fluorescence yield of a given L level is independent of further ionizations in an M or higher level.

The following relations hold:

$$n_1 + n_2 + n_3 = I = A + F \tag{5.1}$$

$$\omega_1 n_1 + \omega_2(n_2 + f_{12} n_1) + \omega_3\left[n_3 + f_{13} n_1 + f_{23}(n_2 + f_{12} n_1)\right] = F \tag{5.2}$$

$$a_1 n_1 + a_2(n_2 + f_{12} n_1) + a_3\left[n_3 + f_{13} n_1 + f_{23}(n_2 + f_{12} n_1)\right] = A \tag{5.3}$$

$$n_1 = n_2/C_2 = n_3/C_3 \tag{5.4}$$

$$\omega_1 n_1 = \frac{\omega_2(n_2 + f_{12} n_1)}{F_2} = \frac{\omega_3\left[n_3 + f_{13} n_1 + f_{23}(n_2 + f_{12} n_1)\right]}{F_3} \tag{5.5}$$

$$a_1 n_1 = \frac{a_2(n_2 + f_{12} n_1)}{A_2} = \frac{a_3\left[n_3 + f_{13} n_1 + f_{23}(n_2 + f_{12} n_1)\right]}{A_3} \tag{5.6}$$

$$1 = f_{12} + f_{13} + \omega_1 + a_1 \tag{5.7a}$$

$$1 = f_{23} + \omega_2 + a_2 \tag{5.7b}$$

$$1 = \omega_3 + a_3 \tag{5.7c}$$

The problem is to determine the quantities represented by small letters when the quantities represented by capital letters are experimentally determined. The equations are however not independent; nor are they sufficient. There are twelve unknowns, the n's, the ω's, the a's and the f's, and of these, three (the n's) refer to primary ionization and nine are independent of this process. There are eight independent quantities (I, C_2, C_3, F, F_2, F_3, A_2 and A_3 - A being dependent on I and F) which can be determined by experiment or otherwise estimated, and three of these (I, C_2, C_3) allow the n's to be calculated. This leaves five determinable quantities and three identities (equations 5.7) for the calculation of the nine coefficients of de-excitation.

Substituting from equation (5.5), equation (5.2) becomes

$$\omega_1 n_1 (1 + F_2 + F_3) = F$$

Multiplying both sides by $1 + C_2 + C_3$ and using (5.1) and (5.4)

$$\omega_1 = \frac{F}{I} \cdot \frac{1 + C_2 + C_3}{1 + F_2 + F_3} \qquad (5.8a)$$

A similar consideration of equation (5.6) yields

$$a_1 = \frac{I - F}{I} \cdot \frac{1 + C_2 + C_3}{1 + A_2 + A_3} \qquad (5.8b)$$

(5.5) and (5.6) give $\frac{\omega_1}{a_1} = \frac{\omega_3 A_3}{a_3 F_3}$ and by

(5.7c) $a_3 = 1 - \omega_3$ so that substituting for ω_1 and a_1 from (5.8) gives

$$\frac{1}{\omega_3} = 1 + \frac{I - F}{F} \cdot \frac{A_3}{F_3} \cdot \frac{1 + F_2 + F_3}{1 + A_2 + A_3} \qquad (5.9a)$$

$$\left(\text{i.e. } 1 + \frac{A_3}{F_3} \cdot \frac{a_1}{\omega_1}\right)$$

and similarly

$$\frac{1}{a_3} = 1 + \frac{F}{I - F} \cdot \frac{F_3}{A_3} \cdot \frac{1 + A_2 + A_3}{1 + F_2 + F_3} \qquad (5.9b)$$

$$\left(\text{i.e. } 1 + \frac{F_3}{A_3} \cdot \frac{\omega_1}{a_1}\right)$$

To proceed it is necessary to acquire an additional source of experimental information or to introduce a simplifying assumption. The assumption $f_{23} = 0$ is mathematically convenient and not likely to be much in error since transitions of the type $L_{II} \longrightarrow L_{III}$ M are energetically impossible for $30 < Z < 90$.

Adopting this assumption (5.7b) reduces to $1 = \omega_2 + a_2$ and we can proceed to find ω_2 and a_2 exactly as for ω_3 and a_3.

$$\frac{1}{\omega_2} = 1 + \frac{I - F}{F} \cdot \frac{A_2}{F_2} \cdot \frac{1 + F_2 + F_3}{1 + A_2 + A_3} \qquad (5.10a)^*$$

$$\left(1 + \frac{A_2}{F_2} \cdot \frac{a_1}{\omega_1}\right)$$

$$\frac{1}{a_2} = 1 + \frac{F}{I - F} \cdot \frac{F_2}{A_2} \cdot \frac{1 + A_2 + A_3}{1 + F_2 + F_3} \qquad (5.10b)^*$$

$$\left(1 + \frac{F_2}{A_2} \cdot \frac{\omega_1}{a_1}\right)$$

* Valid only if $f_{23} = 0$

Then from equation (5.4) and (5.5) in terms of (5.8a) and (5.10a) we obtain

$$f_{12} = \frac{\omega_1 F_2}{\omega_2} - C_2 \qquad (5.11)^*$$

$$f_{13} = \frac{\omega_1 F_3}{\omega_3} - C_3 \qquad (5.12)^*$$

If no assumption is made about f_{23} a second set of experimental data is required with the ratio of primary ionizing events in the three L levels different from $n_1 : n_2 : n_3$. In this particular case this is easily achieved by bombarding a target of bismuth with X-rays. In general this procedure is not possible unless a stable isotope is available.

In the following, dashed letters will be used to represent the second set of experimentally determined quantities, and also to distinguish duplicated values of the coefficients of de-excitation obtained by using these quantities.

By combining the two sets of results (using (5.5) and (5.4)) we then have

$$\omega_2 = \frac{\omega_1 F_2 - \omega_1' F_2'}{C_2 - C_2'} \qquad (5.13a)$$

$$f_{12} = \frac{C_2 \omega_1' F_2' - C_2' \omega_1 F_2}{\omega_1 F_2 - \omega_1' F_2'} \qquad (5.14a)$$

* Valid only if $f_{23} = 0$

Similarly using (5.6 and (5.4)

$$a_2 = \frac{a_1 A_2 - a_1' A_2'}{C_2 - C_2'} \qquad (5.13b)$$

$$f_{12} = \frac{C_2 a_1' A_2' - C_2' a_1 A_2}{a_1 A_2 - a_1' A_2'} \qquad (5.14b)$$

These results enable f_{13} to be obtained from (5.7a) and f_{23} from (5.7b) thus completing the solution of the problem. It can be seen that full duplication of all experimentally determined quantities would provide duplicated values of six of the coefficients (ω_1, a_1, ω_3, a_3, f_{12}, f_{13}) and a single value for the remaining three.

So far no account has been taken of the relative accuracy of the experimental information. It is unlikely that it will all be of the same accuracy and in this particular investigation it will be seen that the values of A_2 and A_3 are difficult to determine with precision. A_2 and A_3 are not involved in the calculation of ω_1, ω_2 and f_{12} from equations (5.8a) (5.13a) and (5.14a) respectively, but they are involved in the calculation of a_1 and ω_3 by equations (5.8b) and (5.9a) and hence in the determination of a_3 and f_{13} using (5.7c) and (5.7a). It is however possible to determine experimentally the ratio $A_3/(1 + A_2)$ more accurately than either A_2 or A_3, so that ω_3 and a_3 will be less in error than a_1 and f_{13}. The coefficients a_2 and f_{12} will be particularly unreliable as they require two sets of Auger intensities

[Equation (5.13b) and (5.14b)] and as f_{23} is calculated from a_2 using equation (5.7b) it will also be unreliable. f_{23} can be calculated alternatively from the relation

$$f_{23} = \frac{\omega_1 F_3/\omega_3 - C_3 - f_{13}}{C_2 + f_{12}} \qquad (5.15)$$

which is obtained from equation (5.5) and(5.4). This may, in favourable circumstances, give a smaller error than the other method of finding f_{23}.

EXPERIMENTAL VALUES FOR BISMUTH

The quantities which we require to determine experimentally are therefore C_2, C_3, F_2, F_3, A_2, A_3 (possibly $\frac{A_3}{1 + A_2}$) and the ratio F/I, with the corresponding dashed quantities. Of these F_2, F_3 and, using auxiliary information, F/I can be measured with the present spectrometer. The remaining quantities (C_2, C_3, A_2, A_3) must be deduced from other experiments or theory.

F_2 and F_3

The energies of the important L X-rays emitted by RaE after internal conversion of the 46.5 Kev γ-ray range from 10.72 Kev (α_2) to 16.27 Kev (γ_4). For this energy range it is easily possible to expose the source at full aperture on the 20 cm. spectrometer, the angles $-\omega_0+\alpha+\theta_1$ and $\omega_0+\alpha+\theta_2$ (See chapter 4) being respectively 0.369 and 0.389 radians for 10.7 Kev and 16.3 Kev.

The RaD source which was obtained from the Radio-chemical

Centre at Amersham consisted of approximately 80 mc. of RaD deposited anodically on a platinum foil 1.5 cm. by 1 cm. The source was covered by a sheet of aluminium of thickness 6.3 mgm. per square cm.

To prevent undue fogging of the G5 nuclear plate a collimating system of lead baffles described by Ewan (1952) was employed. The apertures in the three baffles were just wide enough to allow radiation from any part of the source to impinge on any part of the crystal aperture. The inside of the collimator was lined with thin aluminium sheet covered with paper to absorb as much as possible of the lead L X-rays produced when the γ-rays strike the walls of the collimator.

High energy β-rays are harmful to the crystal and must therefore be deflected or absorbed before reaching it. No suitable magnetic field was available for deflecting β-rays of energy up to 1.2 Mev (end point energy for RaE β-rays) so they were absorbed in a wad of filter paper of thickness 0.45 gms. per $cm.^2$ placed inside the collimator at a distance of about 8 cm. from the source - i.e. about half way along the collimator.

(It should not be placed at the source end of the collimator for then γ-rays suffering wide angle Compton scattering would be contained in the beam reaching the crystal; nor should it be placed at the exit end of the collimator for scattered radiation would then escape out of the beam and cause fogging of the plate.)

An exposure of about three weeks was given and the microphotometer trace obtained from the plate is shown in fig 5.1.

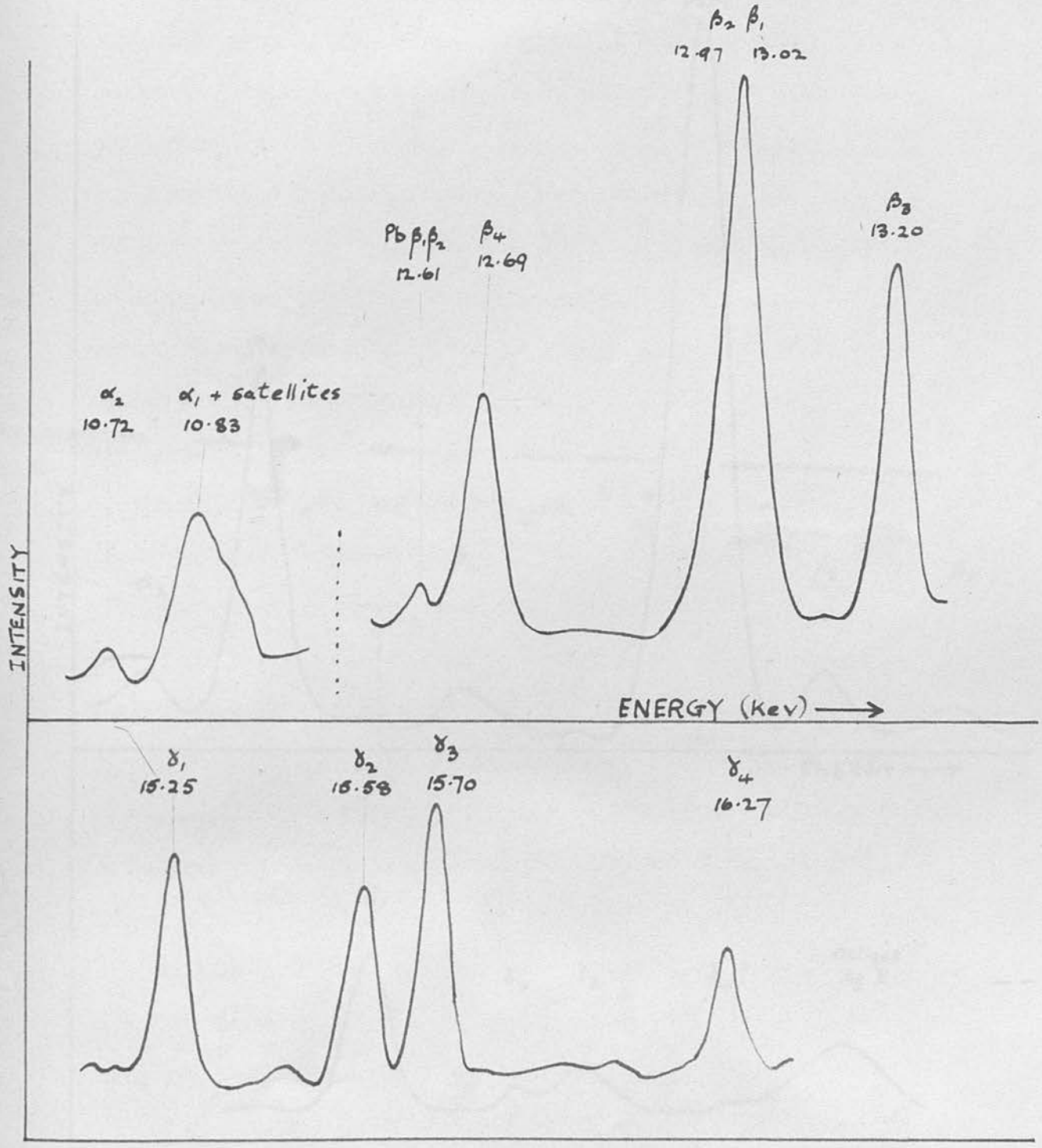

Fig 5.1 : Microphotometer trace of RaE L X-rays

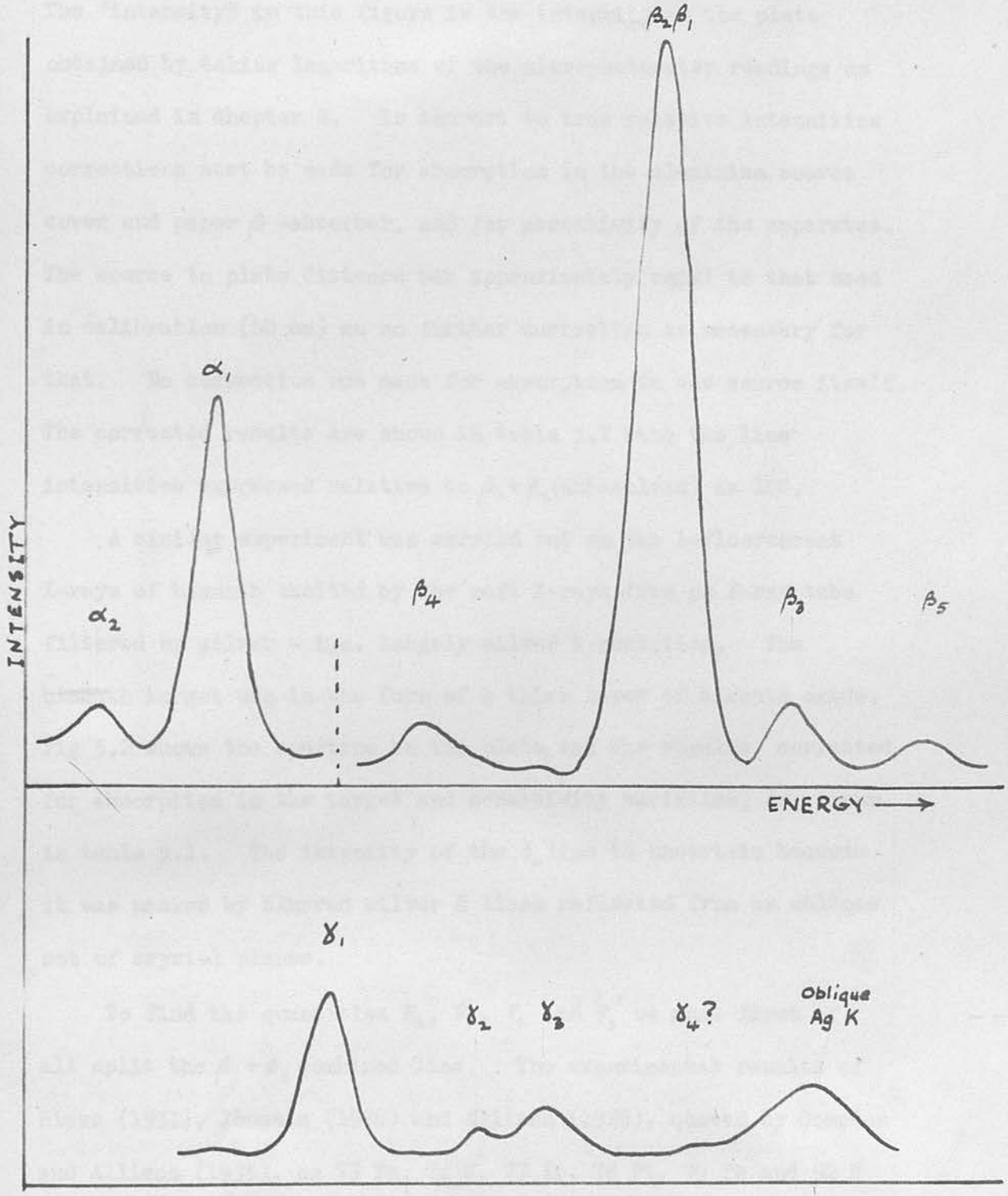

Fig 5.2 : Microphotometer trace of Bi L X-rays (fluorescent excitation)

The "intensity" in this figure is the intensity on the plate obtained by taking logarithms of the microphotometer readings as explained in chapter 2. To convert to true relative intensities corrections must be made for absorption in the aluminium source cover and paper β -absorber, and for sensitivity of the apparatus. The source to plate distance was approximately equal to that used in calibration (60 cm) so no further correction is necessary for that. No correction was made for absorption in the source itself. The corrected results are shown in table 5.1 with the line intensities expressed relative to $\beta_1 + \beta_2$(unresolved) as 100.

A similar experiment was carried out on the L-fluorescent X-rays of bismuth excited by the soft X-rays from an X-ray tube filtered by silver - i.e. largely silver K radiation. The bismuth target was in the form of a thick layer of bismuth oxide. Fig 5.2 shows the spectrum on the plate, and the results, corrected for absorption in the target and sensitivity variation, are shown in table 5.1. The intensity of the γ_4 line is uncertain because it was masked by blurred silver K lines reflected from an oblique set of crystal planes.

To find the quantities F_2, F_3, F_2' and F_3' we must first of all split the $\beta_1 + \beta_2$ combined line. The experimental results of Hicks (1931), Jönsson (1926) and Allison (1928), quoted by Compton and Allison (1935), on 73 Ta, 74 W, 77 Ir, 78 Pt, 90 Th and 92 U were used as auxiliary data. Since α_1 and β_2 originate from the same subshell, L_{III}, their relative intensities will be independent of the method of excitation. Taking a value of 0.248 for β_2/α_1

Table 5.1 : Relative Intensities of L X-ray lines of Bi.

Line	Transition	Intensity	
		RaD Disintegration	Fluorescent Excitation
α_2	$L_{III} - M_{IV}$	15	14.3
α_1	$L_{III} - M_V$	151	122
β_4	$L_I - M_{II}$	40	7.2
β_2	$L_{III} - N_V$	(37)	(29)
		100	100
β_1	$L_{II} - M_{IV}$	(63)	(71)
β_3	$L_I - M_{III}$	39	7.8
β_5	$L_{III} - O_{IV,V}$	3	4.4
γ_1	$L_{II} - M_{IV}$	10.8	12.5
γ_2	$L_I - N_{II}$	8.5	1.9
γ_3	$L_I - N_{III}$	10.8	2.7
γ_4	$L_I - O_{III}$	3.7	0.5

the intensities of β_1 and β_2 become respectively 63 and 37 by RaD disintegration and 71 and 29 by fluorescent excitation.

These values are consistent with other intensities for if we accept the value for β_1 the ratio β_1/γ_1 (which should be the same for both methods of excitation) is 5.7 for RaD disintegration and 5.8 for fluorescent excitation. Furthermore gold L X-rays were excited in the same way as bismuth L, and the results indicate that the ratio 71 : 29 for fluorescent excitation is not much in error. (The gold results cannot give definite confirmation

because, though β_1 and β_2 are resolved, β_2 and β_3 are not.) The β_5 line was not observed in the case of the RaD disintegration. A value of 3 was allotted by a similar argument to that used for separating β_1 and β_2.

The total intensities of radiation from the L_I, L_{II} and L_{III} shells are shown in table 5.2. These are compared with data obtained from the results of Frilley et al. (1951). As a further comparison the relative intensities of the $L\alpha$, $L\beta$ and $L\gamma$ groups measured by Wu et al. (1953) and Hughes (1955) are also shown in table 5.2. Wu et al. made their observations with a proportional counter with krypton and methane filling and Hughes used a proportional counter with pure argon filling. Agreement

Table 5.2: Relative Intensities of Groups of L X-ray lines from Bi.

	RaD Disintegration		Fluorescent Excitation	
	Cochran	Frilley	Cochran	Frilley
L_I	102	94	20	19.2
L_{II}	74	78	84	85
L_{III}	206	211	170	191

	Cochran	Frilley	Hughes	Wu	Cochran	Frilley	Hughes
$L\alpha$	166	170	1.00	1	136	159	1.00
$L\beta$	182	175	1.13	1	119	121	0.98
$L\gamma$	34	38	0.23	0.2	18	15.2	0.19

with the other three sets of results is considered satisfactory and consequently values of F_2, F_3, F_2' and F_3' have been calculated from the present results. They are:

$F_2 = 0.73 \pm 0.05$ $\qquad$ $F_3 = 2.02 \pm 0.2$

$F_2' = 4.20 \pm 0.3$ $\qquad$ $F_3' = 8.5 \pm 0.8$

Hence

$F_2'/F_2 = 5.8 \pm 0.6$ $\qquad$ $F_3'/F_3 = 4.2 \pm 0.6$

$F_3/F_2 = 2.8 \pm 0.3$ $\qquad$ $F_3'/F_2' = 2.0 \pm 0.2$

The errors quoted are reasonable estimates arising mainly from the sensitivity calibration.

Value of F/I

For the case of excitation by soft X-rays we have F/I = 0.402 as determined by Lay (1934).

For the RaD disintegration there is more doubt about the best value. An absolute determination of F by Stahel (1935) gave 0.252 per disintegration and more recent (though probably less reliable) measurements are 0.30 (Gray 1932), 0.27 (Tsien 1944) and 0.19 $\pm$ 0.03 (Damon and Edwards 1954). Two methods have been chiefly employed to measure I - comparison of the total L-conversion intensity with the total intensity of the RaE continuum, or determination of the absolute intensity of L-conversion and the absolute intensity of the source. Results are shown in table 5.3. Butt and Brodie consider their value of I to err on the low side on account of overcorrection for back-scattering in the source.

Table 5.3: Values of I and F/I for RaD disintegration

	Method	I per disintegration	F/I	
Cranberg (1950)	Absolute source strength	0.54	0.465	
Butt & Brodie (1951)	RaE	0.467	0.54	F from
Wu et al.(1953)	RaE	0.64	0.393	Stahel
Bashilov et al. (1953)	RaE	0.45 ± 0.02	0.56	
Kinsey (1948)	Calculation		0.41	
"	Final estimate		0.47	

An alternative method of determining F/I for the RaD disintegration is through the ratios F/R and R/I separately determined. R/I is the reciprocal of the internal conversion coefficient the data for which are given in the next section (table 5.4). The theoretical value is considered to be better than any experimental value at present available and consequently R/I is taken as 0.056.

F/R was determined by comparing the total L X-ray intensity with the intensity of the 46.5 Kev γ-ray. It is not possible to have the γ-ray and the complete L X-ray spectrum simultaneously at full aperture, but by turning the source through 90°, thus effectively reducing its length to 1 cm., it is just possible to

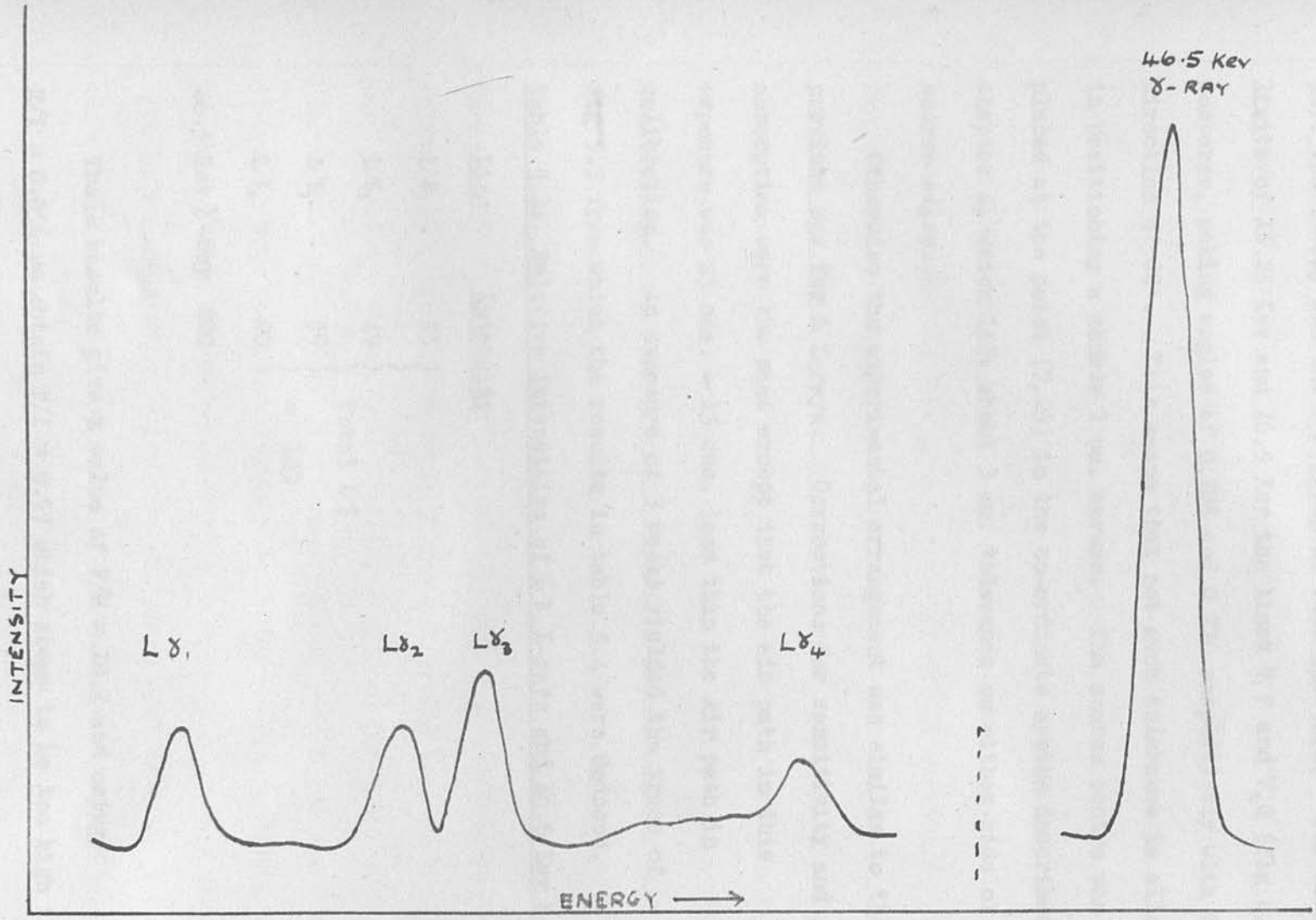

Fig 5.3 : Microphotometer trace of RaD 46.5 Kev γ -ray and RaE Lδ X-rays

have the γ-ray and the L γ group at full aperture. For energy limits of 15.25 Kev and 46.5 Kev the lines V, P and V_2Q (fig 4.1) converge, making angles of 0.286 and 0.276 respectively with the direction of CC'. This means that not much tolerance is allowed in positioning a source 1 cm. across. The source centre was placed at the point (7,25) in the co-ordinate system described in chapter 4, which left about 3 mm. tolerance on either side of the source edges.

Otherwise the experimental arrangement was similar to the previous one for L X-rays. Corrections for sensitivity and absorption were the same except that the air path in this exposure was 45 cms. - 15 cms. less than the air path in calibration. An exposure of 3 weeks yielded the trace of fig 5.3 from which the results in table 5.4 were deduced.

Table 5.4: Relative Intensities of L γ X-rays and 46.5 Kev γ-ray.

Line	Intensity	
L γ_1	55	Total L γ = 183
L γ_2	49	
L γ_3	59	
L γ_4	20	
46.5 Kev γ-ray	200	

These results give a value of F/R = 10.2 and using R/I = 0.056 we obtain F/I = 0.57 which seems to be too high in view of the results in table 5.3. The error involved in comparison of L γ with γ-ray is estimated at 15% and this makes

the total error in the ratio F/R a little less than 20% giving $F/I = 0.57 \pm 0.11$.

Other values of F/R by direct comparison (using a proportional counter and pulse analyser) are 6.74 ± 0.5 (Hughes 1955) and 4.4 ± 0.7 (Wu et al. 1953). Damon and Edwards (1954) used a scintillation spectrometer to make absolute determinations of $F = 0.19 \pm 0.03$ and $R = 0.044 \pm 0.003$ and hence $F/R = 4.3 \pm 0.9$. The last two of these results give a value of F/I of about 0.25 while the determination of Hughes gives $F/I = 0.38 \pm 0.03$.

We thus have values of F/I ranging from 0.25 to 0.57. The former seems clearly too low to be reconciled with the data in table 5.3. The latter agrees with Bashilov et al. but is not in good agreement with any of the other values (remembering that Butt and Brodie's value is considered too high) although reasonable agreement is achieved near the lower limit of the large error. It will be seen when we come to calculate the yields that a value of about 0.40 for F/I is the most acceptable one, though the yields will also be calculated for $F/I = 0.57$. This means that we shall obtain two sets of yields for the first of which, only the measurements made on the L X-ray spectrum with the curved crystal spectrometer will be used. All other data will be obtained elsewhere. For the second set both the L X-ray and the γ-ray measurements with the spectrometer will be used.

The Remaining Experimental Quantities

Best values for remaining experimental quantities (C_2, C_3, A_2 and A_3) are deduced by Ross, Cochran, Hughes and Feather (1955). The following is an abbreviated account.

C_2 and C_3:

The results of recent work on the relative intensities of conversion of the 46.5 Kev γ-ray in Bi following β-disintegration of RaD are shown in table 5.5 together with theoretical values taken from the tables of internal conversion coefficients for magnetic dipole radiation given by Rose et al. (private communication) for the L_I and L_{II} levels, and by Gellmann et al (1952) for the L_{III} level. Agreement between theory and experiment is reasonably good except that the measured L_{III} intensity is considerably higher than the theoretical value.

*** See note overleaf.

Table 5.5 : Relative Intensities of Conversion of the RaD γ-ray in the L levels of Bi.

Level of conversion	Cranberg (1950)	Wu et al. (1953)	Bashilov et al. (1953)	Theoretical M 1	
				Relative	Absolute
L_I	100	100	100	100	16.3
L_{II}	9 ± 1.5	7.5 ± 0.5	15 ± 3	8.9	1.45
L_{III}	1.9 ± 0.4	0.7 ± 0.3	0.86 ± 0.05	0.13	0.022

There are at least two possible reasons for this, (i) that there could be a small amount of electric quadrupole radiation, and (ii) under the conditions of experiment a small amount of

***

Since writing this, recent calculated values of L_{III} internal conversion coefficients for M 1 radiation and Z = 85 have come to hand. Rose (private communication) did not issue these because of disagreement with the results of Gellman et al. It is believed now that Rose's results are correct and they give the L_{III} conversion for the 46.5 Kev γ-ray in Bismuth as about five times the figure quoted in table 5.5. This brings the relative intensity of conversion for L_{III} to about 0.65 which is in much better agreement with the experimental values. This change in value for C_3 has however negligible effect on the values of the yields since C_3 is in any case much smaller than f_{13} and $1 + C_2$.

external conversion in Pb is mistaken for internal conversion. However, no matter what value is accepted for C_3 it will be much smaller than f_{13} and $1 + C_2$ so that variations in it are unimportant. Hence the theoretical values are adopted

$$C_2 = 0.089 \pm 0.002, \quad C_3 = 0.0013.$$

For the case of L ionization by soft X-rays experimental values of the relative intensities of ionization are given by Robinson and Young (1930) but complete data are found in their work only for gold. They find ionization (produced by silver Kα X-rays) proportional to 3.5, 5.3 and 8.5, in the L_I, L_{II} and L_{III} levels respectively, giving $C_2' = 1.5$ and $C_3' = 2.4$.

The relative intensities of ionization can also be estimated from the "absorption jump" ratios. Relative intensities obtained in this way for Bi are 1 : 1.7 : 2.6 (Patten 1934), 1 : 2.1 : 2.26 (Carr 1934), and 1 : 1.77 : 2.74 (Küstner and Arends 1935). The crude theoretical ratio of 2 : 3 for L_{II} and L_{III} ionization agrees with all of these results except that of Carr. Taking a mean of the others gives $C_2' = 1.66 \pm 0.15$ and $C_3' = 2.6 \pm 0.2$.

A_2 and A_3:

High resolution electron spectrometer studies of the L Auger electrons of RaD have been made by Kobayashi (1953) and by Bashilov et al. (1953). Kobayashi gives an analysis of the line intensities after applying a correction for absorption in the source and estimating the level of the background. Ross (1955) has analysed the spectrum of Bashilov et al., and she

concludes that allowing for the latters' higher resolution at energies below about 6 Kev the two analyses give essentially the same results. They are shown in table 5.6.

From the data in this table Ross makes an approximate analysis of the relative intensities arising from the individual subshells. This is shown in table 5.7. From this she concludes that the ratio $\frac{A_2}{1 + A_2} = 1.3 \pm 0.2$ and less confidently $1 < A_2 < 2.5$.

Table 5.6: Relative Intensities of Auger Electron Bands

	Kobayshi	Bashilov et al. (analysis by Ross)
$L_{III} \longrightarrow MM$ + small part $L_{II} \longrightarrow MM$	26.5	25.4
part $L_{II} \longrightarrow MM$ + part $L_I \longrightarrow MM$ + $L_{III} \longrightarrow M(N,O)$	21	21
part $L_I \longrightarrow MM$ + small part $L_{II} \longrightarrow M(N,O)$	4	4.7
part $L_{II} \longrightarrow M(N,O)$ + part $L_I \longrightarrow M(N,O)$	6	6.2
part $L_I \longrightarrow M(N,O)$ + $L_{III} \longrightarrow N(N,O)$	3	2.65
$L_{II} \longrightarrow N(N,O)$ + $L_I \longrightarrow N(N,O)$		0.95

Table 5.7: Approximate Auger Intensities from the Three Subshells

$L_{III} \longrightarrow MM$	25	$L_{III} \longrightarrow M(N,O)$	7	$L_{III} \longrightarrow N(N,O)$	2
$L_{II} \longrightarrow MM$	12	$L_{II} \longrightarrow M(N,O)$	4-	$L_{II} \longrightarrow N(N,O)$)	0.95
$L_I \longrightarrow MM$	7	$L_I \longrightarrow M(N,O)$	2+	$L_I \longrightarrow N(N,O)$)	

The acceptance of such rough data perhaps requires some justification. If we assume $f_{23} = 0$ and use the value F/I = 0.40 a value of ω_2 can be obtained from equation (5.10a). Using the extreme values of 1.0 and 2.5 for A_2, ω_2 is 0.374 and 0.295 respectively. This range for ω_2 is perhaps smaller than might be expected considering the large uncertainty in A_2; this is because of the way in which A_2 appears in the equation. This range lies entirely between the values calculated by Kinsey (0.506) and obtained experimentally by Küstner and Arends (0.255). Values of $A_2 = 1.7 \pm 0.7$ and $A_3 = 3.5 \pm 1.2$ are therefore not greatly in error and we use the ratio $\frac{A_3}{1 + A_2}$ rather than the individual values whenever possible.

For the case of X-ray excitation, the only observations of Auger intensities are those of Robinson and Young (1930) but because of uncertainty in their correction factor for conversion of photographic blackening units to electron intensity, it is probably better to rely on the relations $A_2/F_2 = A_2'/F_2'$ and $A_3/F_3 = A_3'/F_3'$ for values of A_2' and A_3'.

CALCULATION OF THE YIELDS

Kinsey's Results

It will first be shown that the values proposed by Kinsey (1948a) do not give a satisfactory fit with the experimental data adopted here. Using the values of initial ionization, i.e. C_2 and C_3 and Kinsey's values for f_{12} and f_{13}, the total excitation can be calculated. Then using Kinsey's fluorescent and Auger

yields the X-ray and Auger intensities to be expected can be found. The results for the two methods of excitation are shown in table 5.8.

Table 5.8: Intensities expected using Kinsey's Results

	Level	Initial Excitation	f_{12}	f_{13}	Total Excitation	ω	a	X-ray Intensity	Auger Intensity
RaD disintegration	(L_I	1.0	.12	.70	1.0	.11	.07	.11	.07
	(L_{II}	0.089			.209	.506	.494	.106	.103
	(L_{III}	0.0013			.7013	.33	.67	.231	.470
Fluorescent excitation	(L_I	1.0	.12	.70	1.0	.11	.07	.11	.07
	(L_{II}	1.66			1.78	.506	.494	.90	.88
	(L_{III}	2.6			3.30	.33	.67	1.09	2.21

We see from the X-ray intensities that the following values are obtained:

$F_2 = 0.96$ $\quad F_3 = 2.1$
$F_2' = 8.2$ $\quad F_3' = 9.9$

For the RaD disintegration F_2 is slightly different from the observed value of 0.73 ± 0.05 and F_3 agrees with 2.02 ± 0.2. However for fluorescent excitation F_2' is not in agreement with the observed value of 4.2 ± 0.3 and no permissible modification of the initial X-ray excitation can alter it to an acceptable value.

New Values of the Yields

To calculate new values for the yields it is first of all

necessary to choose a value for F/I. When this has been done ω_3 can be calculated from equation (5.9a) and the result compared with the directly determined values of Küstner and Arends (1935) and of Stephenson (1937) for the heavy elements, namely:

	Küstner & Arends	Stephenson
82Pb	$\omega_3 = 0.337$	$\omega_3 = 0.32$
83Bi	$\omega_3 = 0.367$	
90Th		$\omega_3 = 0.42$

Values of F/I of 0.25, 0.40 and 0.57 give ω_3 respectively as 0.24, 0.39 and 0.56 clearly supporting the choice of value of F/I of about 0.40. The yields will therefore be calculated with F/I = 0.40 ± 0.02 and also with F/I = 0.57 ± 0.11 (the value obtained with the curved crystal spectrometer).

The yields can now be calculated in two ways. In the first f_{23} is assumed to be zero and the data from the RaD experiments are used with equations (5.7) (5.8) (5.9a) (5.10a) and (5.12). The resulting yields shown in table 5.9 are then applied to the case of ionization by X-rays following the procedure adopted in table 5.8, i.e. using values of C_2' and C_3'. This gives the calculated values of X-ray intensities as shown in table 5.10, the upper figure in each row of both tables being obtained with the "best" value of F/I - viz. 0.40 - and the lower one (in parenthesis) with 0.57.

The results in table 5.10 give (parenthesis again indicating values obtained using F/I = 0.57):

$F_2' = 4.9 \pm 0.8$ $\qquad$ $F_3' = 10.4 \pm 1.5$

$(F_2' = 5.2 \pm 1.6$ $\qquad$ $F_3' = 10.6 \pm 3)$

Table 5.9: Calculation of Yields Assuming $f_{23} = 0$ and using RaD data

Level	f_{12}	f_{13}	ω	a
L_I	0.18 ± .03 (0.16 ± .05)	0.60 ± .03 (0.60 ± .10)	0.12 ± .01 (0.17 ± .03)	0.105 ± .030 (0.075 ± .025)
L_{II}			0.32 ± .04 (0.49 ± .12)	0.68 ± .04 (0.51 ± .12)
L_{III}			0.39 ± .04 (0.56 ± .12)	0.61 ± .05 (0.44 ± .12)

Table 5.10: Calculated X-ray and Auger Intensities by fluorescent excitation using yields of table 5.9.

Level	Initial Excitation	Total Excitation	X-ray Intensities	Auger Intensities
L_I	1.00	1.00 (1.00)	0.12 ±0.01 (0.17 ±0.03)	0.105 ±0.03 (0.075 ±0.025)
L_{II}	1.66 ± 0.15	1.84 ± 0.16 (1.82 ± 0.16)	0.59 ±0.09 (0.89 ±0.23)	1.25 ± 0.14 (0.93 ± 0.23)
L_{III}	2.6 ± 0.2	3.20 ± 0.20 (3.20 ± 0.22)	1.25 ±0.15 (1.8 ±0.4)	1.95 ± 0.19 (1.4 ± 0.4)

The value of F_2' is in good agreement with the experimental value of 4.2 ± 0.3 and the value of F_3' is reasonably near to the observed 8.5 ± 0.8. F_3'/F_2' is 2.1 ± 0.4 (2.0 ± 0.8) compared with the observed value of 2.0 ± 0.2.

The agreement of calculated and observed values does not confirm absolutely the values of the yields in table 5.9. It indicates that, provided our values of C_2 and C_3 are correct, the values deduced for f_{12} and f_{13} are good and the ratios $\omega_1 : \omega_2 : \omega_3$ are correct.

The second method of calculating the yields is to make no assumption about f_{23} and use the X-ray excitation data. Equations (5.7c), (5.8) and (5.9a) are each used once with the RaD data (giving the values of ω_1, ω_3, a_1, and a_3 already entered in table 5.9) and once with the X-ray excitation data (giving ω_1', ω_3', a_1' and a_3'). Equations (5.13a) and (5.14a) are used once and (5.15), (5.7a) and (5.7b) twice. The results are shown in table 5.11 again using the two values of F/I.

Table 5.11: Yields calculated on the assumption that f_{23} may have a non-zero value

$\omega_1 = 0.12 \pm 0.01$ (0.17 ± 0.03)	$\omega_1' = 0.15 \pm 0.01$
$\omega_3 = 0.39 \pm 0.04$ (0.56 ± 0.12)	$\omega_3' = 0.42 \pm 0.06$
$a_1 = 0.105 \pm 0.03$ (0.075 ± 0.025)	$a_1' = 0.12 \pm 0.03$
$a_3 = 0.61 \pm 0.05$ (0.44 ± 0.12)	$a_3' = 0.58 \pm 0.06$
$\omega_2 = 0.34 \pm 0.05$ (0.32 ± 0.05)	
$f_{12} = 0.17 \pm 0.04$ (0.29 ± 0.08)	
$f_{13} = 0.60 \pm 0.06$ (0.47 ± 0.09)	$f_{13}' = 0.56 \pm 0.05$ (0.44 ± 0.09)
$f_{23} = 0.07 \pm 0.35$ (0.37 ± 0.5)	$f_{23}' = -0.07 \pm 0.3$ (0.00 ± 0.5)
$a_2 = 0.59 \pm 0.35$ (0.31 ± 0.5)	$a_2' = 0.73 \pm 0.3$ (0.68 ± 0.5)

Discussion of Results

Unless otherwise stated the values discussed are those obtained with F/I = 0.40 i.e. the values in the upper line in each case.

The coefficients ω_1 and ω_1' are measured quite independently. The coefficients ω_3, a_1 and a_3 are independent of the corresponding dashed coefficients except for the fact that A_2' and A_3' were derived using A_2, F_2 and A_3, F_3 from the RaD data. Comparison of the values obtained by the two methods for these four coefficients

shows the consistency of the results in the case where the quantity F/I is taken as 0.40 for RaD disintegration. Of course this value was accepted as the "best" value largely on the grounds that it gives a value of ω_3 to agree with direct measurement, but ω_3' is independent of F/I and the agreement is satisfactory.

The values of ω_2 and f_{12} are not significantly altered by abandoning the assumption $f_{23} = 0$ which suggests that this assumption is a good one. Unfortunately (along with a_2) f_{23} is particularly sensitive to variation in A_2 and A_3 and for this reason the error quoted is large. We cannot say, therefore, whether f_{23} is zero or not. The fact that f_{23} is found to be so near zero - compared with the size of the error - is taken to mean that the values of A_2 and A_3 adopted by Ross are better than her error estimates indicate.

MODE OF DISINTEGRATION OF RaD

As we have seen the value of F/I = 0.40 is not much in error. If also Stahel's (1935) value of F = 0.252 per disintegration is accurate then I = 0.63 per disintegration in agreement with Wu et al. (1953) but higher than the other determinations shown in table 5.3. The ratio of conversion in the L shell to conversion in the M and higher shells is about 2.9 (Cranberg 1950, Wu et al 1953) and this gives the total conversion of the γ-ray as 0.84 per disintegration. Using the theoretical value for the total internal conversion coefficient of 17.8 this means that R = 0.035 in good agreement with measured values of 0.031 (Bramson 1930) "somewhat less than 4%" (Gray 1932), 0.036 (van Droste 1933),

0.035 (Stahel 1935) and 0.044 (Damon and Edwards 1954). It does not agree with the value 0.07 calculated by Wu et al (1953) from their measurements of F/R which have been discarded in an earlier section of this chapter.

The value of 0.84 for total conversion and 0.035 for R means that the 46.5 Kev state is excited to about 87.5% of the disintegrations leaving 12.5% to be otherwise accounted for. This quantity is however critically dependent on the values selected for F/I and F and if F/I = 0.38 and F = 0.27 (Tsien 1944) are accepted then the excitation of the 46.5 Kev state is 100%.

If the value of F/I = 0.57 obtained with the curved crystal spectrometer is used then the total excitation of the 46.5 Kev state is only about 62%. This is another indication that the value is much too high and we must conclude that the sensitivity-energy calibration is at present inadequate for dealing with lines which are separated by more than a few Kev.

CHAPTER 6

THE FLUORESCENCE YIELDS OF THE L LEVELS OF URANIUM AND NEPTUNIUM

INTRODUCTION

The L fluorescence yields of elements Z = 92 or 93 can be calculated from experimental observations on U_{92} and Am_{95}^{241}. The latter decays with a half-life of about 470 years by α-emission to Np_{93}^{237} and the γ-rays produced when this nucleus de-excites give rise to Np L X-rays by internal conversion. (Fuller details of the Am decay scheme follow in a later section.) It is not practicable to excite the L X-rays of Np by soft X-rays but it is a simple matter so to excite U L X-rays. The values of the yields differ very little for elements of neighbouring atomic number unless an important Coster-Kronig transition is possible for one and not the other. No such difficulty arises with 92 U and 93 Np hence this method was used as the alternative mode of excitation giving the dashed coefficients as described in Chapter 5.

Because of the absence of some experimental values and unreliability of others it is not possible to calculate completely the nine yields. For this reason a few reasonable assumptions were made and the calculations were performed in a slightly different order from those relating to bismuth.

For neither method of excitation are there any experimental results on intensity of Auger electron emission. Hence none of

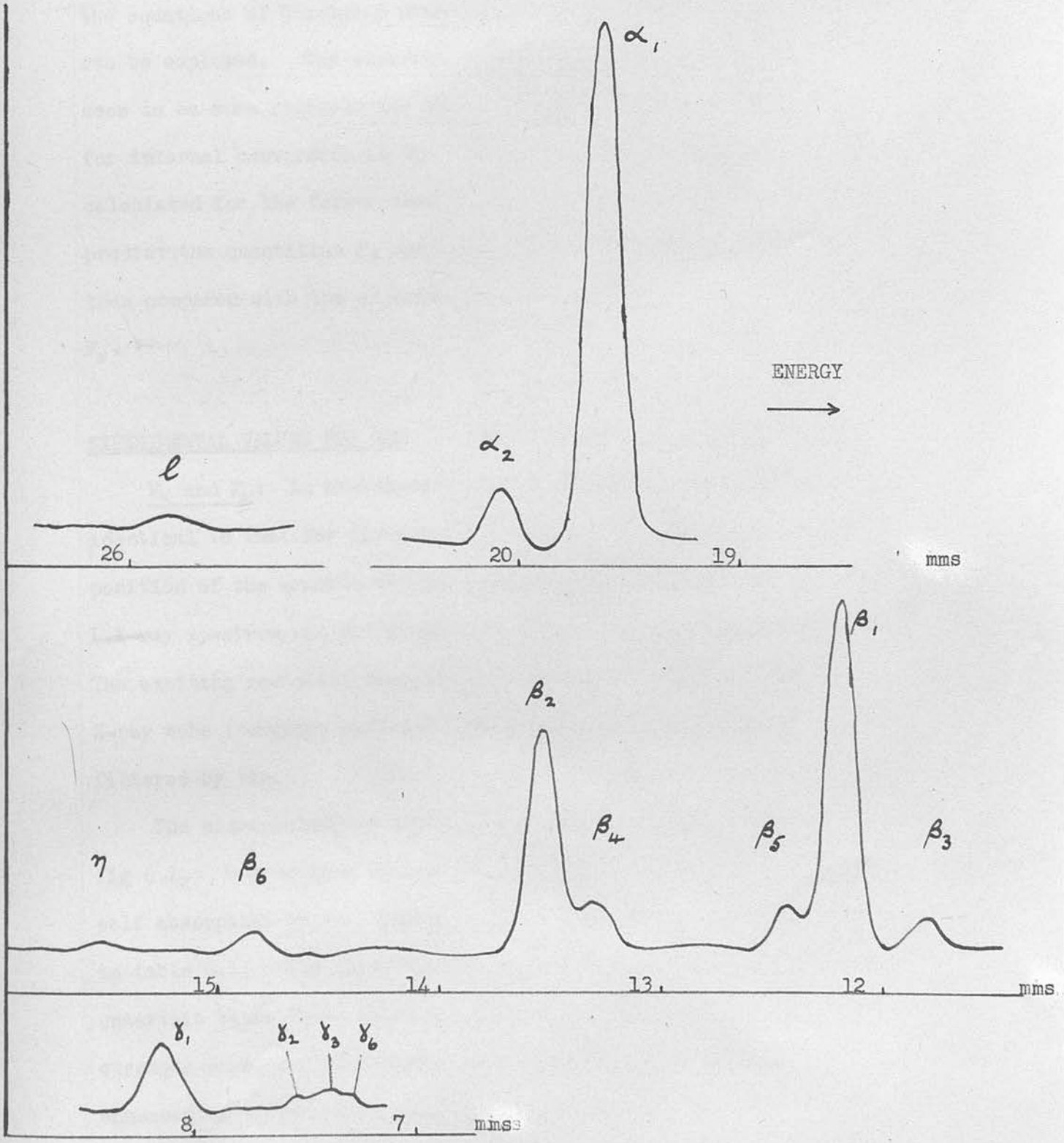

Fig 6.1 : Microphotometer trace of U L X-rays (fluorescent excitation)

the equations of Chapter 5 which involve the quantities A_2 and A_3 can be employed. The experimental values of F/I and C_2 and C_3 seem to be more reliable for the fluorescent excitation of U than for internal conversion in Np. The yields are therefore calculated for the former case first, and the values used to predict the quantities F_2 and F_3 for the latter case. These are then compared with the experimentally determined values of F_2 and F_3.

EXPERIMENTAL VALUES FOR 92U

F_2 and F_3: An experiment was done on the 20 cm. spectrometer identical to that for bismuth fluorescent X-rays except that the position of the uranium nitrate target (12,36) to give the entire L X-ray spectrum was different from that of the bismuth target. The exciting radiation consisted of the white X-rays from the X-ray tube (tungsten anti-cathode) running at about 70 kilovolts filtered by tin.

The microphotometer trace of the U L X-rays is shown in fig 6.1. Corrections applied to this are for sensitivity and self absorption in the target. The results deduced are shown in table 6.1. The figures quoted for β_4 and β_5 are somewhat uncertain since these lines are not completely resolved from stronger ones, and some weak lines are partially obscured, or enhanced by large background fluctuations. In the latter case intensities are obtained by comparison of the ratio of such lines to a stronger line from the same subshell with the same ratio

obtained by electron bombardment quoted by Compton and Allison (1935, p.645).

These values, which are asterisked in table 6.1, have of course always to be consistent with the approximate intensity observed. Thus if calculation from the figures in Compton and Allison had produced relative intensity for γ_2 of 15 this would not have been accepted since the microphotometer trace clearly shows that no line of intensity comparable to γ_1 could exist at γ_2.

Table 6.1: L X-ray spectrum obtained by fluorescent excitation of U

Line	Transition	Energy (Kev)	Intensity (Relative to $\beta_1 = 100$)
l	$L_{III} - M_I$	11.61	12.4
α_2	$L_{III} - M_{IV}$	13.43	39
α_1	$L_{III} - M_V$	13.61	306
η	$L_{II} - M_I$	15.39	2.3
β_6	$L_{III} - N_I$	15.72	5.7
β_2	$L_{III} - N_V$	16.42	79
β_4	$L_I - M_{II}$	16.57	11.2
β_5	$L_{III} - O_V$	17.06	12
β_1	$L_{II} - M_{IV}$	17.21	100
β_3	$L_I - M_{III}$	17.45	8.3
γ_1	$L_{II} - N_{IV}$	20.16	16.5
γ_2	$L_I - N_{II}$	20.48	3.3 *
γ_3	$L_I - N_{III}$	20.71	3.3 *
γ_5	$L_{II} - O_{IV}$	20.84	2.5 *
γ_4	$L_I - O_{III}$	21.55	

There are no results available for comparison of intensities by fluorescent excitation. However in table 6.2 the relative intensities of lines from each subshell are compared with those obtained by electron bombardment and quoted in Compton and Allison (1935, p.645).

Table 6.2: Relative Intensities of Lines from the three L subshells

		Compton & Allison	Cochran	
		U (electron bombardment)	U (fluorescent excitation)	Np (Am^{241} decay)
L_I	β_4	100	100	100
	β_3	102	74	117
	γ_2	36	)	
			) 60	90
	γ_3	34	)	
	γ_4	0	0	
L_{II}	η	2	2.3	
	β_1	100	100	100
	γ_1	24	16.5	26
	γ_6	4.4	2.5	4
L_{III}	ℓ	3.4	4.5	
	α_2	11	12.8	11
	α_1	100	100	100
	β_6	1.6	1.9	
	β_2	28	26	13
	β_5	6.4	3.9	

Agreement is considered to be satisfactory.

The results of table 6.1 give the relative quantum yields as $F_2' = 4.6 \pm 0.5$ $F_3' = 17.4 \pm 2.0$

Other experimental values: F/I is taken as 0.45 (Lay 1934). C_2' and C_3' are determined by absorption jump ratio measurements. The values for these adopted from the results quoted in Compton and Allison (1935, p.529) are

R (I,II) = 1.16, R (II,III) = 1.33, R (III,M) = 2.23.

This gives $C_2' = 1.57 \pm 0.15$ $C_3' = 2.6 \pm 0.2$.

No results are available for Auger intensities.

CALCULATION OF YIELDS

There are not sufficient experimental data to calculate the yields completely. However certain of them can be calculated and the others estimated by making two assumptions.

Using equation 5.8a we can immediately find $\omega_1 = 0.10 \pm 0.01$.

The value of ω_2 can also be found if we assume that $f_{12} = 0$. This cannot be much in error since transitions of the type L_I-L_{II} M and L_I - L_{II} ($N_{I,II,III,IV}$) are energetically impossible for Z = 92. Therefore f_{12} is likely to be very nearly zero or at any rate very small compared with C_2'. Hence we may assume a zero value in order to calculate ω_2, the expression for which then becomes (using equation 5.5) $\omega_2 = \omega_1 \frac{F_2'}{C_2'} = 0.30 \pm 0.04$.

No reasonable assumption can enable us to calculate ω_3 from the results but a direct determination of ω_3 was made by Stephenson (1937) for Z = 82, 90 and 92 and he obtained 0.44 for U. Küstner and Arends (1935) also did direct determinations of ω_3 for

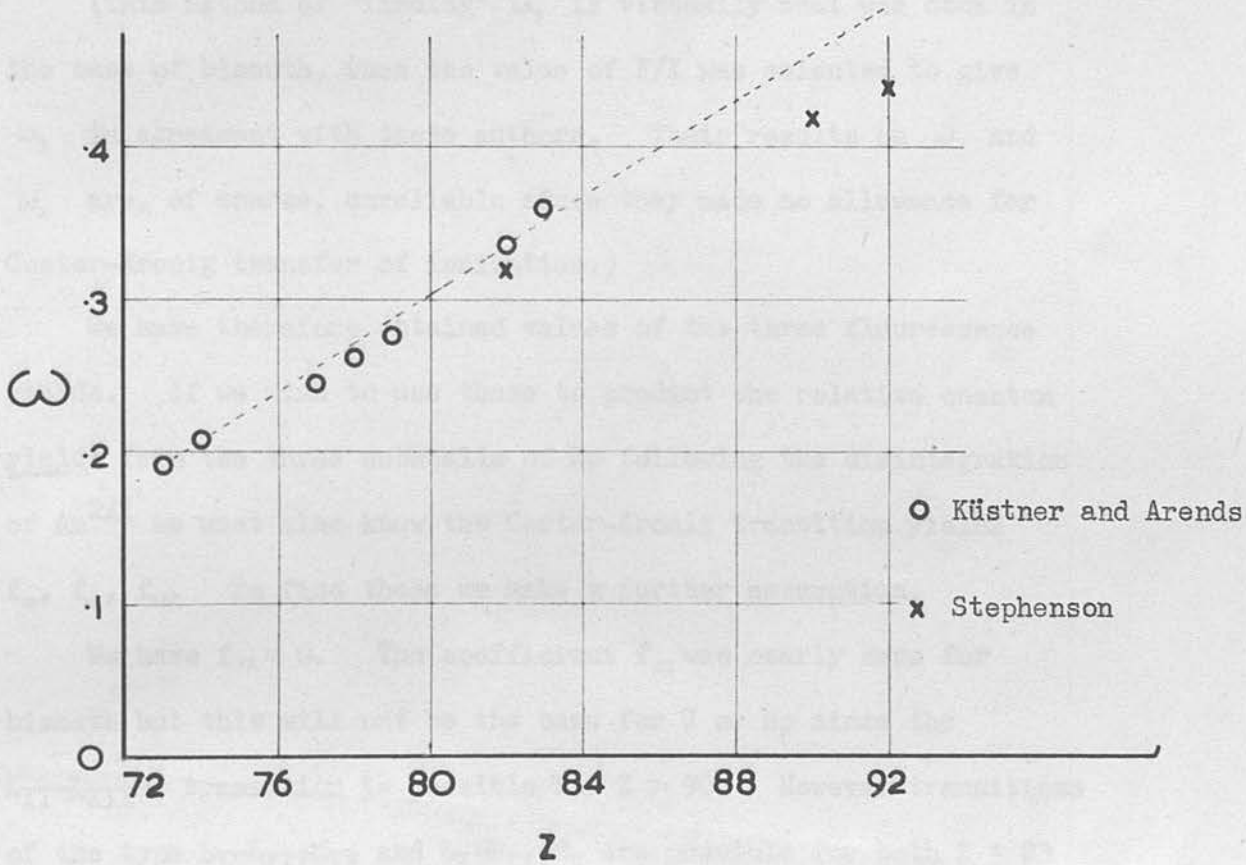

Fig 6.2 : Fluorescence yield of the L_{III} level according to Küstner and Arends (1935) and Stephenson (1937)

seven elements from Z = 73 to Z = 83 and their results agree fairly well with Stephenson's. The two sets of results are plotted in fig 6.2 and it can be seen that extrapolation of the values of Küstner and Arends produces a slightly higher result for 92 U than that obtained by Stephenson. The value adopted for ω_3 is therefore 0.46 ± 0.02.

(This method of "finding" ω_3 is virtually what was done in the case of bismuth, when the value of F/I was selected to give ω_3 in agreement with these authors. Their results on ω_1 and ω_2 are, of course, unreliable since they made no allowance for Coster-Kronig transfer of ionization.)

We have therefore obtained values of the three fluorescence yields. If we wish to use these to predict the relative quantum yields from the three subshells of Np following the disintegration of Am^{241} we must also know the Coster-Kronig transition yields f_{12}, f_{13}, f_{23}. To find these we make a further assumption.

We have $f_{12} = 0$. The coefficient f_{23} was nearly zero for bismuth but this will not be the case for U or Np since the L_{II}-$L_{III}M_V$ transition is possible for $Z > 90$. However transitions of the type L_I-$L_{III}M_{IV}$ and L_I-$L_{III}M_V$ are possible for both Z = 83 and Z = 92 or 93 and these are the only possible transitions in this range of Z involving the emission of M electrons. Hence the coefficient f_{13} will not vary much between Z = 83 and Z = 92 - or at any rate there will be no sudden jump in its value. Kinsey's (1948a) calculations suggest that, for Z = 92, f_{13} is about 10% lower than for Z = 83 and if we adopt the value of f_{13} found for

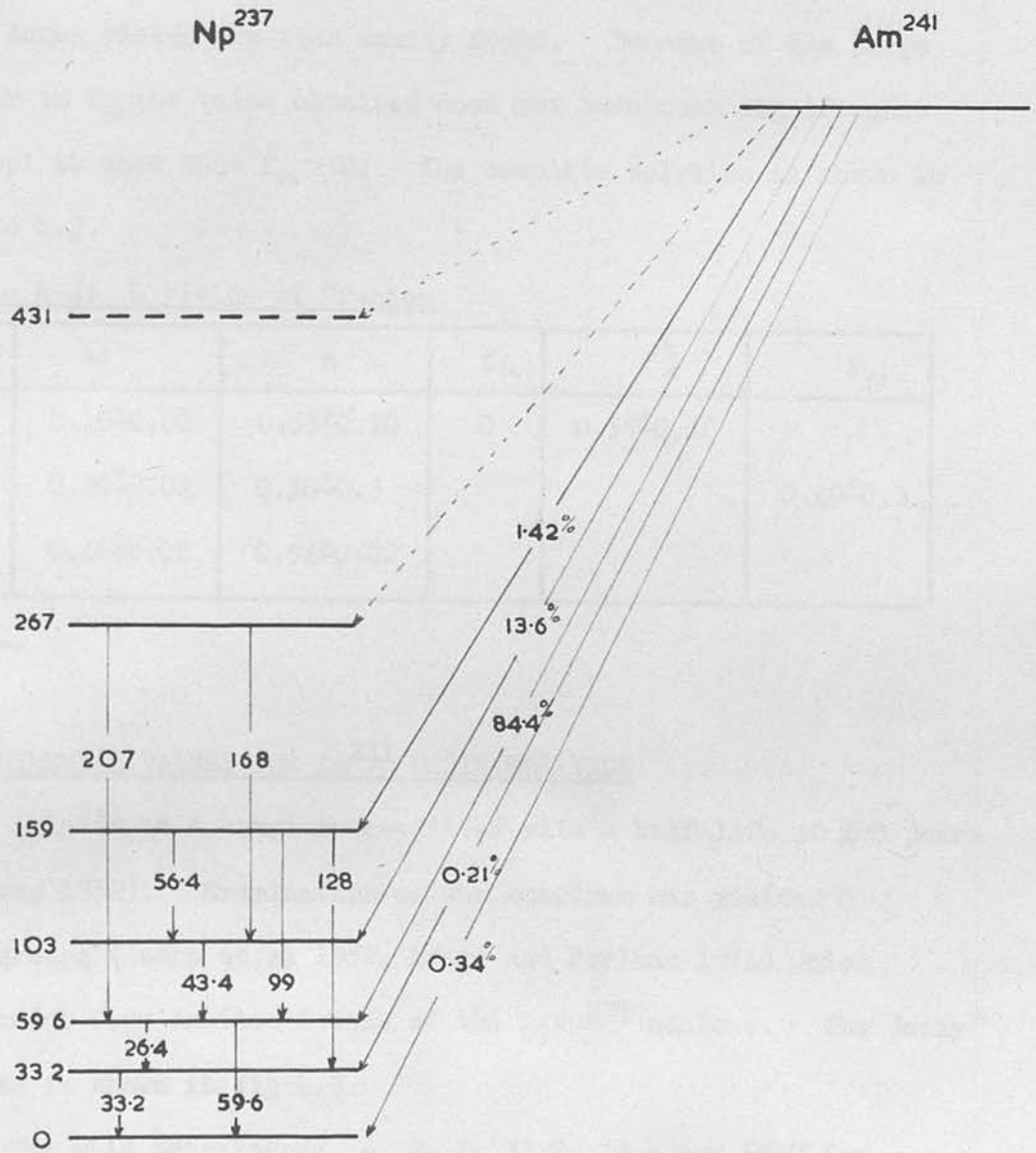

Fig 6.3 : Decay scheme of Am^{241} (energies in Kev)

bismuth in Chapter 5 of 0.60 ± 0.06, f_{13} for Z = 92 or 93 becomes approximately 0.55 with an error of, say, ± 0.1.

If we accept this value for f_{13} the remaining Coster-Kronig coefficient f_{23} is calculated from equation 5.15 as 0.40 ± 0.3 and the Auger yields are then easily found. Because of the large error in f_{23} the value obtained does not have much significance except to show that $f_{23} > 0$. The complete solution is shown in table 6.3.

Table 6.3: L yields of Uranium

	ω	a	f_{12}	f_{13}	f_{23}
L_I	0.10±0.01	0.35±0.10	0	0.55±0.10	
L_{II}	0.30±0.04	0.30±0.3			0.40±0.3
L_{III}	0.46±0.02	0.54±0.02			

EXPERIMENTAL VALUES FOR Am^{241} DISINTEGRATION

$_{95}Am^{241}$ is a complex α-emitter with a half-life of 470 years (Harvey 1952). Examination of the spectrum has yielded 5 α-groups (Asaro et al 1952, Asaro and Perlman 1954) which determine four excited levels of the $_{93}Np^{237}$ nucleus. The decay scheme is shown in fig 6.3.

The main transitions - 26.4, 33.2, 43.4 and 59.7 Kev - have been observed either directly or by their conversion electrons (Freedman et al 1952, Beling et al 1952, West et al 1952, Newton and Rose 1953, Jaffe et al 1955, Day 1955). The results of the last two seem to confirm the existence of other weaker transitions

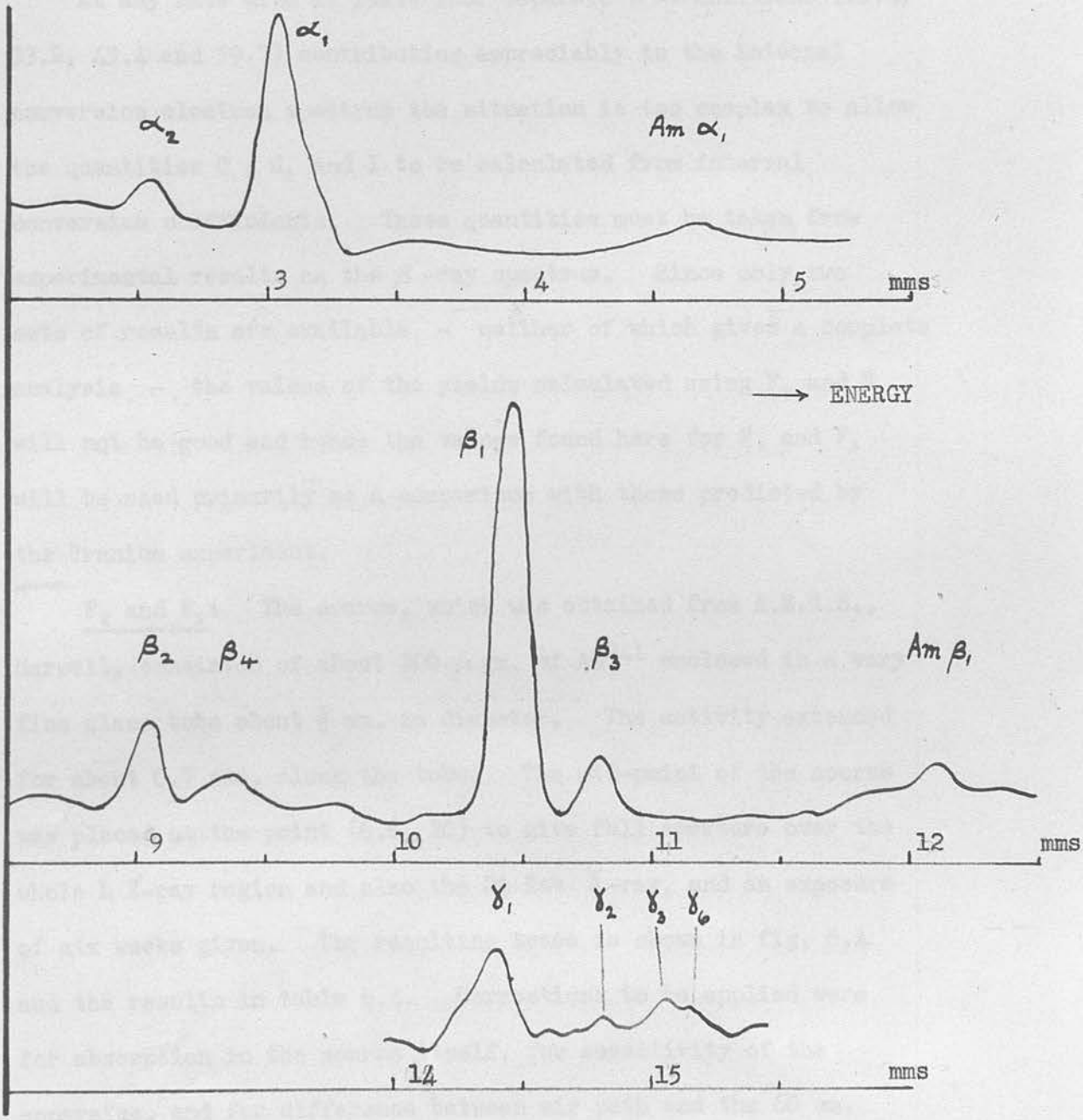

Fig 6.4 : Microphotometer trace of Np L X-rays after Am^{241} disintegration

56.4, 99, 128, 168 and 207 Kev - and Day's results suggest the existence of a level at about 431 Kev above the ground state of Np^{237}.

At any rate with at least four separate γ-transitions (26.4, 33.2, 43.4 and 59.7) contributing appreciably to the internal conversion electron spectrum the situation is too complex to allow the quantities C_2, C_3 and I to be calculated from internal conversion coefficients. These quantities must be taken from experimental results on the β-ray spectrum. Since only two sets of results are available - neither of which gives a complete analysis - the values of the yields calculated using F_2 and F_3 will not be good and hence the values found here for F_2 and F_3 will be used primarily as a comparison with those predicted by the Uranium experiment.

F_2 and F_3: The source, which was obtained from A.E.R.E., Harwell, consisted of about 300 μgm. of Am^{241} enclosed in a very fine glass tube about $\frac{1}{2}$ mm. in diameter. The activity extended for about 0.7 cms. along the tube. The mid-point of the source was placed at the point (6.6, 20) to give full aperture over the whole L X-ray region and also the 26 Kev γ-ray, and an exposure of six weeks given. The resulting trace is shown in fig. 6.4 and the results in table 6.4. Corrections to be applied were for absorption in the source itself, for sensitivity of the apparatus, and for difference between air path and the 60 cm. path used in calibration.

The first correction is not easy to make accurately since the L X-rays of Np fall among the L absorption edges of Am. The values of absorption coefficients were deduced by extrapolating

the values for Th and U for wave-lengths shorter than the L_I edge, and the rest of the absorption coefficient-wave-length curve drawn by finding the absorption jump ratios at the L_I, L_{II} and L_{III} edges of Am also by extrapolation (of data quoted in Compton and Allison p.529, 1935). The source was regarded as being infinitely thick. This should not introduce much error since the mass absorption coefficient of Am at the wave-length of the L X-rays of Np is approximately 30 - 40 $cm^2 gm^{-1}$. This means that in a distance equal to the radius of the glass tube the L X-rays of Np will be reduced by a factor of at least 40 or 50. The thickness of the glass of the tube is not known but it is estimated that absorption in it will amount to not more than two per cent for the softest X-rays and differences in absorption over the wave-length range in question can be neglected.

The final corrected intensities are shown in table 6.4 and the relative intensities of lines from each of the three subshells is compared with the values for U in table 6.2. Once again the asterisked values in table 6.4 indicate that though a line was observed it was either partially obscured by large background variations or else incompletely resolved from another and the value was obtained as explained for Uranium. Such values are inserted only where there is clear evidence on the trace for the existence of a line. The energy of the L X-rays of Np will be discussed in the next chapter.

The results are also compared with those of Jaffe et al (1955) and Day (1955). These two authors used a bent topaz crystal

Table 6.4: L X-ray spectrum of Np by disintegration of Am^{241}.

Line	Transition	Intensity		
		Cochran	Jaffe et al	Day
ℓ	$L_{III} - M_I$			3.5
α_2	$L_{III} - M_{IV}$	23 *	7 (9)	7.7
α_1	$L_{III} - M_V$	210	64 (81)	69.2
η	$L_{II} - M_I$		2 (2)	3.3
β_6	$L_{III} - N_I$		1 (1)	1.4
β_2	$L_{III} - N_V$	28	13 (14)	18
β_4	$L_I - M_{II}$	11	16 (17)	11.5
β_5	$L_{III} - O_{IV,V}$		3 (3)	2.7
β_1	$L_{II} - M_{IV}$	100	100 (100)	100
β_3	$L_I - M_{III}$	13	13 (13)	9.1
γ_5	$L_{II} - N_I$		2 (2)	0.8
γ_1	$L_{II} - N_{IV}$	26	34 (29)	23
γ_2	$L_I - N_{II}$	5 *	8 (7)	2.5
γ_3	$L_I - N_{III}$	5 *	7 (6)	3.0
γ_6	$L_{II} - O_{IV}$	4 *	10 (8)	6.0
γ_4	$L_I - O_{II,III}$		3 (2)	2.7

spectrometer (10" radius in both cases) but they employed different corrections for the reflecting power of the crystal. Jaffe et al assumed that it varied inversely as the square of the energy ($1/E^2$), the justification being that the reflectivity of a

quartz crystal was found to vary approximately as $1/E^2$ for energies between 25 Kev and 1.3 Mev (Lind et al. 1950) and that "lines widely spaced in energy" maintained the same intensity ratio when reflected from both quartz and topaz (Browne, 1952). Day uses a $1/E$ correction because this gives better agreement than $1/E^2$ between the intensity ratio of the 59.7 Kev γ-ray to total L X-rays as found by the topaz spectrometer and by a scintillation counter.

In view of the experiences of the present author (Chapter 3) with mica neither a $1/E^2$ nor a $1/E$ assumption may be entirely reliable over the range 13 - 22 Kev. However in order to compare the two sets of results those of Jaffe et al. are tabulated both as they calculate them and, in brackets, assuming a $1/E$ variation of reflectivity. Agreement between Jaffe et al. and Day is fairly good but the present work is in disagreement for the lower energy lines. As a further comparison table 6.5 shows the relative intensities of the three groups, $L\alpha$, $L\beta$ and $L\gamma$. The results of Beling et al. (1952) were obtained with a proportional counter.

The present results are in disagreement with the other three sets between which agreement is fairly good. This seems to indicate that the present results are in error, particularly for the $L\alpha$ group. However it does seem possible that in choosing their reflectivity variation Jaffe et al. and Day were in some way influenced by the results of Beling et al. This is perhaps more apparent in the case of the ratio of the 59.7 Kev γ-ray to the

Table 6.5: Relative Intensities of 3 L X-ray groups of Np.

	Cochran	Jaffe et al.	Day	Beling et al.
Lα	5.8	1.1 (1.7)	2	2
Lβ	3.8	2.4 (2.8)	3.8	3.5
Lγ	1	1 (1)	1	1

26.4 Kev γ-ray. Beling et al. obtain 1 : 0.069 ± 0.007. Both Day and Jaffe et al. obtain comparable values, 1 : 0.082 and 1 : 0.1 despite the fact that their reflectivity corrections differ by a factor of 2.26. In fact if a 1/E correction be applied to Jaffe's results the ratio becomes 1 : 0.226.

The present results are so much in disagreement with the others that there is little point in compromising between them so for the moment each set will be accepted and treated separately. When we come to calculate the yields it will be seen that the present results give more reasonable values than the others. The values of the F's then are

$F_2 = 3.8 \pm 0.5$	$F_3 = 7.7 \pm 1$	Cochran
$F_2 = 3.2$	$F_3 = 1.9$	Jaffe et al
$F_2 = 4.6$	$F_3 = 3.6$	Day.

Other experimental quantities

Even if the internal conversion coefficients for the four chief γ-transitions were accurately known the decay scheme is too complex to use them to calculate C_2 and C_3.

These quantities have been estimated from the β -ray spectrometer results of Jaffe et al. (1955) and Turner (1955). Their results, shown in table 6.6, agree fairly well and since those of Jaffe et al. are more nearly complete than those of Turner they were used in the calculation of C_2 and C_3 except where otherwise stated. Unfortunately additional information was required in several places. This was deduced as follows:-

The 59.7 Kev transition: The L_I and L_{II} conversion lines are unresolved. This transition is assumed to be E1 on the basis of its total L conversion coefficient and so from the theoretical ratio of L_I to L_{II} conversion the double line can be resolved. Unfortunately this may not be reliable since the ratio of $L_I + L_{II}$ conversion to L_{III} conversion is considerably larger than theory predicts (2 - 3 times according to these authors). It is suggested that this is due to the presence of a certain amount of M2, which is possible on account of the abnormally long lifetime of the 59.7 Kev state. This could produce the necessary increase in $L_I + L_{II}$ to L_{III} conversion ratio and it would at the same time make the $L_I : L_{II}$ ratio higher than for a pure E1 transition. For the pure E1 transition this ratio is about 1.05 (internal conversion coefficients are $L_I \sim 0.130$, $L_{II} \sim 0.123$ by interpolation in the values of Rose et al. (private communication)) giving the conversion electrons as 0.121 and 0.115 per α -particle from the L_I and L_{II} shells respectively.

Assuming that the discrepancy in the $(L_I + L_{II}) : L_{III}$ ratio is in fact due to the presence of M2, the amount can be roughly estimated from the total L conversion. Thus the total L

Table 6.6: Intensity of Internal Conversion Electrons in Decay of Am^{241}.

γ-ray Energy (Kev)	Shell	Intensity (e^-/α) Jaffe et al.	Intensity (e^-/α) Turner
26.3	M	-	0.016
	N	0.0068	0.007
33.2	L_I	0.067	
	M_I	0.018	0.032
	M_{III}	0.0012	
	N	0.004	0.016
43.4	L_I	0.017	0.05
	L_{II}	0.035	
	L_{III}	0.039	0.031
56.4	L_IL_{II}	-	0.0042
	L_{III}	0.0015	-
59.7	L_IL_{II}	0.236	0.225
	L_{III}	0.054	0.035
	M	0.064	0.10
	N	0.014	
99	L_IL_{II}	0.00062	
	L_{III}	0.00037	-
	M	0.00031	

conversion coefficient for E1 radiation is about 0.38 (L_{III} data are not so well known as L_I and L_{II}) and for M2 is > 1000. These

figures in conjunction with the electron intensities in table 6.6 and the result of 0.40 59.7 Kev quanta per α (Beling et al 1952) indicate that about 10% of M2 would be required. The ratio of $L_I : L_{II} : L_{III}$ conversion for M2 radiation of 59.7 Kev for Z = 93 is about 16 : 1 : 7 and this would mean that instead of being of roughly equal intensity the L_I conversion line would be about 1.8 times as intense as L_{II} - i.e. approximately 0.152 and 0.084 L_I and L_{II} electrons per α respectively. This second pair of values is believed to be better than those obtained assuming pure E 1 but the values adopted are 0.14 $\pm$ .02 and 0.095 $\pm$ .02 which cover both sets with a slight inclination towards the latter pair.

<u>26.4 Kev Transition</u>: There are no L conversion electron measurements for this transition. However from the available results the vacancies caused in the three L subshells can be estimated in two ways.

From his measurements on M + N conversion intensities and knowledge of transition branching ratios Turner estimates the total L conversion coefficient for the 26.4 Kev line as 6.7 $\pm$ 3.0 in agreement with an E 1 assignment. Beling et al. find that the 26.4 Kev γ-ray is emitted 0.028 $\pm$ 0.003 times per α. These two figures give a total of 0.187 $\pm$ 0.08 L electrons per α and using the theoretical ratio of internal conversion coefficients for E 1 transitions this means 0.029, 0.065 and 0.092 electrons per α from the L_I, L_{II} and L_{III} shells respectively.

However it might be argued that since the 26.4 Kev transition is from the same long lived level as the 59.7 Kev one, a more

accurate value of the L vacancies would be obtained by making the ratios of L_I, L_{II} and L_{III} electrons to M + N electrons the same as for the 59.7 Kev transition. This method would use more of the experimental results and rely less on theory, and does not assume a pure E 1 character for the transition. On the other hand, it is based on the difficult measurement of a weak conversion line and it makes the doubtful assumption that the conversion ratios of the three L subshells is the same at 26.4 Kev as at 59.7 Kev.

The results of Jaffe et al who give only the N conversion line for 26.4 Kev, give a total of 0.14 L electrons per α and assuming the values for the 3 subshells are in the ratio of those adopted for the 59.7 Kev line, then for the 26.4 Kev transition these are 0.067, 0.046 and 0.026 L_I, L_{II} and L_{III} electrons respectively.

The results of Turner, who gives M and N conversion lines for 26.4 Kev, give only 0.06 L electrons per α with a corresponding reduction in the individual subshell values.

The difference in the two sets of values obtained by this latter method illustrates how large the uncertainties involved are. It is believed that the figures obtained by the first method are better and hence the values adopted for L_I, L_{II} and L_{III} conversion are respectively 0.029 ± 0.013, 0.065 ± 0.03, 0.092 ± 0.04.

33.2 Kev transition: The L conversion lines of this transition unfortunately fall in the region of the Auger electrons

so absolute intensities are difficult to arrive at, and the only L conversion line observed by Jaffe et al is for L_I - 0.067 per α

The transition is either E2 or M1, or a mixture, because of parity conditions and the lower limit for its total internal conversion coefficient. If the $L_{II} + L_{III}$ conversion electron intensity is as low as, say, 0.01 per α compared with 0.067 for L_I then the transition would be largely M 1 (>90%) which is unlikely in view of the total internal conversion coefficient. (A mixture of 90% M 1 + 10% E 2 would give a total L internal conversion coefficient of about 150 compared with > 240 (Turner 1955) and > 400 deduced from the upper limit set by Beling et al. (1952) of 0.0005 33.2 Kev quanta per α .)

Nearly all of the excited Np nuclei pass through the 59.7 Kev state and as about 76% go direct to ground state (0.36 conversion electrons + 0.40 γ-rays) there remains 24% to go by the two stages 26.4 + 33.2. Hence there ought to be approximately 0.2 L electrons per α from this source. To make the total L conversion up to a reasonable figure the L_{II} and L_{III} conversion would have to be comparable with L_I. This would be the case with roughly 70% E 2 and 30% M 1 and would give a total L internal conversion coefficient of about 400 in better agreement with the values mentioned above.

The figures adopted are therefore 0.067, 0.06 $\pm$ 0.02, 0.06 $\pm$ 0.02 for the L_I, L_{II} and L_{III} shells respectively.

Other transitions: The three L conversion lines of the 43.4 Kev transition are resolved by Jaffe et al and their results

agree well with Turner who does not resolve L_I and L_{II}.

The 56.4 Kev and 100 Kev transitions are not sufficiently important to require detailed consideration. L shell vacancies caused by them are allocated using the conversion intensities in table 6.6 and assuming both are E 2.

Table 6.7 summarises the deductions of the preceding pages. Errors are shown in the entries only for values which have been deduced - and then only for important transitions. From the results $C_2 = 1.02 \pm 0.2$ and $C_3 = 0.98 \pm 0.2$.

Table 6.7: Observed and Deduced Conversion Electron Intensities for Am^{241} Decay.

Multipole Order	Energy (Kev)	L_I	L_{II}	L_{III}
E 1	26.4	0.029 ± 0.013	0.065 ± 0.03	0.092 ± 0.04
E 2 + M 1	33.2	0.067	0.06 ± 0.02	0.06 ± 0.02
E 2 (+M 1?)	43.4	0.017	0.035	0.039
E 2 ?	56.4	0.0001	0.0017	0.0015
E 1 (+ M 2?)	59.7	0.14 ± 0.02	0.095 ± 0.02	0.054
E 2	100	0.00002	0.0006	0.00037
		0.25312 ± 0.024	0.2573 ± 0.041	0.24687 ± 0.045

Total L vacancies = 0.757 ± 0.065

The ratio F/I is determined by finding absolute values for F and I. From table 6.7 I is taken as 0.76 ± 0.07.

Beling et al (1952) find a total of 1.035 ± 0.059 L X-ray quanta per 59.7 Kev γ-ray and using their value of 0.40 ± 0.015 per α for the latter, F = 0.41 ± 0.03. This gives F/I = 0.54 ± 0.06.

FITTING URANIUM YIELDS TO Am^{241}.

Using the values deduced for the Coster-Kronig yields of U the second column of table 6.8 is deduced from the first and using the U fluorescence yields the relative yields to be expected from the L levels of Np are found. These results give

$F_2 = 3.1 \pm 0.8$ $F_3 = 8.5 \pm 1$

compared with the present results

$F_2 = 3.8 \pm 0.5$ $F_3 = 7.7 \pm 1$

and those of Jaffe et al, and Day respectively, 3.2 and 1.9, and 4.6 and 3.6.

Table 6.8

	Initial Vacancies	Total Vacancies	ω	Relative Yield
L_I	1	1	0.10 ± 0.01	0.10 ± 0.01
L_{II}	1.02 ± 0.20	1.02 ± 0.20	0.30 ± 0.04	0.31 ± 0.07
L_{III}	0.98 ± 0.20	1.94 ± 0.39	0.46 ± 0.02	0.85 ± 0.1

The present results are in much better agreement with the predicted fluorescence, particularly with regard to F_3/F_2 which both Jaffe et al and Day find to be <1. This agreement is perhaps not surprising since the uranium yields were found using the present instrument. However if the present values of F_2 and F_3 are used to calculate ω_1 and ω_2 for Np independent of the U results - using the values of C_2, C_3 and F/I deduced earlier and assuming $f_{12} = 0$-then values of 0.13 ± 0.02 and 0.48 ± 0.06 are obtained not in violent disagreement with those obtained for uranium. Indeed if the ratio F/I were reduced by about 25% the agreement between the Am and U results would be good. The value of F has been obtained from the results of Beling et al (1952) and we saw earlier that those results were not in agreement with the present ones. Thus we can at least say that there is nothing in the present results which rules out the possiblity of a lower value for F.

If the values of F_2 and F_3 found by Jaffe et al. and Day are used, the values of ω_1 and ω_2 obtained are 0.27 and 0.87 (Jaffe), and 0.18 and 0.83 (Day). These values of ω_2 verge on the impossible and it would require a large reduction in F/I, or a large value for f_{12}, to bring ω_2 to a reasonable value.

The weighted means of the Am and U results give the values $\omega_1 = 0.11 \pm 0.01$ and $\omega_2 = 0.35 \pm 0.06$, and, along with $\omega_3 = 0.46 \pm 0.02$, these are the "best" results obtainable from the present series of experiments.

CHAPTER 7

ENERGY MEASUREMENTS

INTRODUCTION

The object of the present research was to make intensity measurements with the curved crystal spectrometers - but in doing so several plates were obtained, from which energies could be found where they were of interest. They are of some interest in two cases - Am^{241} and Xe^{133}. It must be stressed that in every case the primary object was to measure intensities, and energies were measured only when sufficient plates were available to "waste" one by putting calibration lines on it. The values quoted are therefore probably not so accurate as might have been possible if the sole object had been to measure energy.

METHOD OF MEASURING ENERGY

I. The method which gives best results is to put on the plate a large number of calibration lines which span completely the lines whose energy is to be found. For the energies for which the present spectrometers are useful, a convenient way of doing this is to use the characteristic X-rays of elements which can be excited by the X-ray tube.

The positions on the plate of every line are determined, either by the microphotometer or by a travelling microscope, and the unknown energies found by interpolation. Naturally the nearer one can find a calibration line to the suspected energy of

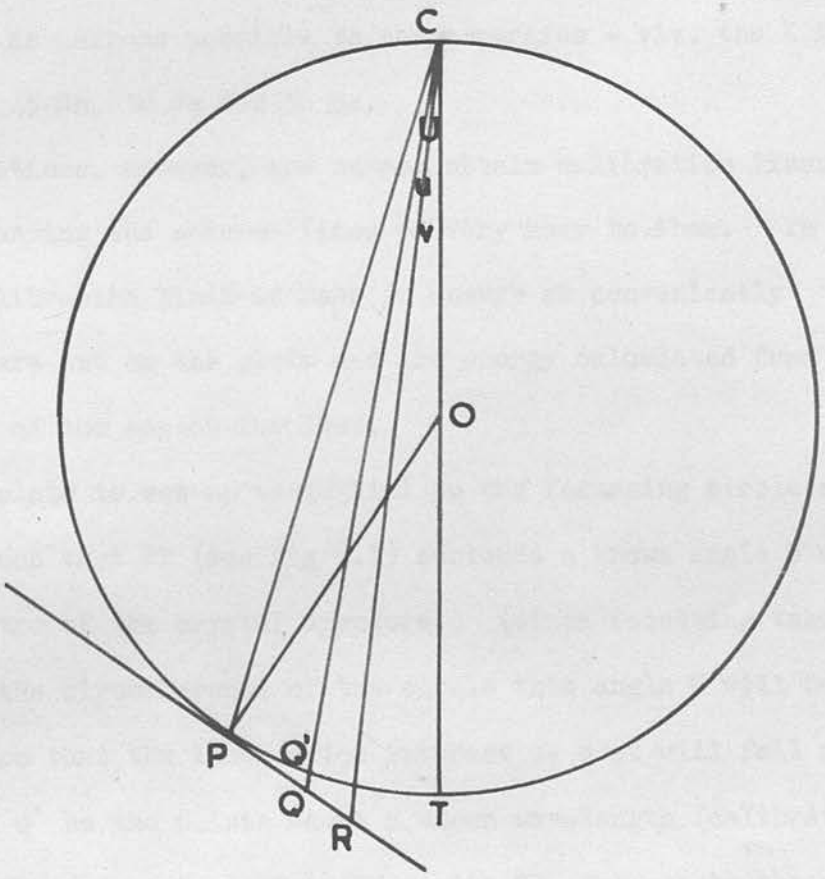

Fig 7.1 : Positions of lines on a plate tangential to the focussing circle

the unknown line the more accurately will the latter be determined. For example in the measurement of the $L\beta_1$ and $L\gamma_1$ X-rays of Np and the lowest energy γ-ray of Am^{241} it was known from extrapolation of X-ray data and from previous results that the energies were approximately 17.8, 20.8 and 26.4 Kev respectively. Calibration lines were therefore chosen to cover the whole range and to be as near as possible to these energies - viz. the K X-rays of 42 Mo, 45 Rh, 50 Sn and 56 Ba.

II. Sometimes, however, one cannot obtain calibration lines either spanning the unknown lines or very near to them. In such a case calibration lines as near in energy as conveniently possible are put on the plate and the energy calculated from a knowledge of the angles involved.

The plate is set up tangential to the focussing circle at a point P such that PT (see fig 7.1) subtends a known angle U at C, the centre of the crystal aperture. (Since focussing takes place on the circumference of the circle this angle U will be selected so that the lines which interest us most will fall near P.) Let Q and Q' be the points where a known wavelength (calibrating line), reflected at C at an angle u with CT, intersects the plate and focussing circle respectively. Then in an exact focussing spectrometer all radiation of this wavelength reflected from the whole crystal aperture passes through Q'. Only the radiation reflected from C passes through Q but since the aperture is small and $QQ' \ll CQ'$ then Q is approximately the point on the plate where the line falls - in the approximate as well as the exact focussing case.

Calculation of the exact position of the middle of the line on the plate is not difficult in principle. One requires to know from what portion of the crystal surface reflection of that particular wave length has taken place and this is readily obtained from a knowledge of the source position and source size. The distance from P to the centre of the line on the plate can then be shown to be $\frac{2r\left[\sin u - \sin U \cos (U + \omega - u)\right]}{\cos (2U + \omega - u)}$ where ω is the angle subtended at T by the arc of the crystal extending from C to the centre of the region from which reflection takes place. For high precision measurements - for example, on a large radius spectrometer - this expression should be used, but in view of the errors involved in making the measurements and the "spread" of the line on the plate it is an unnecessary refinement here and the point Q is therefore taken to be the middle of the line on the plate. Then $PQ = \frac{2r \cos U \sin (U - u)}{\cos (2U - u)}$ where $r = OP$ (7.1) and this serves to determine the position of P on the plate since Q represents a known line.

If now an unknown line occurs at R on the plate the angle v, which it makes with the normal to the crystal after reflection is given by the relation, $\tan v = \frac{r \sin 2U - s \cos 2U}{r(1+\cos 2U) + s \sin 2U}$ (7.2)

Where s = the distance PR which is found in practice by measuring QR and adding to it PQ as found from (7.1).

Equation (7.2) is found from the equation corresponding to equation (7.1) involving PR and v instead of PQ and u.

From v the Bragg angle, θ, and hence the wavelength can be found.

Since the angle which the reflecting planes make with the

normal to the crystal surface is 10°10' the angles U, u and v have always been small - i.e. in the range + 8° to - 2°. This means that very approximately PQ and PR are 2R (U - u) and 2R (U - v) and hence QR = 2R (u - v). This approximation is good enough only in exceptional cases but it does show that QR is not critically dependent on the angle U. This is of importance since the 20cm. spectrometer is not equipped to measure angles accurately and errors of ± 1° in U are possible. On the only occasion on which this spectrometer was used for energy measurements - for the weaker L X-rays of neptunium - U was 2° and u and v were between +4° and 0° so that an error of ± 1° in U made no significant difference to the energy measurement.

AMERICIUM 241

The energies of all the clearly visible L X-rays and the two strong γ-rays - those which have been called 59.7 Kev and 26.4 Kev- were measured.

59.7 Kev line: This was measured on the 46.4 cm spectrometer and the calibration lines used were the K X-rays of 74 W obtained from the X-ray tube running at 80 kilovolts. To avoid obscuring the γ-ray a strip of lead about 0.5 cms wide was placed lengthwise in front of the middle of the plate (i.e. parallel to the long sides). The K X-rays of tungsten then appeared on the unshielded parts of the plate above and below the γ-ray. The energies of these X-rays are (Fine and Hendee, 1955):

W $K\alpha_2$ = 57.973 Kev

W $K\alpha_1$ = 59.310 Kev

W $K\beta_1$ = 67.233 Kev

Using these values the energy of the Am^{241} γ-ray was found to be 59.66 ± 0.03 Kev.

26.4 Kev γ-ray and L X-rays: These were obtained on a plate exposed on the 46.4 cm spectrometer and the K X-rays of 42 Mo, 45 Rh, 50 Sn and 56 Ba were used as calibration lines. There were then twelve good calibration lines (α_2, α_1 and β_1) at conveniently spaced intervals from 17.373 Kev to 36.376 Kev. The energy values adopted were those quoted by Fine and Hendee (1955).

On this particular plate only the $L\beta_1$, $L\gamma_1$ X-rays and 26.4 Kev γ-ray were clearly visible and the energy of these three lines was found by interpolation from the twelve calibration lines. The energies of the remaining lines of the L X-ray spectrum were found by measuring their positions on the trace of fig. 64(20 cm spectrometer) relative to the three lines $L\beta_1$, $L\gamma_1$ and 26.4 Kev γ-ray. Since three known energies are not enough to interpolate from, the second method already described was employed to calculate the remaining energies. The complete results are shown in table 7.1 compared with those obtained by Jaffe et al. (1955) and Day (1955) and by extrapolation (Hill et al. 1952, Fine and Hendee 1955).

The results are in good agreement with those of the other two authors and confirm that the X-ray energies are a little higher than those obtained by extrapolation.

XENON 133

The γ-ray emitted from the excited Cs 133 nucleus has an

Table 7.1: Energies of lines in the electro-magnetic spectrum of Am^{241} (kev)

	Cochran	Jaffe et al.	Day	Extrapolation
NpLα_2	13.76 ± 0.05	13.79 ± 0.04	13.776 ± 0.003	13.76
NpLα_1	13.96 ± 0.04	13.98 ± 0.04	13.961 ± 0.003	13.95
NpLβ_2	16.85 ± 0.03	16.89 ± 0.02	16.857 ± 0.006	16.84
NpLβ_4	17.10 ± 0.04	17.10 ± 0.02	17.075 ± 0.006	17.05
NpLβ_1	17.78 ± 0.02	17.78 ± 0.01	17.764 ± 0.003	17.74
NpLβ_3	18.03 ± 0.03	18.02 ± 0.02	18.001 ± 0.005	17.98
NpLγ_1	20.82 ± 0.02	20.82 ± 0.02	20.796 ± 0.005	20.77
NpLγ_2	21.16 ± 0.06	21.12 ± 0.04	21.108 ± 0.020	21.09
NpLγ_3	21.36 ± 0.06	21.31 ± 0.04	21.340 ± 0.017	21.33
NpLγ_6	21.54 ± 0.06	21.51 ± 0.04	21.476 ± 0.015	21.49
AmLα_1	14.60 ± 0.06	14.66 ± 0.03	14.629 ± 0.003	14.62
AmLβ_1	18.90 ± 0.03	18.76 ± 0.04	18.871 ± 0.005	18.83
γ-rays	26.40 ± 0.03	26.38 ± 0.04	26.363 ± 0.014	
	59.66 ± 0.04	59.62 ± 0.06	59.568 ± 0.017	

energy of about 81 Kev. The nearest calibration line which could conveniently be produced was the $K\beta_2$ line of tungsten at 69.090 Kev. It was therefore necessary to use method II for calculation of energy and the value found was 82.3 $\pm$ 0.3 Kev.

Hughes (private communication) using a proportional counter found another line at 63 $\pm$ 1 Kev with an intensity of about 10% of the 82.3 Kev line. A careful scan of the plate in the microphotometer revealed no trace of such a line and it is estimated that it would have been detected if its intensity had been greater than 0.5% of the 82.3 Kev line.

CHAPTER 8

CONCLUSION

Having made several sets of intensity measurements we are now in a position to comment on the performance of the curved crystal spectrometers as instruments for measuring relative intensities of X-rays and soft γ-rays. It must be admitted that the difficulties of making such measurements accurately have proved greater than was anticipated.

In Chapter 3 it was seen that sensitivity calibration was in practice a different procedure, very liable to error on account of the "step by step" nature of the method adopted. This method was adopted because of the absence of suitable sources to provide a more reliable method. The comparison, in Chapter 5, of the RaD γ-ray with the RaE L X-rays showed that the curve obtained was, in fact, unreliable for this energy difference.

However, the difficulties are not merely practical ones. Though the calibration curve may be unreliable for large energy differences it does show that the sensitivity of the spectrometers in their present form is rapidly varying in a non-uniform way over the energy region in which they are most useful. Thus good sensitivity-energy calibration is inherently difficult, quite apart from the practical difficulty of finding suitable calibrating lines.

The problem, then, is to make the sensitivity more uniform over the range for which the present spectrometers are useful.

We should like, in the first place, to see if this can be done without making any drastic alteration in the way in which they are used (i.e. with an extended source and photographic recording).

The sensitivity has to be increased at both the low and high energy ends of the curve. The steep fall-off at low energies is to a certain extent due to decreasing sensitivity of the emulsion but the main cause is rapidly increasing absorption in the path between source and detector. This could be reduced in two ways. Firstly, by placing the whole apparatus in vacuum to eliminate absorption in air and, secondly, by using a thinner crystal. The reduction in crystal thickness must not be carried too far, however, since reflections from the whole crystal thickness contribute to the image. While reduction in intensity due to this may be less than the gain due to smaller absorption for low energies, the reverse is likely to be true for higher energies where absorption is unimportant. The crystals at present employed are 0.25 mm. thick, in which distance a line of energy 10 Kev is reduced by a factor of 7 by absorption, whereas one of 100 Kev is reduced by a factor of 1.01. If the crystal thickness is halved the absorption factors become 2.6 and 1.005. This means that for the 10 Kev line the nett gain in intensity would be $\frac{7}{2.6} \times \frac{1}{2} = 1.35$ whereas the 100 Kev would be reduced by half. One must, therefore, ensure that the thickness is not reduced by so much that the sensitivity gained at low energies is lost two- or three-fold at high energies. From the rough figures quoted it can be seen that the thickness should not be reduced by a factor of more than 2 if the instrument is to be used over the

whole range of 0 - 100 Kev or so. Of course if higher energies are not required then a further reduction could be tolerated.

Assuming the intensity of the image to be proportional to $de^{-\mu d}$ where d = crystal thickness, and μ = total linear absorption coefficient of the crystal for a given energy, then the optimum thickness for that energy is $1/\mu$. The thickness must be chosen to give the most uniform response over the range required.

The fall-off in sensitivity at high energies is due to decreasing reflecting power of the crystal planes and decreasing sensitivity of the emulsion. The reflecting power of the crystal cannot be increased except by using a different crystal but not much improvement is possible here. In any case if it were increased it would be increased for all energies and would not, therefore, produce more uniform sensitivity.

The total reflection from the crystal could of course be increased by using a thicker crystal but here all the remarks about reducing thickness apply in reverse. This would however be profitable if the spectrometer were to be used in the range 50 - 100 Kev, say. Notice, however, that the optimum thickness for 100 Kev is about 1.8 cm. and, even supposing a good enough crystal could be obtained of such a thickness, it would be very difficult to bend it with the required precision.

The sensitivity of the plate could be increased by using a thicker emulsion but for high energies the gain in sensitivity is approximately proportional to the increase in thickness, and as

G5 emulsions several hundred microns thick are very difficult to process, not much can conveniently be gained in this way. In addition, background stain is increased so that contrast between a line and the background is not much improved. A more promising possibility is to increase the absorption of the emulsion by soaking it in a solution of a lead compound before exposing - or by using specially manufactured emulsion containing lead.

To sum up, therefore, we can say that if a spectrometer is to be used for intensity measurements over its entire useful range (up to 120 Kev) then a little improvement can be expected by evacuating the apparatus and impregnating the emulsion with lead. If, however, we do not wish to cover the whole range at once, but could divide it into a few smaller ranges (even two, from 0 - 25 Kev, and from 25 Kev upwards) and could use a different spectrometer for each energy band, then considerable improvement might be expected by a judicious choice of crystal thickness. For instance, the optimum thickness for 100 Kev mentioned above would give about 30 times the intensity of the crystal at present used.

For energies above 120 Kev the instruments would have to be used like Dumond's (1947) - with a line source on the focussing circle and a counter with suitable collimation on the other side of the crystal. The performance of such a spectrometer as regards precision intensity measurements is beyond the scope of the present research but it is quite evident that here again the sensitivity must vary rapidly - though presumably continuously decreasing for energies above 100 Kev or so.

REFERENCES

ALLISON, (1927) Phys. Rev., 29, 375; (1928) Ibid. 32, 1.

AMALDI and RASETTI, (1939) Ricerca Scientifica, 10, 111.

ASARO and PERLMAN, (1954) Phys. Rev., 93, 1423.

ASARO, REYNOLDS and PERLMAN, (1952) Phys. Rev., 87, 277.

AUGER, (1925) J. Phys. Radium, 6, 205.

BACKHURST, (1936) Phil. Mag., 22, 737.

BASHILOV, DZHELEPOV and CHERVINSKAYA, (1953) Izv. Akad. Nauk SSSR, Ser. Fiz., 17, 428

BELING, NEWTON and ROSE, (1952) 86, 797; 87, 1144.

BERGSTRÖM, (1951) Phys. Rev., 81, 638.

BERGSTRÖM and THULIN, (1950) Phys. Rev., 79, 538.

BRAGG, JAMES and BOSANQUET, (1921) Phil. Mag., 41, 309.

(1922) Ibid., 42, 1.

BRAMSON, (1930) Z. Phys., 66, 721.

BROWNE, (1952) Ph.D. Thesis, Univ. of Calif. Radiation Lab. Unclassified Document UCRL - 1764 (unpublished).

BUTT and BRODIE, (1951) Proc. Roy. Soc. A 64, 791.

CARR, (1934) Phys. Rev., 46, 92.

CAUCHOIS, (1934) Ann. Phys., Paris, 1, 215.

COMPTON, (1917) Phys. Rev., 10, 95.

COMPTON and ALLISON, (1935) X-rays in Theory and Experiment (D. van Nostrand Co., Inc., New York).

COSTER and KRONIG, (1935) Physica 2, 13.

CORK, BRANYAN, STODDARD, KELLER, LEBLANC and CHILDS (1951) Phys. Rev., 83, 681

CRANBERG, (1950) Phys. Rev., 77, 155.

CURRAN, ANGUS and COCKROFT, (1949) Phil. Mag., 40, 36.

DAMON and EDWARDS, (1954) Phys. Rev., 95, 1698.

DARWIN, (1914) Phil. Mag., 27, 325; 675.

DAVIS and STEMPEL, (1921) Phys. Rev., 17, 608.

DAY, (1955) Phys. Rev., 97, 689.

von DROSTE, (1933) Z. Phys., 84, 17.

DUMOND, (1947) Rev. Sci. Instr., 18, 626.

DUMOND and KIRKPATRICK, (1930) Rev. Sci. Instr., 1, 88.

EWAN, (1952) Thesis, Univ. of Edinburgh (account to be published)

FINE and HENDEE, (1955) Nucleonics, 13 (3), 36.

FREEDMAN, WAGNER and ENGELKEMEIR, (1952) Phys. Rev. 88, 1155.

FRILLEY, GOKHALE and VALADARES, (1951) C.R. Acad. Sci., Paris, 232, 157.

GELLMAN, GRIFFITH and STANLEY, (1952) Phys. Rev., 85, 944.

GOLDHABER and HILL, (1952) Rev. Mod. Phys., 24, 179.

GRAHAM and BELL, (1953) Canad. J. Phys., 31, 377.

GRAY, (1932) Nature, 130, 738.

HARVEY, (1952) Phys. Rev., 85, 482.

HICKS, (1931) Phys. Rev., 38, 572.

HILL, CHURCH and MIHELICH, (1952) Rev. Sci. Instr., 23, 523.

HUGHES, (1955) See ROSS et al (1955)

JAFFE, PASSELL, BROWNE and PERLMAN, (1955), Phys. Rev., 97, 142.

JÖNSSON, (1926) Z. Phys., 36, 426.

KINSEY, (1948a) Canad. J. Res. A 26, 404.

(1948b) Ibid., 26, 421.

KOBAYASHI, (1953) J. Phys. Soc. Japan, 8, 440.

KÜSTNER and ARENDS, (1935) Ann. Phys. Lpz., 22, 443.

LAY, (1934) Z. Phys., 91, 533.

LIND, WEST and DUMOND, (1950) Phys. Rev., 77, 475.

MARTIN and EGGLETON, (1937) Proc. Roy. Soc. A 158, 46.

NEWTON and ROSE, (1953) Phys. Rev., 89, 1157.

PATTEN, (1934) Phys. Rev., 45, 662.

PRINGLE, (1951) Private Communication.

ROBINSON and YOUNG, (1930) Proc. Roy. Soc. A 128, 92.

ROSS, COCHRAN, HUGHES and FEATHER, (1955) Proc. Phys. Soc. A 68, 612.

ROSS and EWAN, (1953) Nature, 170, 760.

SALGUEIRO, (1944) Portugaliae Physica, 1, 2, 67.

STAHEL, (1935) Helv. Phys. Acta., 8, 651.

STEPHENSON, R.J. (1937) Phys. Rev., 51, 637.

TSIEN, (1944) C.R. Acad. Sci., Paris, 218, 503.

TSIEN, (1946) Phys. Rev., 69, 38.

TURNER, (1955) Phil. Mag., 46, 687.

ULREY, (1918) Phys. Rev., 11, 401.

WAGNER and KULENKAMPFF, (1922) Ann. Phys. Lpz., 68, 369.

WEST, DAWSON and MANDELBERG, (1952) Phil. Mag., 43, 875.

WEST and ROTHWELL, (1950) Phil. Mag., 41, 873.

WILLIAMS, (1933) Phys. Rev., 44, 146

WU, BOEHM and NAGEL, (1953) Phys. Rev., 91, 319.